Bisectors and Voronoi Diagrams for Convex Distance Functions

Vom Fachbereich Informatik
der FernUniversität Hagen
genehmigte

Dissertation

zur Erlangung des akademischen Grades eines
Doktors der Naturwissenschaften
(Dr. rer. nat.)

von
Dipl.-Math.
Lihong Ma

Erster Gutachter: Prof. Dr. Rolf Klein, FernUniversität Hagen
Zweiter Gutachter: Prof. Dr. Heinrich Müller, Universität Dortmund

Tag der mündlichen Prüfung: 5. April 2000

Contents

List of Figures

Chapter 1

Introduction

Let S be a finite set of point sites in d-dimensional space, we consider the subdivision of d-space such that each site p in S is associated with a region consisting of all points x for which p is the *nearest* site of S, see Figure 1.0.1. These structures have a long

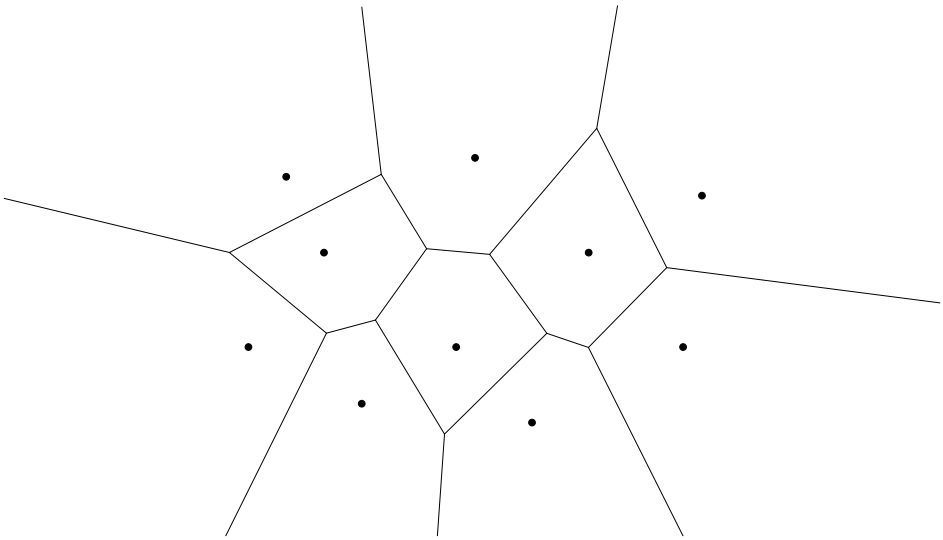

Figure 1.0.1: A set of point sites in the plane and the partition of the plane into regions each containing one site which is the nearest site for all points of the region. This structure is known as the Voronoi diagram.

history in the mathematical sciences, they have been reinvented several times, are used in many different contexts and have been given denominations like Dirichlet tesselations and Thiessen polygons. In computational geometry, scientists have agreed on the name *Voronoi diagram*, which reminds of the Russian mathematician Georges Voronoi (Georgy Fedoseevich Voronoy, 1868 – 1908). Voronoi diagrams can be considered as planar graphs, and their dual is usually denoted as *Delaunay triangulation*, honoring the Russian mathematician Boris Delaunay (Boris Nikolaevich Delone, 1890 – 1980).

Since the first worst-case optimal algorithm for constructing Voronoi diagrams by Shamos and Hoey [76] an immense number of papers on Voronoi diagrams has appeared in computational geometry. Surveys about this also including more details about the history of Voronoi diagrams can be found in Aurenhammer [2], Aurenhammer and Klein [4], Okabe et al. [69], or Fortune [29, 30]. Introductions to computational geometry including Voronoi diagrams and Delaunay triangulations were written by Preparata and Shamos [70], Klein [50], Boissonnat and Yvinec [10, 11], and de Berg et al. [23].

There are many possible generalizations of Voronoi diagrams. Shamos and Hoey [77] have introduced Voronoi diagrams of higher order. Lee and Drysdale [62] have considered diagrams for more general objects than points. Aurenhammer and Edelsbrunner [3] observed weighted Voronoi diagrams. Edelsbrunner and Seidel [28] defined Voronoi diagrams as the lower envelope of a set of functions. Klein et al. [24, 48, 49, 52, 65] have introduced abstract Voronoi diagrams which are not based on the notions of sites and distance, but on the concept of bisecting curves.

Instead of the usual Euclidean distance one can consider the more general concept of convex distance functions, see Section 1.1 for basic definitions. Voronoi diagrams based on convex distance functions are interesting for several reasons. First they can used for planning translational motions of a convex robot [17, 68, 64, 72] and for location problems [36]. The convex distance functions express the influence or attractions of a point on its environment. Second, since the convex distance functions are a natural generalization of the Euclidean distance, investigating their Voronoi diagrams is a natural and necessary step towards a unifying theory.

Two-dimensional Voronoi diagrams based on convex distance functions were studied by Lee [61] for the L_p-metric for $1 \leq p \leq \infty$, by Widmayer et al. [80] for convex distance functions defined by symmetric polygons, and by Chew and Drysdale [17] in the general case. A generalization in which each site is associated its own, different, convex distance function was considered by Icking et al. [41].

Voronoi diagrams for general distance functions in 3-dimensional space are interesting and have important applications, but not much is really known about their structure and how to compute them. Most of the few known results focus on their complexity. Boissonat et al. [7] show an upper bound of $O(n^2)$ for the complexity of a Voronoi diagram of n point sites under L_1 and L_∞, as well as for a tetrahedral distance, and generalizations of this for higher dimensions. Tagansky [79] obtains a more general bound of $O(k^3\alpha(k)n^2 \log n)$ for polyhedral distances with k facets in 3-space. Lê [57] shows that the complexity of Voronoi diagrams under L_p distances is bounded in any dimension, independent of p. Chew et al. [18] prove an upper bound of $O(n^2\alpha(n) \log n)$ for the complexity of a Voronoi diagram of lines under a polyhedral distance.

In this work we investigate the properties of bisectors and Voronoi diagrams based on convex distance functions in the plane and in 3-space. The bisectors do have some important properties in common with Euclidean bisectors, but we will show that there are substantial differences of the bisector systems of convex distance functions to the Euclidean metric. This disproves the general belief that Voronoi diagrams based on convex distance functions are, in any dimension, analogous to Euclidean Voronoi diagrams. We specially concentrate on solving all cases of degeneracies without excluding them by definition. This work is organized as follows.

Chapter 1 contains the basic definition and the important ray theorem by Desargues.

In Chapter 2 we describe the general properties of bisectors and Voronoi diagrams based on convex distance functions in the plane. In Section 2.1 we define the concept of chosen bisectors to deal with the degenerate cases, and we consider the properties of the chosen bisectors and their Voronoi diagrams. In Section 2.2 we use the properties of the convex polygons to construct the bisectors of two sites based on convex polygonal distance functions. We give an algorithm to determine the existence of the bisector of three sites. In Section 2.2.6 we explain an *on-line* algorithm for constructing Voronoi diagrams based on convex polygonal distance functions.

In Chapter 3 we turn to three dimensions. We consider the bisectors for general convex distance functions and show that there is no upper bound for the complexity of the bisector of four sites. More precise bounds are developped for polyhedral and special L_p distances.

1.1 Convex distance functions

Let C be a compact, convex body in 2-space or 3-space (not necessarily symmetric) which contains the origin O, called the center of C, in its interior. For two points p and a, we translate C by vector p and consider the ray from p through a. Let v denote the unique point on the boundary of C hit by this ray; see Figure 1.1.1. Then by

$$d_C(p,a) := \frac{||a-p||}{||v-p||}$$

a *convex distance function* d_C *based on* C is defined. Here $||a-p||$ denotes the Euclidean distance between p and a. The quantity $d_C(p,a)$ is exactly the factor that C centered at p must be expanded or contracted for its boundary to touch a.

The function d_C holds two properties of metrics.

1. $d_C(p,a) \geq 0$ and $d_C(p,a) = 0$ iff $p = a$,
2. $d_C(p,a) \leq d_C(p,b) + d_C(b,a)$, triangle inequality.

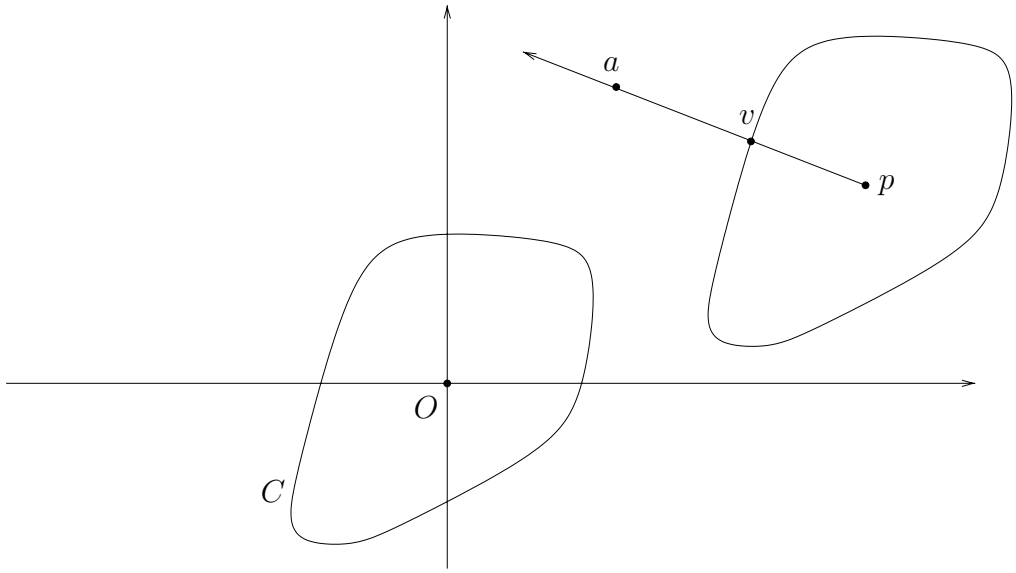

Figure 1.1.1: A convex distance function.

The symmetry relation $d_C(p,a) = d_C(a,p)$ holds, i. e. d_C is a metric, iff C is symmetric with respect to its center. For an asymmetric convex body C, the distance using the convex body C from p to a is not necessarily as same as the distance from a to p.

Clearly, C is the *unit ball* of all points a satisfying $d_C(0,a) \leq 1$, equality holding only for the points on the boundary of C, we also call the boundary of C the *unit circle* in the plane and *unit sphere* in 3-space.

Lemma 1.1.1 *Let D denote the body C reflected about its center, then the convex distance based on C from p to q is the same as the convex distance based on D from q to p.*

Proof. Let $C+p$ denote C translated by vector p, and let q' be the intersection point of the ray from p through q and the boundary of $C+p$, then

$$d_C(p,q) = \frac{||q-p||}{||q'-p||}$$

Let p' be the intersection point of the ray from q through p and $D+q$, then

$$d_D(q,p) = \frac{||p-q||}{||p'-q||}$$

By the fact that D is the reflection of C, the lengths $||q'-p||$ and $||p'-q||$ are the same, therefore $d_C(p,q) = d_D(q,p)$. □

With the above Lemma 1.1.1 we have the following result; see Figure 1.1.2.

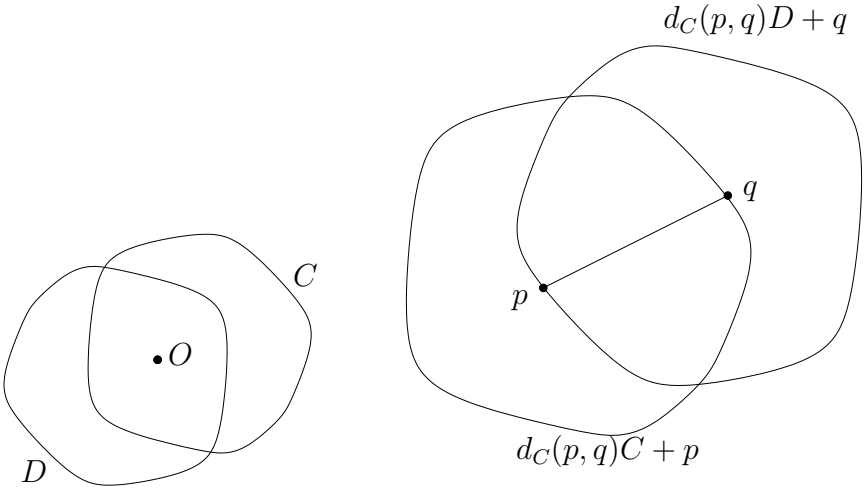

Figure 1.1.2: The unit circle C and its reflection D, as well as C, centered at p and expanded such that its boundary touches q, and D centered at q and expanded by the same factor.

Corollary 1.1.2 *The boundary of C centered at point p and expanded or contracted by factor $d_C(p,q)$ touches the point q. The symmetric assertion holds for $d_C(p,q)D+q$ which touches point p.*

The distance function d_C (and C itself) is called *strictly convex* if the boundary of C does not contain a line segment. It is called *smooth* if it admits, at each point of its boundary, a unique tangent.

Well-known examples of convex distance functions are the L_p metrics, $1 \leq p \leq \infty$, defined by $||x||_p = \sqrt[p]{|x_1|^p + |x_2|^p + |x_3|^p}$, among them the Euclidean distance, L_2. The L_p convex distance functions with $1 < p < \infty$ are smooth and strictly convex, but L_1 and L_∞ are neither smooth nor strictly convex.

We recall the following definition of the central projection into the boundary of a convex body C.

Definition 1.1.3 Let C be a compact convex body containing a point p, For each $x \neq p$ the ray $\overrightarrow{p\,x}$ from p through x intersects the boundary ∂C in a unique point x'. The mapping f, defined by

$$f(x) = x', \quad x' = \overrightarrow{p\,x} \cap \partial C,$$

is called the *central projection* on ∂C centered at p, the point x' is the *foot point* of x from p.

Kelly and Weiss [43] have shown the following theorem.

Theorem 1.1.4 *Central projections are continuous mappings.*

1.2 The ray theorem of Desargue

The following theorem by the French mathematician Girard Desargue (1591 – 1661), see [66], will turn out quite useful for constructing bisectors based on a convex polygon or polytope.

Theorem 1.2.1 *Let $\triangle(a_1, b_1, c_1)$ and $\triangle(a_2, b_2, c_2)$ be two triangles in 3-space. If the three lines $a_1\,a_2$, $b_1\,b_2$ and $c_1\,c_2$ pass through a common point u, then the intersection points p, q and r of $a_1\,b_1$ and $a_2\,b_2$, $b_1\,c_1$ and $b_2\,c_2$, $a_1\,c_1$ and $a_2\,c_2$, respectively, are collinear, see Figure 1.2.1.*

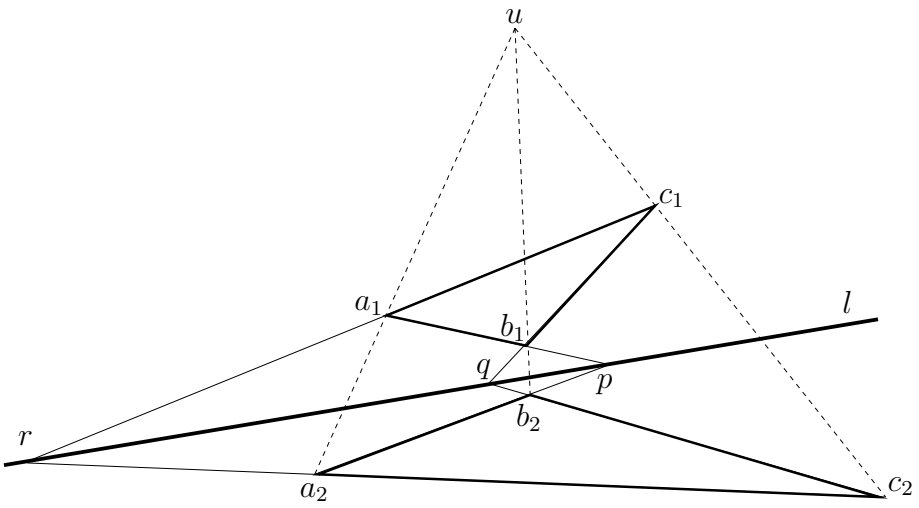

Figure 1.2.1: The ray theorem of Desargue.

Proof. In the case that the two triangles $\triangle(a_1, b_1, c_1)$ and $\triangle(a_2, b_2, c_2)$ are homothetic, the points p, q and r do not exist, because the corresponding edges of two triangles are parallel.

Suppose that $\triangle(a_1, b_1, c_1)$ and $\triangle(a_2, b_2, c_2)$ are not homothetic. There are at least two pairs of lines, for example, $a_1\,c_1$ and $a_2\,c_2$, $a_1\,b_1$, and $a_2\,b_2$, that are not parallel. Because u, a_1, c_1, a_2, and c_2 lie on a plane, the two lines $a_1\,c_1$ and $a_2\,c_2$ intersect in a point r. Analogously, $a_1\,b_1$ and $a_2\,b_2$ also intersect in a point p. If $\triangle(a_1, b_1, c_1)$ and $\triangle(a_2, b_2, c_2)$ are not coplanar, then the two planes spanned by the two triangles, respectively, intersect in a line l. Hence, the intersection points p, q and r of the corresponding lines have to lie on line l. In particular, if $b_1\,c_1$ and $b_2\,c_2$ are parallel, then the line passing through p and r is parallel to $b_1\,c_1$.

Assume, that $\triangle(a_1, b_1, c_1)$ and $\triangle(a_2, b_2, c_2)$ lie on a same plane π. Let b_1^* be an arbitrary point on the line that is perpendicular to π und intersects π in b_1, let b_2^* be the intersection point of the line passing through u and b_1^* and the line that is perpendicular to π und intersects π in b_2. The two triangles $\triangle(a_1, b_1^*, c_1)$ and

$\triangle(a_2, b_2^*, c_2)$ are not coplanar. Hence, the intersection points of $a_1\, b_1^*$ and $a_2\, b_2^*$, $b_1^*\, c_1$ and $b_2^*\, c_2$, $a_1\, c_1$ and $a_2\, c_2$ are collinear. The perpendicular projection of the intersection line onto π is a line. The points b_1 and b_2 are the projections of b_1^* and b_2^*, respectively. Hence, the intersection points p, q and r, are collinear. □

This ray theorem of Desargue is also true if the lines $a_1\, a_2$, $b_1\, b_2$, and $c_1\, c_2$ are parallel. It is also true in two dimensions, of course, as a special case of the above.

Chapter 2

Bisectors and Voronoi diagrams in 2-space

2.1 General convex distance functions

In this section we derive some properties of bisectors of convex distance functions in 2-space. Some of these properties have so far tacitly been taken for granted, but they nevertheless deserve a formal proof, because not everything which seems "intuitively clear" turns out to be true, for example look at Section 3.1.5. Independently of this work, Mazón and Recio have given proofs for some of these results, see [21, 22].

Let a_1, a_2 be two distinct sites in the plane, and let d_C be a 2-dimensional convex distance function defined by the convex set C.

Definition 2.1.0.1 The *bisector* $B_C(a_1, a_2)$ based on the convex distance function d_C (or simply on C) consists of all points p such that $d_C(a_1, p) = d_C(a_2, p)$.

A well-known example is the Euclidean bisector which is the line perpendicular to the line segment $\overline{a_1\, a_2}$ through the midpoint of a_1 and a_2. In general, $B_C(a_1, a_2)$ is not a line.

Definition 2.1.0.2 The *bisector of three sites* $B_C(a_1, a_2, a_3)$ is the set of all points p such that $d_C(a_1, p) = d_C(a_2, p) = d_C(a_3, p)$.

Clearly we have $B_C(a_1, a_2, a_3) = B_C(a_1, a_2) \cap B_C(a_1, a_3)$.

If the set C' results from scaling C by factor s then for its associated distance function, $d_{C'}$, we have $d_{C'} = \frac{1}{s} d_C$. Clearly, d_C and $d_{C'}$ yield the same bisector systems, so in our figures we sometimes draw C "sufficiently small" such that two copies of C translated to two sites are disjoint.

Let C_i denote the copy of C translated to a_i, for $i = 1, 2$, etc.

2.1.1 The bisector of two sites

W. l. o. g. we may assume that the line $a_1\,a_2$ is horizontal, and a_1 lies to the left of a_2. By U and L we denote the *upper* and the *lower* outer common supporting lines of C_1 and C_2 that are parallel to the line $a_1\,a_2$.

The *top point* of C_1, denoted by t_{12}, is the leftmost point of the intersection of C_1 and U, and the *bottom point* of C_1, d_{12}, is the corresponding point on L. The top and bottom points of C_2, t_{21}, d_{21}, are defined analogously, i. e. "leftmost" is replaced by "rightmost", see Figure 2.1.1.1.

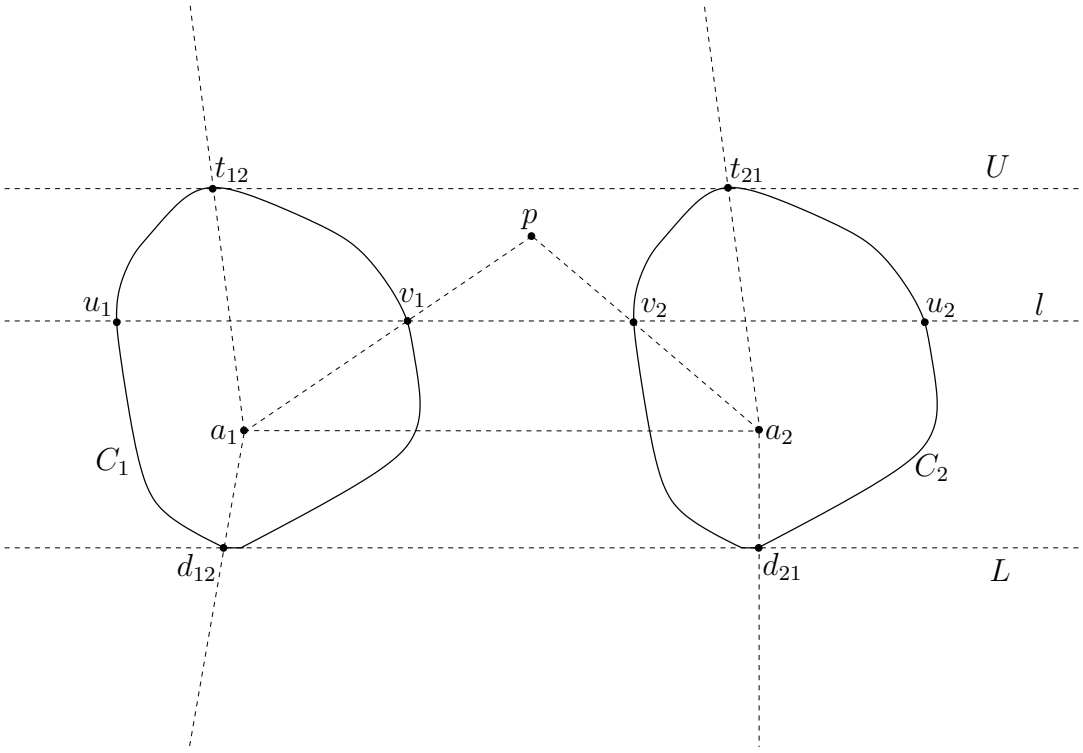

Figure 2.1.1.1: Analyzing the bisector $B_C(a_1, a_2)$.

The next lemma shows that a bisector of two sites normally behaves similar to a line.

Lemma 2.1.1.1 *If $a_1\,a_2$ is not parallel to any line segment of ∂C then the bisector $B_C(a_1, a_2)$ is homeomorphic to a line. It is fully contained in the interior of the bent strip defined by the rays $\overrightarrow{a_1\,t_{12}}$, $\overrightarrow{a_2\,t_{21}}$, $\overrightarrow{a_1\,d_{12}}$, and $\overrightarrow{a_2\,d_{21}}$.*

Proof. Let p be a point in $B_C(a_1, a_2)$ that lies strictly above the line $a_1\,a_2$, and let v_i be the foot point from a_i, for $i = 1, 2$. Since p lies in $B_C(a_1, a_2)$, we have

$$\frac{||p - a_1||}{||v_1 - a_1||} = \frac{||p - a_2||}{||v_2 - a_2||} \tag{2.1}$$

which implies that the line segments $\overline{a_1\,a_2}$ and $\overline{v_1\,v_2}$ are parallel. The line l through v_1 and v_2 intersects the boundary of each C_i in a second point, u_i. Clearly, v_1 and v_2 must be the innermost points of $\{u_1, u_2, v_1, v_2\}$ on l, as depicted in Figure 2.1.1.1, or the rays $\overrightarrow{a_1\,v_1}$ and $\overrightarrow{a_2\,v_2}$ would not intersect. Therefore, p lies in the open strip defined by $\overrightarrow{a_1\,t_{12}}$, $\overrightarrow{a_2\,t_{21}}$, and $\overrightarrow{a_1\,a_2}$.

The central projection $f : p \to v_1$ is a continuous mapping from $B_C(a_1, a_2)$ into the open boundary piece of C_1 between t_{12} and d_{12} (which in turn is homeomorphic to a line), by Theorem 1.1.4. It remains to show that f is bijective and that the inverse function f^{-1} is also continous.

Let l be an arbitrary line parallel to (but not incident with) $a_1\,a_2$ that intersects the interior of both C_1 and C_2, and let v_1, v_2 denote the neighboring pair of intersection points in $\partial C_1 \cap l$ and $\partial C_2 \cap l$. Then the rays $\overrightarrow{a_1\,v_1}$ and $\overrightarrow{a_2\,v_2}$ must intersect in some point p, and p belongs to $B_C(a_1, a_2)$, due to (2.1). The line segment $\overline{a_1\,a_2}$ contains exactly one point of $B_C(a_1, a_2)$. Hence f is surjective.

If there were two points, p and p', of $B_C(a_1, a_2)$ on the same ray $\overrightarrow{a_1\,v_1}$, then $\overrightarrow{a_2p'} \cap \partial C_2$ would consist of a point v_2' different from v_2. The points v_1, v_2, v_2' are collinear on a horizontal line, this implies that U or L contain a line segment of ∂C_2, a contradiction. Thus, the inverse mapping of f exists; it is given by the above construction of p.

Let p be a point in $B_C(a_1, a_2)$ above $a_1\,a_2$ having the foot point $v_1 \in \partial C_1$. For a neighbourhood, $[u_1, w_1]$, of v_1 in the image of f there is a corresponding interval $[u_2, w_2]$ on ∂C_2 such that the intersections $\overrightarrow{a_1\,u_1} \cap \overrightarrow{a_2\,u_2}$ and $\overrightarrow{a_1\,w_1} \cap \overrightarrow{a_2\,w_2}$ are bisector points. We consider the two cones bounded by $\overrightarrow{a_1\,u_1}$ and $\overrightarrow{a_1\,w_1}$ resp. $\overrightarrow{a_2\,u_2}$ and $\overrightarrow{a_2\,w_2}$. If only the interval $[u_1, w_1]$ is chosen small enough then the two cones intersect in a quadrilateral which is contained in any given neighbourhood of p. Therefore f^{-1} is continous. □

Only in certain special *degenerate* cases the bisector is not similar to a line, but contains one or two 2-dimensional areas.

Corollary 2.1.1.2 *The bisector $B_C(a_1, a_2)$ contains one resp. two infinite regions if and only if $a_1\,a_2$ is parallel to one resp. two line segments of ∂C.*

Proof. Let $\overline{t_{12}\,t_{12}'}$ be the line segment of ∂C_1 parallel to $a_1\,a_2$ which lies on the upper outer common supporting line U, let $\overline{t_{21}'\,t_{21}}$ be the corresponding line segment of ∂C_2. The cone bounded by the two rays $\overrightarrow{a_1\,t_{12}'}$ and $\overrightarrow{a_2t_{21}'}$ is a subset of the bisector $B_C(a_1, a_2)$, see Figure 2.1.1.2.

The converse follows from Lemma 2.1.1.1. □

Now it is useful to introduce a notation for the set of the foot points on the boundary of a unit circle.

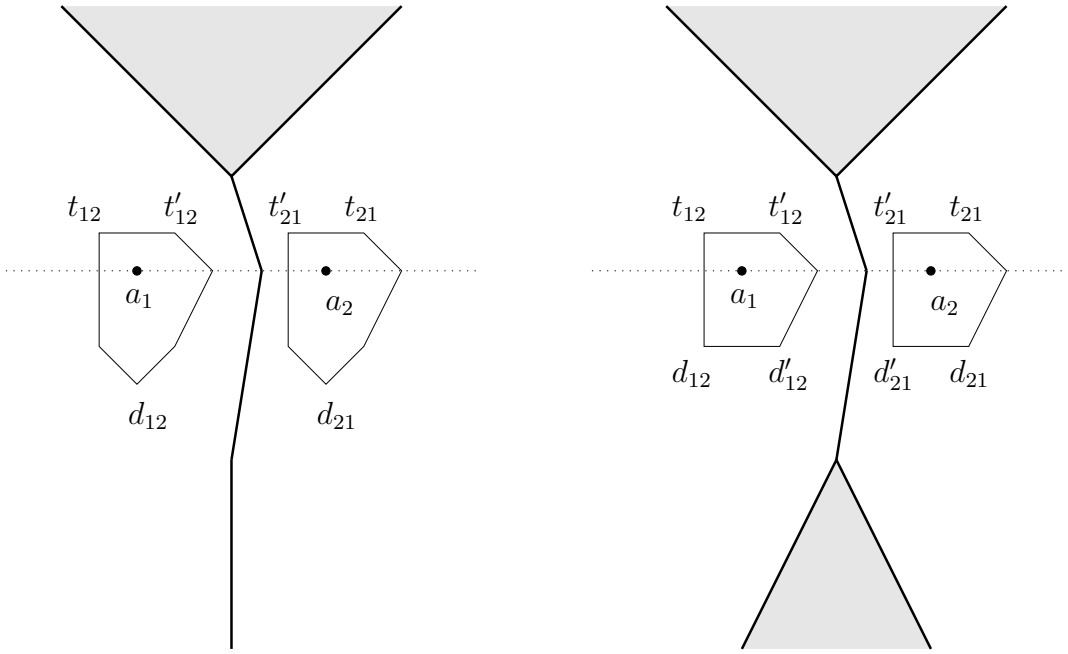

Figure 2.1.1.2: A special case: line $a_1\,a_2$ is parallel to one resp. two line segments of ∂C, the bisector contains one resp. two infinite regions.

Definition 2.1.1.3 Let H_{12} and H_{21} be the sets of the foot points of the bisector $B_C(a_1, a_2)$ on the boundaries of C_1 resp. C_2, translated back to ∂C.

From Lemma 2.1.1.1 follows that in the non-degenerate case H_{12} and H_{21} are also homeomorphic to the bisector and partition the boundary of C.

Corollary 2.1.1.4 *$H_{12} + a_1$ and $H_{21} + a_2$ are exactly the open boundaries of C_1 resp. C_2 contained in the bent strip bounded by the rays $\overrightarrow{a_1\,t_{12}}$, $\overrightarrow{a_2\,t_{21}}$, $\overrightarrow{a_1\,d_{12}}$, and $\overrightarrow{a_2\,d_{21}}$. H_{12} and H_{21} are homeomorphic to $B_C(a_1, a_2)$ and $H_{12} \cap H_{21} = \emptyset$ if and only if $a_1\,a_2$ is not parallel to a line segment of ∂C.*

2.1.2 The bisector of three sites

In this section we consider the geometric properties of bisectors of three sites and give a method to construct them.

Lemma 2.1.2.1 *For three sites a_1, a_2, a_3 in the plane, the bisectors $B_C(a_1, a_2)$ and $B_C(a_2, a_3)$ have at most one point in common, provided that each of $B_C(a_1, a_2)$, $B_C(a_1, a_2)$, and $B_C(a_2, a_3)$ is homeomorphic to a line.*

Proof. Assume that $B_C(a_1, a_2, a_3)$ contains two points. Then due to Corollary 1.1.2, there are two reflected unit circles of C, D_1 and D_2, of possibly different sizes, passing through a_1, a_2, a_3. Let T_1 and T_2 be the common outer supporting lines to D_1 and

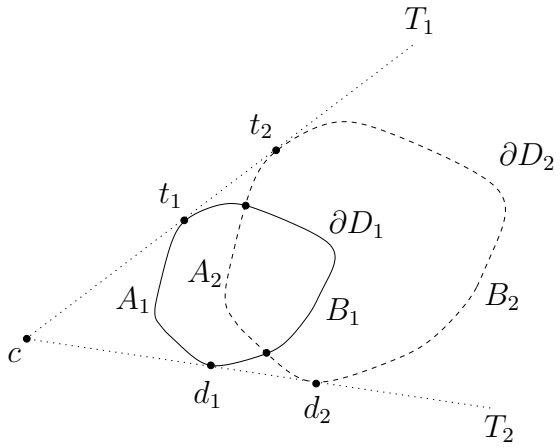

Figure 2.1.2.1: Two reflected circles intersect in at most two points.

D_2. First we assume that T_1 and T_2 touch ∂D_1 and ∂D_2 only in the points t_1, d_1, t_2, and d_2, as shown in Figure 2.1.2.1. Assume that T_1 and T_2 intersect in some point c. (The case where T_1 and T_2 are parallel can be dealt with in the same way.) Let $A_i, B_i, i = 1, 2$, denote the open segments of ∂D_i between t_i and d_i such that A_1 is on the same side as A_2 and closer to c. Clearly, we have

$$A_1 \cap A_2 = \emptyset, \qquad A_1 \cap B_2 = \emptyset, \qquad B_1 \cap B_2 = \emptyset.$$

Thus, $\partial D_1 \cap \partial D_2 = A_2 \cap B_1$. Because of the convexity of C we have $|A_2 \cap B_1| \leq 2$, a contradiction to the assumed existence of a_1, a_2, a_3.

Now we consider the case that T_1 or T_2 contain a line segment of ∂D_1 and ∂D_2. If these line segments do not overlap we can argue as before. Otherwise there are at least two of the three sites a_1, a_2, a_3 that must lie on the overlapping line segment. Due to Corollary 2.1.1.2, the bisector of these two sites is not homeomorphic to a line, a contradiction to the assumption. □

Note that in the previous paragraph we have shown the following result which will be used later.

Corollary 2.1.2.2 *The boundaries of two different but homothetic convex compact sets D_1 and D_2, intersect in at most two points, or one point and one line segment, or two line segments.*

Let us remember that the Euclidean bisector of three sites in the plane is a point in the general case and is empty if the three sites are collinear. The following theorem shows how this property generalizes to convex distance functions.

Theorem 2.1.2.3 *Let each of $B_C(a_1, a_2)$, $B_C(a_1, a_3)$, and $B_C(a_2, a_3)$ be homeomorphic to a line.*

(i) The bisector $B_C(a_1, a_2, a_3)$ is either empty or a single point.

(ii) If a_1, a_2, a_3 are collinear then $B_C(a_1, a_2, a_3) = \emptyset$.

(iii) If a_1, a_2, a_3 are not collinear then $B_C(a_1, a_2, a_3)$ consists of a single point, provided that C is smooth.

Proof. We consider the intersection points of the boundaries of C_i, $i = 1, 2, 3$, with the common outer supporting lines of C_1 and C_2 resp. C_2 and C_3; see Figure 2.1.2.2. Due to Lemma 2.1.1.1, $B_C(a_1, a_2)$ and $B_C(a_2, a_3)$ are confined to the interiors of the

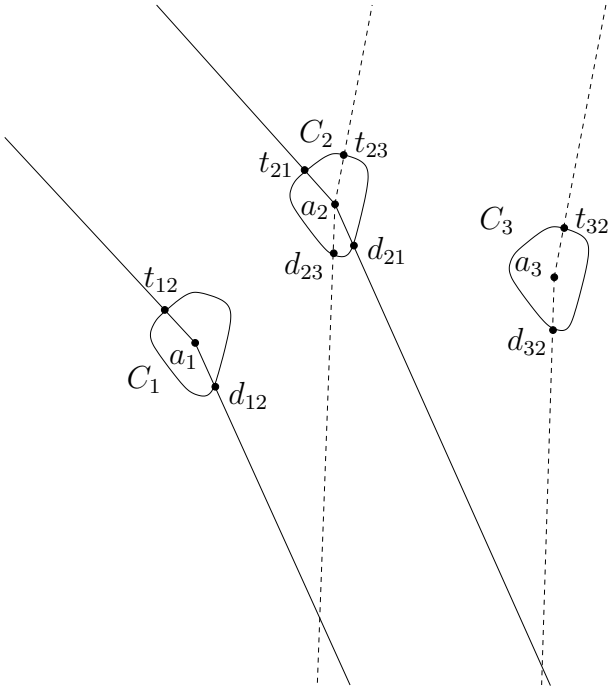

Figure 2.1.2.2: Analyzing the bisector $B_C(a_1, a_2, a_3)$ in the plane.

depicted strips. If a_1, a_2, a_3 are collinear then C_1, C_2, and C_3 have the same outer supporting lines, so the strips are disjoint. If a_1, a_2, a_3 are not collinear then the strips—hence the bisectors—cross, provided that $t_{21} \neq t_{23}$ and $d_{21} \neq d_{23}$ hold for the supporting points on ∂C_2. But this is guaranteed if ∂C_2 is smooth. Due to Lemma 2.1.2.1 we have

$$|B_C(a_1, a_2, a_3)| = 1$$

in this case. □

Note that the smoothness assumption is necessary. For example, if C results from a Euclidean circle by removing a parallel slice in the middle and glueing together the remaining two pieces, then the two resulting cusps could be the common supporting points for C_1 and C_2 as well as for C_2 and C_3, so that the strips are disjoint, see Figure 2.1.2.3.

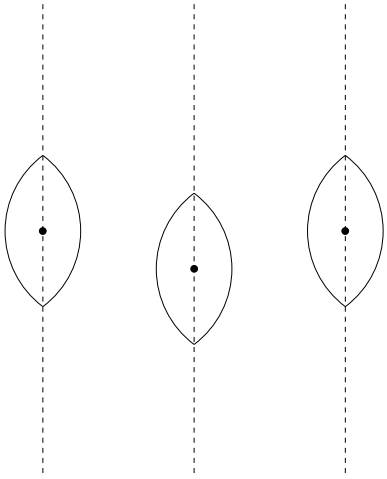

Figure 2.1.2.3: Three non-collinear sites without a common bisector.

As an abbreviation we write $H_{123} = H_{12} \cap H_{13}$, $H_{213} = H_{21} \cap H_{23}$ and $H_{312} = H_{31} \cap H_{32}$. Their geometric meaning becomes clear in the next lemma.

Lemma 2.1.2.4 *Let each of $B_C(a_1, a_2)$, $B_C(a_1, a_3)$, and $B_C(a_2, a_3)$ be homeomorphic to a line. The three sets H_{123}, H_{213}, H_{312} partition ∂C into three disjoint subsets.*

Proof. We assume that $a_1\,a_2$ is horizontal, a_1 lies to the left of a_2, and a_3 is below $a_1\,a_2$, see Figure 2.1.2.4. For simplicity of our presentation let t_{12}, d_{12}, etc. always denote these points after translation to ∂C, in this proof.

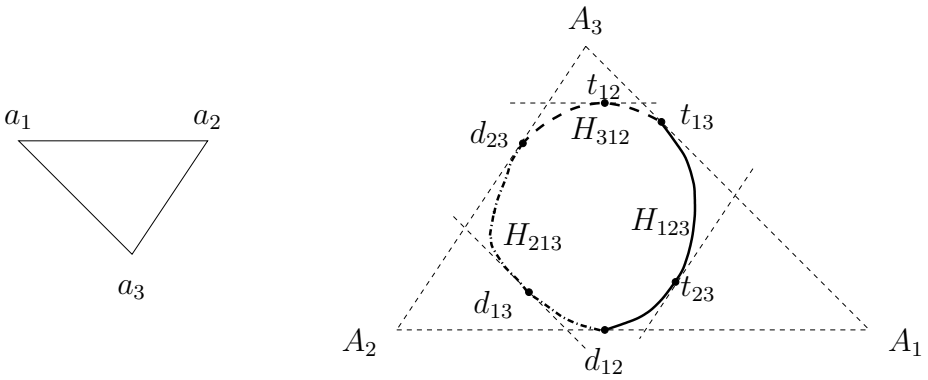

Figure 2.1.2.4: The boundary of C is partitioned into H_{123}, H_{213}, and H_{312}.

Due to the assumption, the sets H_{12} and H_{21} do not intersect, since they are separated by the top point, t_{12}, and bottom point, d_{12}. So the three sets H_{123}, H_{213}, and H_{312} also do not intersect. From the assumed position of a_1, a_2, a_3 to each other follows that the top and bottom points on ∂C have the following counterclockwise order $t_{12}, d_{23}, d_{13}, d_{12}, t_{23}, t_{13}, t_{12}$, some of these points may be identical. The set H_{12} is the counterclockwise, open interval (d_{12}, t_{12}), etc., and we have $H_{123} = (d_{12}, t_{13})$, $H_{213} = (d_{23}, d_{12})$, and $H_{312} = (t_{13}, d_{23})$. □

In the case that the line $a_1\,a_2$ is parallel to a line segment of ∂C the sets H_{123} etc. may still behave just like in the lemma above or two of them may overlap.

In Lemma 2.1.2.4 the three supporting lines through d_{12}, t_{13}, and d_{23} form a triangle $\triangle(A_1, A_2, A_3)$ which is congruent to $\triangle(a_1, a_2, a_3)$. We call $\triangle(A_1, A_2, A_3)$ the *supporting triangle*.

The next lemma shows the relation of $B_C(a_1, a_2, a_3)$ and the sets H_{123}, H_{213}, and H_{312}.

Lemma 2.1.2.5 *Let $p \in B_C(a_1, a_2, a_3)$ be a point of the bisector with foot point v_i on ∂C_i, $i = 1, 2, 3$. The points v_1, v_2, v_3 lie in $H_{123} + a_1$, $H_{213} + a_2$, and $H_{312} + a_3$, respectively, and the triangle $\triangle(v_1, v_2, v_3)$ is homothetic to $\triangle(a_1, a_2, a_3)$.*

Proof. Because of $p \in B_C(a_1, a_2) \cap B_C(a_1, a_3)$ the foot point v_1 lies in $H_{12} + a_1 \cap H_{13} + a_1$, the line segment $\overline{v_1\,v_2}$ is parallel to $\overline{a_1\,a_2}$, see the proof of Lemma 2.1.1.1 and Figure 2.1.2.5. Hence $\triangle(v_1, v_2, v_3)$ is homothetic to $\triangle(a_1, a_2, a_3)$. □

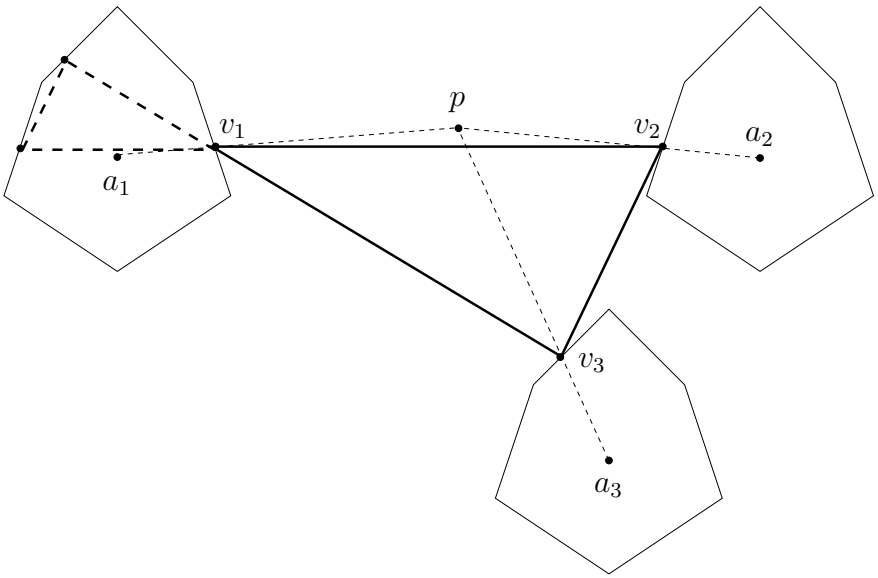

Figure 2.1.2.5: $\triangle(v_1, v_2, v_3)$ and $\triangle(a_1, a_2, a_3)$ are homothetic.

After translating the three foot points to ∂C, they form a triangle which is homothetic to the reflected triangle $\triangle(A_1, A_2, A_3)$.

Corollary 2.1.2.6 *Let u_1, u_2, u_3 be v_1, v_2, v_3 translated to ∂C, respectively. The triangle $\triangle(u_1, u_2, u_3)$ is homothetic to the supporting triangle $\triangle(A_1, A_2, A_3)$.*

Conversely if we have found a triangle T with vertices on ∂C which is homothetic to the supporting triangle then we know a point in $B_C(a_1, a_2, a_3)$.

Lemma 2.1.2.7 *Let $T = \triangle(u_1, u_2, u_3)$ be a triangle with vertices on ∂C which is homothetic to the supporting triangle $\triangle(A_1, A_2, A_3)$. Then there is a bisector point $p \in B_C(a_1, a_2, a_3)$ whose foot points are the points $u_i + a_i$, $i = 1, 2, 3$.*

Proof. Because T is homothetic to $\triangle(A_1, A_2, A_3)$, the points u_1, u_2, u_3 must lie in the sets H_{123}, H_{213} and H_{312}. So the triangle $\triangle(u_1+a_1, u_2+a_2, u_3+a_3)$ is homothetic to $\triangle(a_1, a_2, a_3)$, and $p := \overrightarrow{a_1\,(u_1 + a_1)} \cap \overrightarrow{a_2\,(u_2 + a_2)} \cap \overrightarrow{a_3\,(u_3 + a_3)} \in B_C(a_1, a_2, a_3)$. □

So, for constructing the bisector of three sites one can try to find a triangle with vertices on ∂C which is homothetic to the supporting triangle. In the following lemma we see how this is done.

Lemma 2.1.2.8 *Let a_1, a_2, a_3 be not collinear. Let each of H_{123}, H_{213} and H_{312} be not empty. There is a triangle T contained in C whose three vertices lie on the sets H_{123}, H_{213} and H_{312}, and which is homothetic to the supporting triangle $\triangle(A_1, A_2, A_3)$. It can be found using the prune-and-search technique.*

Proof. In this proof let t_{12} etc. denote the points translated to ∂C. All intervals of points in ∂C are given in counterclockwise order.

We consider the non-degenerate case that H_{123}, H_{213}, and H_{312} are disjoint. From Lemma 2.1.2.4 we know that $H_{123} = (d_{12}, t_{13})$, $H_{213} = (d_{23}, d_{12})$, and $H_{312} = (t_{13}, d_{23})$, see Figure 2.1.2.6.

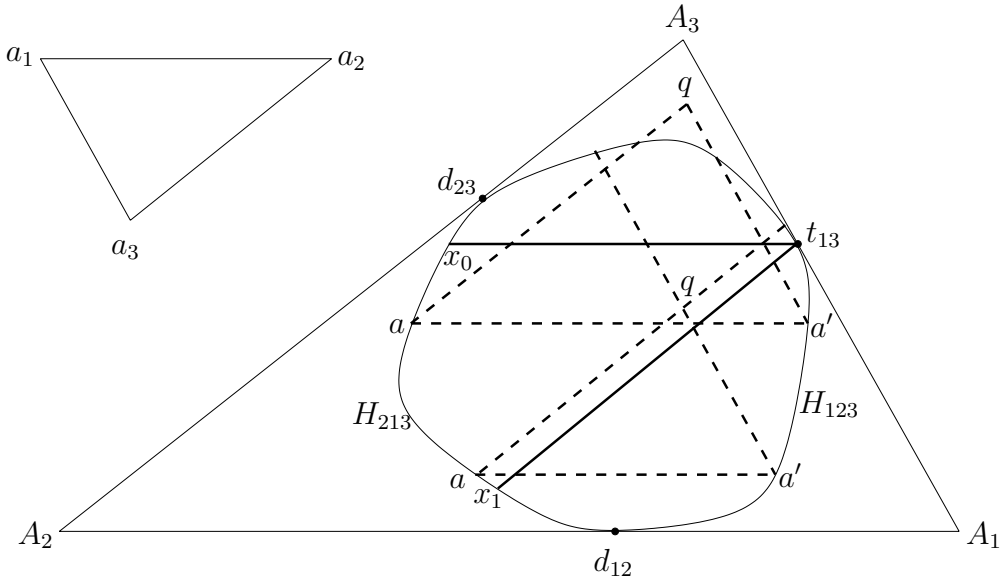

Figure 2.1.2.6: The triangle $\triangle(a_1, a_2, a_3)$ and its supporting triangle $\triangle(A_1, A_2, A_3)$. There are two cases for the point q: inside or outside of C.

We shoot two rays from t_{13} into C, one is parallel to $a_1\,a_2$ and intersects ∂C in point x_0, the other is parallel to $a_2\,a_3$ intersecting ∂C in point x_1.

Let $[y_0, y_1] = [d_{23}, d_{12}] \cap [x_0, x_1]$. For a point $a \in (y_0, y_1)$ we shoot a ray parallel to $a_1\,a_2$ into C which intersects ∂C in a point $a' \in H_{123}$. Now we shoot two more rays into C, one from a parallel to $a_2\,a_3$ and one from a' parallel to $a_1\,a_3$, they intersect in a point q. We definde the function $f : (y_0, y_1) \to \mathbf{R}^2$ by $f(a) = q$.

It is clear that if point a is sufficiently close to y_0 then point $q = f(a)$ lies outside of C, and if a is sufficiently close to y_1 then q is contained in C. Since f is continous the image of f must be connected, thus there must be a point $a_0 \in (y_0, y_1)$ such that $f(a_0) \in \partial C$. In particular, we have $f(a_0) \in H_{312}$, so we have found the triangle T we have looked for. In the non-degenerate case it is unique, by Lemma 2.1.2.1.

To construct T we can use the following prune-and-search technique. We choose point a in the middle of (y_0, y_1). If $q = f(a)$ lies outside C, as shown in Figure 2.1.2.6, we discard the intervals (y_0, a) from H_{213} and retain (a, y_1) for further refinement, and vice versa if q lies inside C. In this way, we continue and obtain a sequence of triangles that converges to the triangle T if the interval is (approximately) halved at each step.

This technique can be adapted to the degenerate case, too. In case of a polygonal unit ball C we can stop after a finite number of steps, as we will see in Section 2.2.4. □

The following corollary gives an interesting equivalent criterion for the bisector of three sites being empty in terms of the sets of foot points. The proof follows directly from the previous lemmata.

Corollary 2.1.2.9 *The bisector $B_C(a_1, a_2, a_3)$ is not empty iff $H_{123} \neq \emptyset$, $H_{213} \neq \emptyset$, and $H_{312} \neq \emptyset$.*

For finding out if the bisector of three sites is empty or not we have Theorem 2.1.2.3 for the non-degenerate case and for smooth C. For a non-smooth C we could, in principle, use Corollary 2.1.2.9 for deciding about the existence of $B_C(a_1, a_2, a_3)$ without computing the intersection of two bisectors. But we can do better without referring to H_{12} etc. For given C and a_1 and a_2 we will obtain the exact region for a_3 such that $B_C(a_1, a_2, a_3)$ is empty in Lemma 2.1.2.13.

W. l. o. g. we assume that the line $a_1\,a_2$ is horizontal. Let t_{12} and d_{12} be the top resp. bottom points of C_1, and let U and L be the two upper and lower outer common supporting lines of C_1 and C_2, see Figure 2.1.2.7. So t_{12} and d_{12} are the two boundary points of $H_{12} + a_1$.

Definition 2.1.2.10 Let T_{21} be the steepest tangent to $C + a_2$ at point t_{21}, and let T_{12} be the least steep tangent to $C + a_1$, see Figure 2.1.2.7. T_{21} and T_{12} are identical to the upper supporting line U iff C is smooth at the top point. Correspondingly, let D_{12} be the steepest tangent to $C + a_1$ at d_{12}, and let D_{21} the least steep tangent to $C + a_2$ at d_{21}.

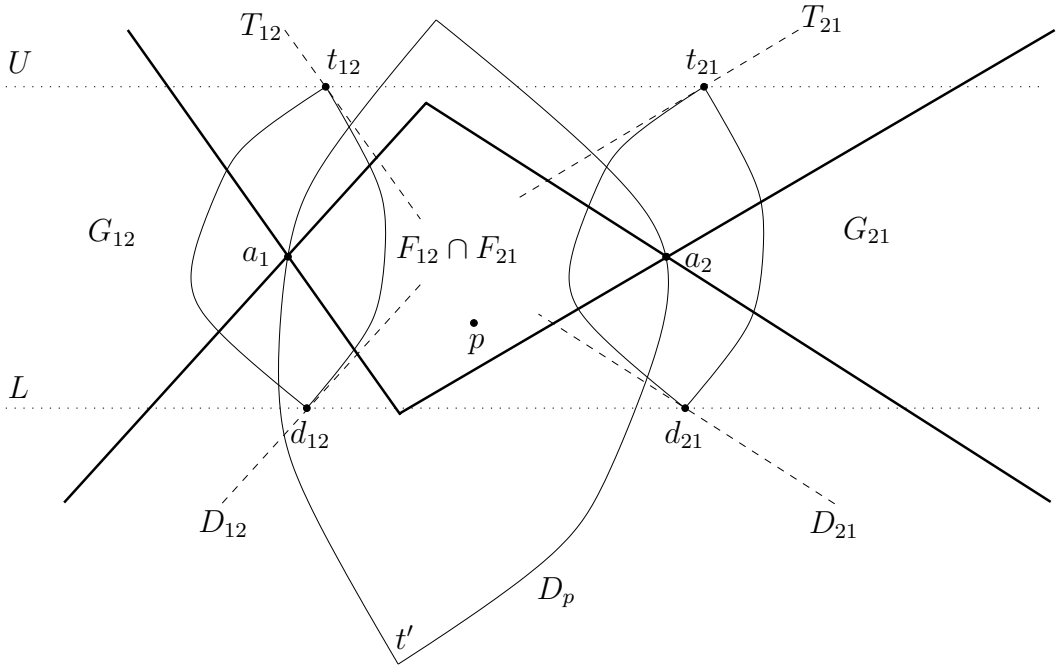

Figure 2.1.2.7: The F and G regions, see Definition 2.1.2.11 and Lemma 2.1.2.12.

Definition 2.1.2.11 We consider the four cones with apex a_1 defined by the lines through a_1 parallel to T_{12} resp. D_{12}. Let F_{12} denote the cone bounded by the line parallel to D_{12} from above and by the line parallel to T_{12} from below, and let G_{12} be the opposite cone. Analogously we have F_{21} and G_{21} with apex a_2, see Figure 2.1.2.7.

The interiors of F_{12}, G_{12}, F_{21}, and G_{21} are empty iff $a_1\,a_2$ is parallel to two line segments of ∂C, or if C is smooth at the top and bottom points.

We will show an interesting geometric interpretation of $F_{12} \cap F_{21}$, G_{12}, and G_{21}.

Lemma 2.1.2.12 *The set $F_{12} \cap F_{21}$ consists of all points that are contained in the interior of each reflected unit circle of C passing through a_1 and a_2. On the other hand, the set $G_{12} \cup G_{21}$ consists of the points that do not lie in any such reflected unit circle. These assertions hold under the assumption that the boundary of C does not contain a line segment ending at the top or bottom points.*

Proof. Let D_p be a reflected unit circle passing through a_1 and a_2. Its center point, p, must be in $B_C(a_1, a_2)$, see Figure 2.1.2.7.

Let t' be the point on the boundary of D_p which corresponds to the top point of C, i. e. it is on the bottom of D_p, and consider the two extreme tangents to D_p at t'. They are parallel to and below the bottom edges of $F_{12} \cap F_{21}$, due to the convexity of D_p. The analogous holds for the top edges of $F_{12} \cap F_{21}$, so this set is contained in D_p. Very similar arguments show that no point of $G_{12} \cup G_{21}$, except a_1 and a_2, is contained in D_p. □

For brevity let FG_{12} denote the set $G_{12} \cup (F_{12} \cap F_{21}) \cup G_{21}$. The line $a_1\, a_2$ is always contained in FG_{12}. Now we have a simple criterion to determine if $B_C(a_1, a_2, a_3)$ is empty.

Lemma 2.1.2.13 *For three sites a_1, a_2, a_3 we have $B_C(a_1, a_2, a_3) = \emptyset$ if and only if either*

- *a_3 is contained in the interior of the set FG_{12},*

or

- *a_3 lies on one of the boundary line segments of FG_{12} and the tangent to C where this line segment stems from does not contain a boundary line segment of ∂C.*

Proof. Assume that $B_C(a_1, a_2, a_3) = \emptyset$ and a_3 is not contained in the interior of the set FG_{12}, so a_3 lies on the boundary of FG_{12} or in the complement of FG_{12}.

If a_3 lies in the complement of FG_{12} then there is a reflected unit circle, D_1, centered at $p_1 \in B_C(a_1, a_2)$ passing through a_1 and a_2 such that $a_3 \in In(D_1)$, so $d_C(a_1, p_1) > d_C(a_3, p_1)$. And there is another reflected unit circle, D_2, centered at $p_2 \in B_C(a_1, a_2)$ passing through a_1 and a_2 such that $a_3 \notin In(D_2)$, so $d_C(a_1, p_2) \leq d_C(a_3, p_2)$. Now consider the continous function defined by $f(p) := d_C(a_1, p) - d_C(a_3, p)$ for $p \in B_C(a_1, a_2)$. Because of $f(p_1) > 0$ and $f(p_2) \leq 0$ there is a $p_0 \in B_C(a_1, a_2)$ such that $f(p_0) = 0$, this means that $p_0 \in B_C(a_1, a_2, a_3)$, a contradiction.

Therefore a_3 lies on one of the boundary line segments or boundary rays of FG_{12}. So this line segment must be contained in any reflected unit circle passing through a_1 and a_2. If now the tangent where this line segment stems from contains a boundary line segment of ∂C, see Figure 2.1.2.8, then there are reflected unit circles passing through a_1 and a_2 that contain a_3 and the line segment or (part of) the ray on their boundary.

The reversed assertions follow directly from Lemma 2.1.2.12. □

2.1.3 Fulfilling the triangle equality

In the Euclidean metric the triangle equality

$$d_C(p, q) = d_C(p, r) + d_C(r, q)$$

for three points p, q, and r holds if and only if they are collinear. For general convex distance functions this can be different. From [49, Corollary 1.2.11] we know that the triangle equality is fulfilled for some non-collinear points iff the unit ball contains a line segment in its boundary.

The following lemma characterizes precisely for which points p, q, and r the triangle equality holds.

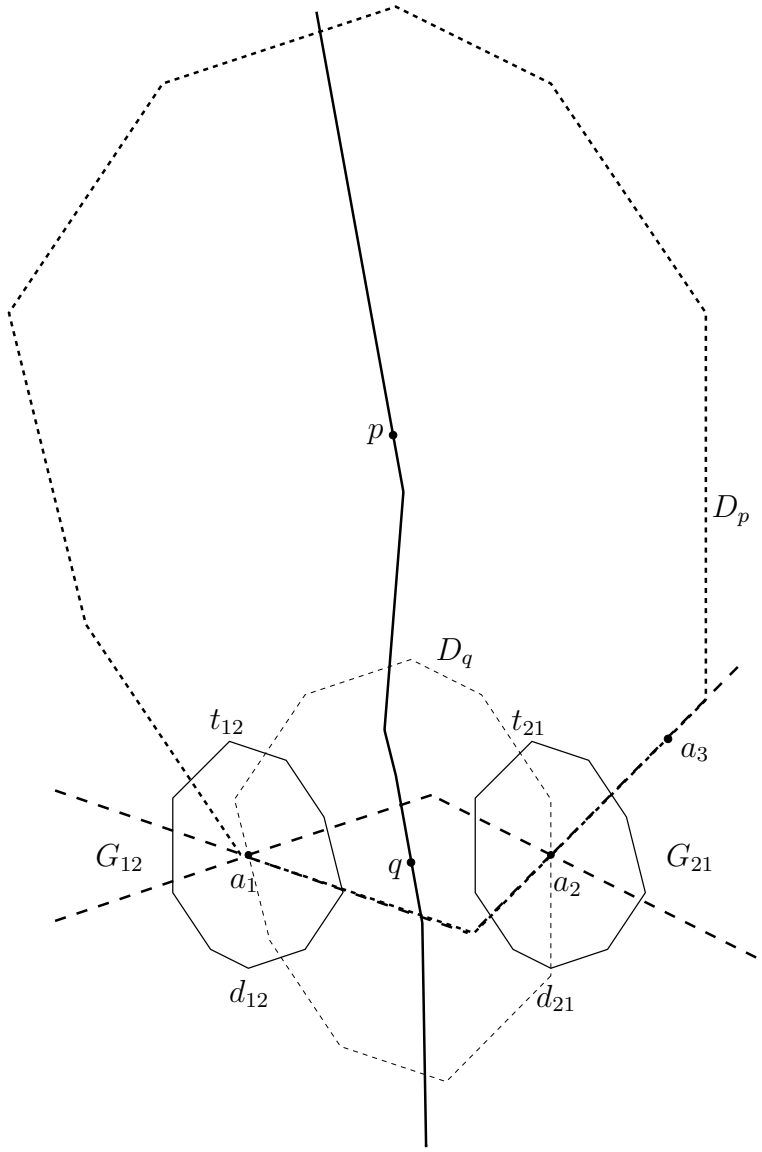

Figure 2.1.2.8: Here, a_3 lies on a boundary ray of FG_{12} which is parallel to a line segment of ∂C. We can find a reflected unit circle, D_p, passing through a_1, a_2, and a_3, if we choose its center point, p, on the ending ray of $B_C(a_1, a_2)$.

Lemma 2.1.3.1 *The triangle equality $d_C(p,q) = d_C(p,r) + d_C(r,q)$ holds if and only if there is a point $t \neq p, q, r$, such that r is on the line segment $\overline{pt}$ and p and r are contained in the same unbounded region of the degenerate bisector $B_D(q,t)$, where D is the unit circle C, reflected at its center point.*

Proof. Suppose $d_C(p,q) = d_C(p,r) + d_C(r,q)$ holds. Let V be a copy of C translated to p with scalar factor $d_C(p,q)$, so q lies on the boundary of V. Let t be the intersection point of the ray $\overrightarrow{pr}$ and ∂V. By $d_C(p,t) = d_C(p,q)$ the point r lies in the interior of V. Because of $d_C(p,t) = d_C(p,r) + d_C(r,t)$ we have $d_C(r,q) = d_C(r,t)$, this implies $d_D(q,r) = d_D(t,r)$. Therefore, p and r are points in $B_D(q,t)$. Because t lies on the

ray $\overrightarrow{p\,r}$, the bisector $B_D(q,t)$ is degenerate and contains an unbounded region.

Conversely, let r lie on the line segment $\overline{p\,t}$, then $d_D(t,p) = d_D(t,r) + d_D(r,p)$, see Figure 2.1.3.1. By $d_D(t,r) = d_D(q,r)$ and $d_D(q,p) = d_D(t,p)$ we have $d_D(q,p) = d_D(q,r) + d_D(r,p)$. Because of $d_D(q,p) = d_C(p,q)$ etc. the equality $d_C(p,q) = d_C(p,r) + d_C(r,q)$ holds. □

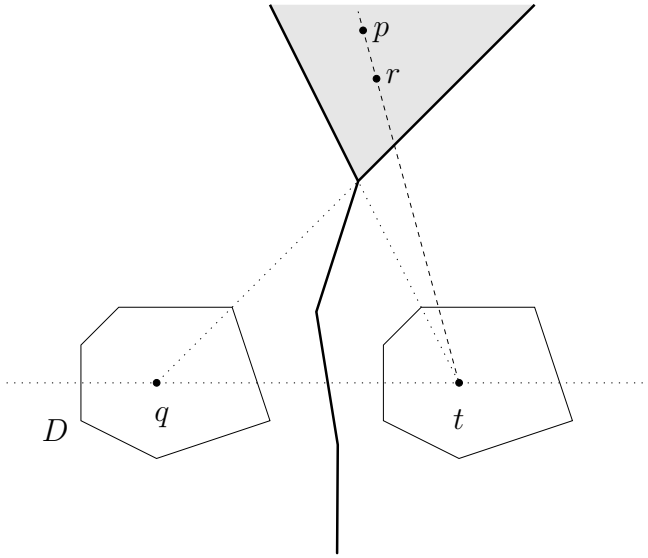

Figure 2.1.3.1: Points p and r are collinear with t and lie in the region of $B_D(q,t)$, thus the triangle equality $d_C(p,q) = d_C(p,r) + d_C(r,q)$ holds.

From Lemma 2.1.3.1 also follows that this phenomenon does not happen for strictly convex distance functions because a degenerate bisector implies that a line segment is contained in the boundary of the unit circle.

2.1.4 Voronoi diagrams

From previous sections we know that the bisector $B_C(a_1,a_2)$ separates the plane into two regions where one contains a_1 and the other one a_2. We also know that $B_C(a_1,a_2)$ contains two-dimensional areas if $a_1\,a_2$ is parallel to line segments of ∂C. But for considering Voronoi diagrams these areas are rather annoying, on the other hand we do not want to exclude such degenerate positions of two sites. Therefore, we make use of a convention first proposed by Klein and Wood [53] introducing a lexicographical ordering of the sites that avoids degenerate bisectors.

Definition 2.1.4.1 Let $\prec$ denote the lexicographical order, i. e. $p \prec q$ iff the x and y coordinates satisfy either $p_x < q_x$ or $p_x = q_x$ and $p_y < q_y$. For $a_1 \prec a_2$ let the region of a_1 with respect to a_2, $D_C(a_1,a_2)$, be the set $\{p : d_C(a_1,p) \leq d_C(a_2,p)\}$, and $D_C(a_2,a_1)$ is its complement. The boundary of $D_C(a_1,a_2)$ is called the *chosen bisector* $B^*_C(a_1,a_2)$.

The chosen bisector differs from the original bisector in that the possible two-dimensional areas of a degenerate bisector are now contained in the region of the lexicographically smaller site. All chosen bisectors are homeomorphic to a line, either by Lemma 2.1.1.1 or by this convention.

Before we consider Voronoi diagrams, we have to know the properties of the chosen bisectors which behave similarly to bisectors in the Euclidean metric.

Lemma 2.1.4.2 *If a_1, a_2, a_3 are collinear then the chosen bisectors $B^*_C(a_1, a_2)$ and $B^*_C(a_2, a_3)$ do not intersect.*

Proof. For three collinear sites it is clear that $B^*_C(a_2, a_3)$ is a translation of $B^*_C(a_1, a_2)$ in direction $a_1\,a_2$, and they do not contain a line segment parallel to $a_1\,a_2$. So they are disjoint. □

As an example, in Figure 2.1.4.1 the sites a_1, a_2, a_3 are collinear, the (real) bisectors $B_C(a_1, a_2)$ and $B_C(a_2, a_3)$ intersect in two regions, but their chosen bisectors do not intersect. Note that the converse of Lemma 2.1.4.2 does not hold, see Figure 2.1.2.3.

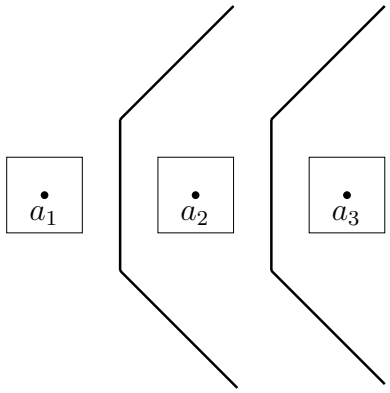

Figure 2.1.4.1: The sites a_1, a_2, a_3 are collinear and in degenerate position, their chosen bisectors do not intersect.

Now let us turn to the bisector of three sites.

Lemma 2.1.4.3 *The intersection of the chosen bisectors $B^*_C(a_1, a_2)$, $B^*_C(a_1, a_3)$, and $B^*_C(a_2, a_3)$ is either empty or a point or a ray. It is a ray, iff two of the lines $a_1\,a_2$, $a_1\,a_3$, and $a_2\,a_3$ are parallel to two adjacent line segments of ∂C.*

Proof. Suppose the chosen bisectors $B^*_C(a_1, a_2)$, $B^*_C(a_1, a_3)$, and $B^*_C(a_2, a_3)$ have two points, p_1 and p_2, in common then the boundaries of two copies D_1 and D_2 of the reflection of C centered at p_1 resp. p_2 with different radii intersect in a_1, a_2, a_3. So the intersection of ∂D_1 and ∂D_2 contains a line segment by Corollary 2.1.2.2. Therefore and by Lemma 2.1.4.2 exactly two points of a_1, a_2, a_3 must lie on this line segment, say a_1, a_2 with $a_1 \prec a_2$. This means that we have a situation as shown in

Figure 2.1.4.2, i. e. the bisector $B_C(a_1, a_2)$ is degenerate, and p_1, p_2 lie on the boundary of its degenerate part.

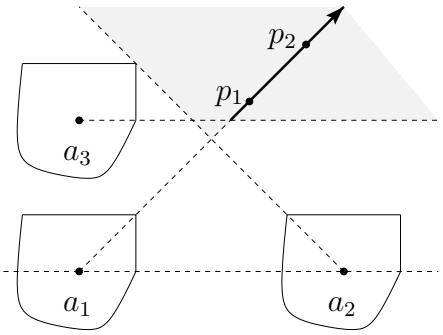

Figure 2.1.4.2: In this doubly degenerate case the chosen bisectors coincide in a ray.

The foot point of p_1 and p_2 on ∂C_1 must be the endpoint of a line segment on ∂C_1 which is parallel to $a_1\, a_2$. So a_1 is the endpoint of the corresponding line segments of ∂D_1 and ∂D_2.

But this can only be the case in the doubly degenerate situation that there is a second line segment on ∂C, and this one is parallel to $a_1\, a_3$ and $a_1 \prec a_3$. The intersection of $B^*_C(a_1, a_2)$, $B^*_C(a_1, a_3)$, and $B^*_C(a_2, a_3)$ contains a ray passing through p_1 and p_2. □

The fact that the intersection of $B^*_C(a_1, a_2)$, $B^*_C(a_1, a_3)$, and $B^*_C(a_2, a_3)$ may be more than a single point, namely a whole ray, is equally annoying as the existence of the degenerate bisectors. Therefore we make another convention regarding the bisector of three sites.

Definition 2.1.4.4 The *chosen bisector* $B^*_C(a_1, a_2, a_3)$ *of three sites* is defined to be the intersection $B^*_C(a_1, a_2) \cap B^*_C(a_1, a_3) \cap B^*_C(a_2, a_3)$ except for the case of a ray where it is only the ray's starting point.

Thereby we have reestablished the behavior known from the Euclidean case: the bisector of three sites is empty or a single point. Remark, however, that in special cases $B^*_C(a_1, a_2, a_3)$ can be empty while $B_C(a_1, a_2, a_3)$ is not, as we have seen in Figure 2.1.4.1.

The Voronoi regions and the Voronoi diagram can now be defined in the usual way.

Definition 2.1.4.5 Let $S = \{a_1, \ldots, a_n\}$ be a set of sites. We call

$$VR_C(a_i, S) = \bigcap_{j \neq i} In(D_C(a_i, a_j)),$$

the *Voronoi region* of a_i. Here, *In* denotes the interior of a set.

The Voronoi regions defined as above are clearly disjoint, each point of the plane belongs to exactly one Voronoi region or lies on a boundary. The boundary of a Voronoi region consists only of pieces of chosen bisectors.

Definition 2.1.4.6 The *Voronoi diagram* of $S = \{a_1, \ldots, a_n\}$ is defined as the union of the boundaries of all Voronoi regions.

$$V_C(S) = \bigcup_i \partial\, VR_C(a_i, S).$$

A Voronoi region is not necessarily convex, as it is for the Euclidean distance, for example see Figure 2.1.4.3. But each region is star-shaped.

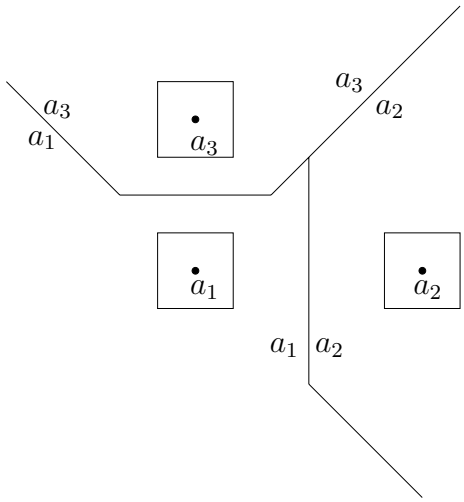

Figure 2.1.4.3: The Voronoi diagram of three sites based on L_∞.

Lemma 2.1.4.7 *Every Voronoi region $VR_C(a_1, S)$ is star-shaped with nucleus a_1.*

Proof. Take an arbitrary point u in the region $VR_C(a_1, S)$. Suppose there exists a point v on the line segment $\overline{a_1\, u}$ which is contained in a different region $VR_C(a_2, S)$. In case of $d_C(a_1, v) > d_C(a_2, v)$ we have

$$d_C(a_1, u) = d_C(a_1, v) + d_C(v, u) > d_C(a_2, v) + d_C(v, u) > d_C(a_2, u),$$

a contradiction to $u \in VR_C(a_1, S)$. If $d_C(a_1, v) = d_C(a_2, v)$ then the line $a_1\, a_2$ is parallel to a line segment of ∂C and v lies in the bisector region of $B_C(a_1, a_2)$. If $a_1 \prec a_2$ then all points on the line segment $\overline{a_1\, u}$ lie in $D_C(a_1, a_2)$, so $v \in D_C(a_1, a_2)$, a contradiction to $v \in VR_C(a_2, S)$. If $a_2 \prec a_1$ then $u \in D_C(a_2, a_1)$, a contradiction to $u \in VR_C(a_1, S)$. □

By Lemma 2.1.4.3 it is clear that each chosen bisector of two sites contributes at most one connected component to the Voronoi diagram.

Definition 2.1.4.8 A maximal connected component of a chosen bisector of two sites that is contained in the Voronoi diagram is called a *Voronoi edge*. Its end points, if they exist, are called *Voronoi vertices*.

Every Voronoi edge is the intersection of the boundaries of two Voronoi regions, and every Voronoi vertex is a chosen bisector of three sites.

Every Voronoi vertex is also the center of a reflected unit circle that passes through three or more sites and that does not include any other sites in its interior. The converse is true in the Euclidean case but not for general convex distance functions. For example, the Voronoi diagram of three sites a_1, a_2, and a_3 in Figure 2.1.4.4 consists of only the two chosen bisectors $B^*_C(a_1, a_3)$ and $B^*_C(a_2, a_3)$. There are no Voronoi vertices, although each reflected unit circle centered at a point of $B^*_C(a_2, a_3)$ passing through a_2 and a_3 also passes through a_1.

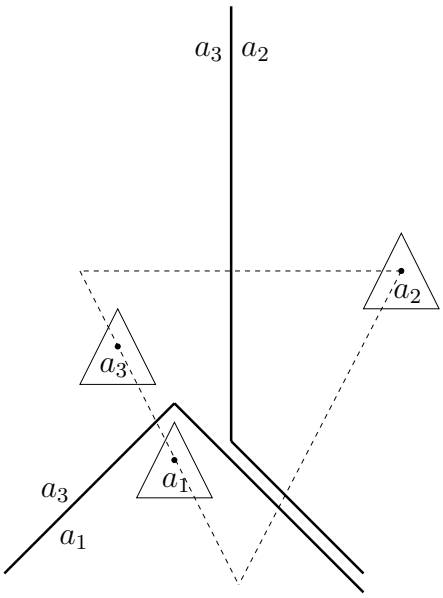

Figure 2.1.4.4: Any point of the bisector $B^*_C(a_2, a_3)$ is the center of a reflected unit circle passing through all three sites, nevertheless there is no Voronoi vertex.

The following result gives the exact criteria for two Voronoi regions being neighbors.

Lemma 2.1.4.9 *The boundaries $\partial VR_C(a_1, S)$ and $\partial VR_C(a_2, S)$ share a Voronoi edge (i. e. they are adjacent) if and only if one of the following holds.*

1. *There exists a point u such that the reflected unit circle D_u centered at u passing through a_1 and a_2 does not include any other site of S in its interior and on its boundary.*

or

2. *There is a open line segment of $B_C^*(a_1, a_2)$ such that for each point u in it the reflected unit circle D_u centered at u through a_1 and a_2 does not include any other site of S in its interior but contains sites $a_1, r_1, \ldots, r_m \in S$ on one line segment and $a_2, s_1, \ldots, s_k \in S$ on another line segment. Either $a_1 \prec r_i$ for all i and $a_2 \prec s_j$ for all j, or there is a site $r \in \{r_1, \ldots, r_m\} \cap \{s_1, \ldots, s_k\}$ such that $r \prec a_1 \prec r_i$ and $r \prec a_2 \prec s_j$ for all $r_i, s_j \neq r$.*

Proof. If (1) holds then the Voronoi regions of a_1 and a_2 are adjacent and u is in the Voronoi diagram, due to Definition 2.1.4.5. Now assume that condition (2) is fulfilled by the open line segment $\overline{u_0\, u_1} \subset B_C^*(a_1, a_2)$. If $\{r_1, \ldots, r_m\} \cap \{s_1, \ldots, s_k\} = \emptyset$ then $\overline{u_0\, u_1}$ lies in $D(a_1, r_i) \cap D(a_2, s_j)$ because of $a_1 \prec r_i$ for all i and $a_2 \prec s_j$ for all j. It is also contained in $D(a_1, a_l) \cap D(a_2, a_l)$ for $a_l \in S \setminus \{r_1, \ldots, r_m, s_1, \ldots, s_k\}$. Hence $\overline{u_0\, u_1}$ lies on the boundaries of $VR_C(a_1, S)$ and $VR_C(a_2, S)$. If, on the other hand, $\{r\} = \{r_1, \ldots, r_m\} \cap \{s_1, \ldots, s_k\}$ then $\overline{u_0\, u_1}$ is on the intersection ray of the chosen bisectors $B_C^*(a_1, a_2)$, $B_C^*(a_1, r)$, and $B_C^*(a_2, r)$, due to Lemma 2.1.4.3, so by Definition 2.1.4.5 it lies on the boundaries of $VR_C(a_1, S)$ and $VR_C(a_2, S)$.

Conversely, let (u_0, u_1) be an open connected subset on the boundaries of $VR_C(a_1, S)$ and $VR_C(a_2, S)$. So for any point $u \in (u_0, u_1)$ there are no sites of S that lie in the interior of the reflected unit circle D_u centered at u passing through a_1 and a_2.

We assume that (1) does not hold, so for each $u \in (u_0, u_1)$ the reflected unit circle D_u always includes at least one site $r \in S$ such that r and a_1 or r and a_2 lie on the same line segment of D_u, due to Corollary 2.1.2.2. Therefore at least one of the bisectors $B_C(a_1, r)$ and $B_C(a_2, r)$ is degenerate, so (u_0, u_1) is a line segment.

Assume that only $B_C(a_1, r)$ is degenerate, this means that a_1 and r are on the same line segment of D_u, but not a_2 and r. If $r \prec a_1$ then $\overline{u_0\, u_1}$ lies in the set $D(r, a_1)$, therefore $\overline{u_0\, u_1}$ can not be on the boundaries of $VR_C(a_1, S)$ and $VR_C(a_2, S)$, a contradiction. Hence we have $a_1 \prec r$ and therefore (2).

If both, $B_C(a_1, r)$ and $B_C(a_2, r)$, are degenerate then r is the intersection vertex of the two line segments of D_u containing a_1 resp. a_2. Due to Lemma 2.1.4.3, the line segment $\overline{u_0\, u_1}$ lies on the intersection ray of the chosen bisectors $B_C^*(a_1, r)$, $B_C^*(a_2, r)$, and $B_C^*(a_1, a_2)$, in particular, $r \prec a_1$ and $r \prec a_2$. Furthermore there are no sites of S that lie on the line segments $\overline{a_1\, r}$ and $\overline{a_2\, r}$, otherwise the Voronoi regions of a_1 and a_2 would not be adjacent. □

For example, in Figure 2.1.4.4, a_3 and a_1 lie on the same edge of the reflected unit circle centered at points on the bisector ray of $B_C(a_2, a_3)$, and $a_3 \prec a_1$, so due to Lemma 2.1.4.9 the Voronoi regions of a_3 and a_2 are adjacent. Figure 2.1.4.5 shows a L_1 circle, and the sites r, a_1, r_1 lie on one of its edges, while the sites r, a_2, s_1 lie on another edge and the conditions $r \prec a_1 \prec r_1$ and $r \prec a_2 \prec s_1$ hold, so the Voronoi regions of a_1 and a_2 share an edge.

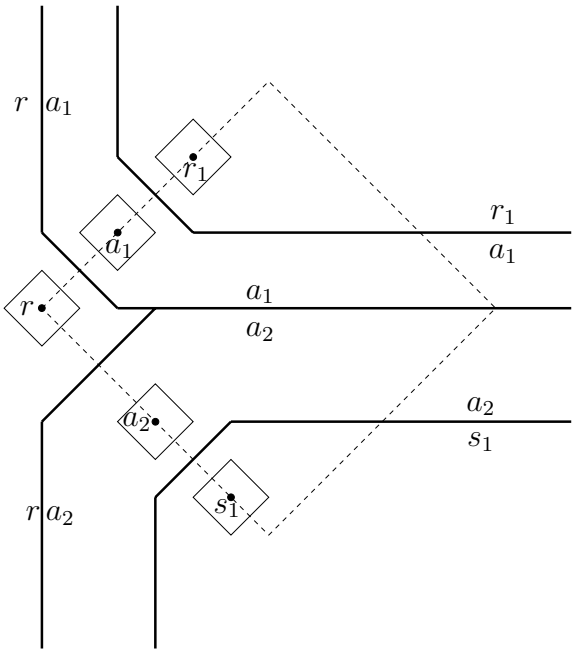

Figure 2.1.4.5: The Voronoi diagram of the sites r, a_1, a_2, r_1, s_1 based on the L_1-metric.

2.1.5 The dual graph of a Voronoi diagram

The notions of Voronoi edges and Voronoi vertices indicate that we will also understand the Voronoi diagram as a graph (which is always planar, of course). The dual of this graph is the generalization of the well-known Delaunay triangulation for the Euclidean case.

Definition 2.1.5.1 The *dual graph*, $D_C(S)$, is the dual of the Voronoi diagram $V_C(S)$, considered as a graph. The vertices of $D_C(S)$ are the sites of S. Two sites of S are connected if and only if their Voronoi regions share a Voronoi edge.

In general, $D_C(S)$ does not inherit all nice properties which are known from the Delaunay triangulation. For example, the Delaunay triangulation is a triangulation of the convex hull of S, but the dual graph $D_C(S)$ for a general distance function can be an only incomplete triangulation, see Figure 2.1.5.1.

Nevertheless we have the following result for "nice" unit circles.

Lemma 2.1.5.2 *Assume that C is strictly convex and smooth. Then the dual graph, $D_C(S)$, is a triangulation of the convex hull of S. The unbounded Voronoi regions belong to exactly those sites that are vertices of the convex hull of S.*

The proof is analogous to the proof for the Euclidean case which can be found in [50, Section 5.2], for example. The strict convexity and smoothness are necessary,

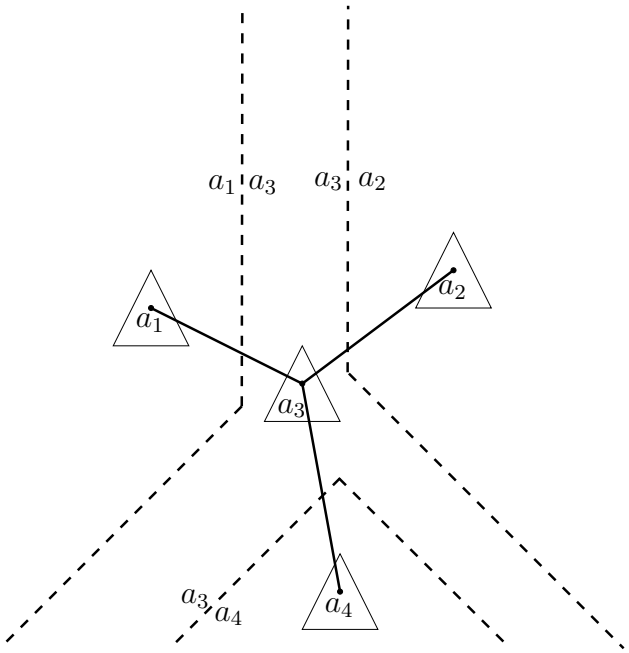

Figure 2.1.5.1: The Voronoi diagram and the dual graph of four sites based on a triangular distance function. Site a_3 is not on the boundary of the convex hull of the sites, but it has an unbounded Voronoi region, therefore the dual graph is only an incomplete triangulation of the convex hull.

otherwise there could be unbounded Voronoi regions for sites which are not vertices of the convex hull, as shown in Figure 2.1.5.1.

Another difference to the Euclidean case concerns nearest neighbours. First we observe that there are two different kinds of nearest neighbours if the distance function is not symmetric.

Definition 2.1.5.3 Let $S = \{a_1, \ldots, a_n\}$ be a set of sites.

1. If we have
$$d_C(a_i, a_j) = \min_{\substack{1 \le k \le n \\ k \neq i}} \{d_C(a_i, a_k)\}$$
then a_j is called a *nearest neighbour of a_i with respect to C*.

2. If we have
$$d_C(a_j, a_i) = \min_{\substack{1 \le k \le n \\ k \neq i}} \{d_C(a_k, a_i)\}$$
then a_j is called a *reverse nearest neighbour of a_i with respect to C*.

In other words the expanded unit circle resp. the expanded reflected unit circle centered at a_i passing through a_j does not contain any other site in its interior. Nearest neighbours are not necessarily unique.

In the Euclidean case for any site the edge to its nearest neighbour site (even to each of its nearest neighbours, if there are more than one) is contained in the Delaunay triangulation, see [70, Section 5.5.1]. The generalization of this to convex distance functions is not always true.

For example, in Figure 2.1.5.2 the site a_2 is the nearest neighbour of a_1, because the expanded triangular unit circle centered at a_1 passing through a_2 does not contain a_3, so $d_C(a_1, a_2) < d_C(a_1, a_3)$. But the Voronoi regions of a_1 and a_2 are not adjacent due to Lemma 2.1.4.9, because every reflected unit circle passing through a_1 and a_2 contains the site a_3. The reason for this is that a_3 lies in the set $F_{12} \cap F_{21}$ and Lemma 2.1.2.12 applies.

For the reverse nearest neighbour, however, we have the following result which is quite similar to the Euclidean case.

Lemma 2.1.5.4 *The Voronoi regions of site a_1 and its lexicographically smallest reverse nearest neighbour site are adjacent.*

Proof. We consider the reflected unit circle expanded and translated such that it is centered at a_1 and passes through all reverse nearest neighbours, say D_1. Let a_2 be the lexicographically smallst reverse nearest neighbour. We consider a second reflected unit circle, say D_2, namely the one passing through a_1 and a_2 and centered at the intersection of $B_C^*(a_1, a_2)$ and the line segment $\overline{a_1\, a_2}$. This construction guarantees that D_2 is enclosed in D_1 and contains no site in its interior. Therefore $VR_C(a_1, S)$ and $VR_C(a_2, S)$ are adjacent either by Lemma 2.1.4.9 (1) if a_1 and a_2 are the only sites on the boundary of D_2, or otherwise by Lemma 2.1.4.9 (2), because then a_2 is the lexicographically smallest site on its boundary line segment of D_2. □

For a triangle in the dual graph we can define its circumcircle.

Definition 2.1.5.5 The *circumcircle* of three sites (or of the triangle with these vertices) whose chosen bisector exists is the reflected unit circle passing through the three sites and centered at the chosen bisector.

Lemma 2.1.5.6 *Let a_1 be a site of the set S with a bounded Voronoi region, and let $a_2, \ldots, a_k$ be its neighbours in this order in the Voronoi diagram of S. Then $VR_C(a_1, S)$ is contained in the union of the circumcircles of $\triangle(a_1, a_2, a_3), \ldots, \triangle(a_1, a_k, a_2)$, i. e. the circumcircles that are centered at the Voronoi vertices of $VR_C(a_1, S)$.*

Proof. Let p be an arbitrary point in the Voronoi region $VR_C(a_1, S)$, i. e. p is in the interior or on the boundary of $VR_C(a_1, S)$. Then the ray $\overrightarrow{a_1\, p}$ intersects the boundary of $VR_C(a_1, S)$ in a point $q \in B_C^*(a_1, a_j)$ for $2 \leq j \leq k$. The line segment $\overline{a_1\, q}$ lies in the reflected unit circle centered at q passing through a_1 and a_j. If q is also a Voronoi

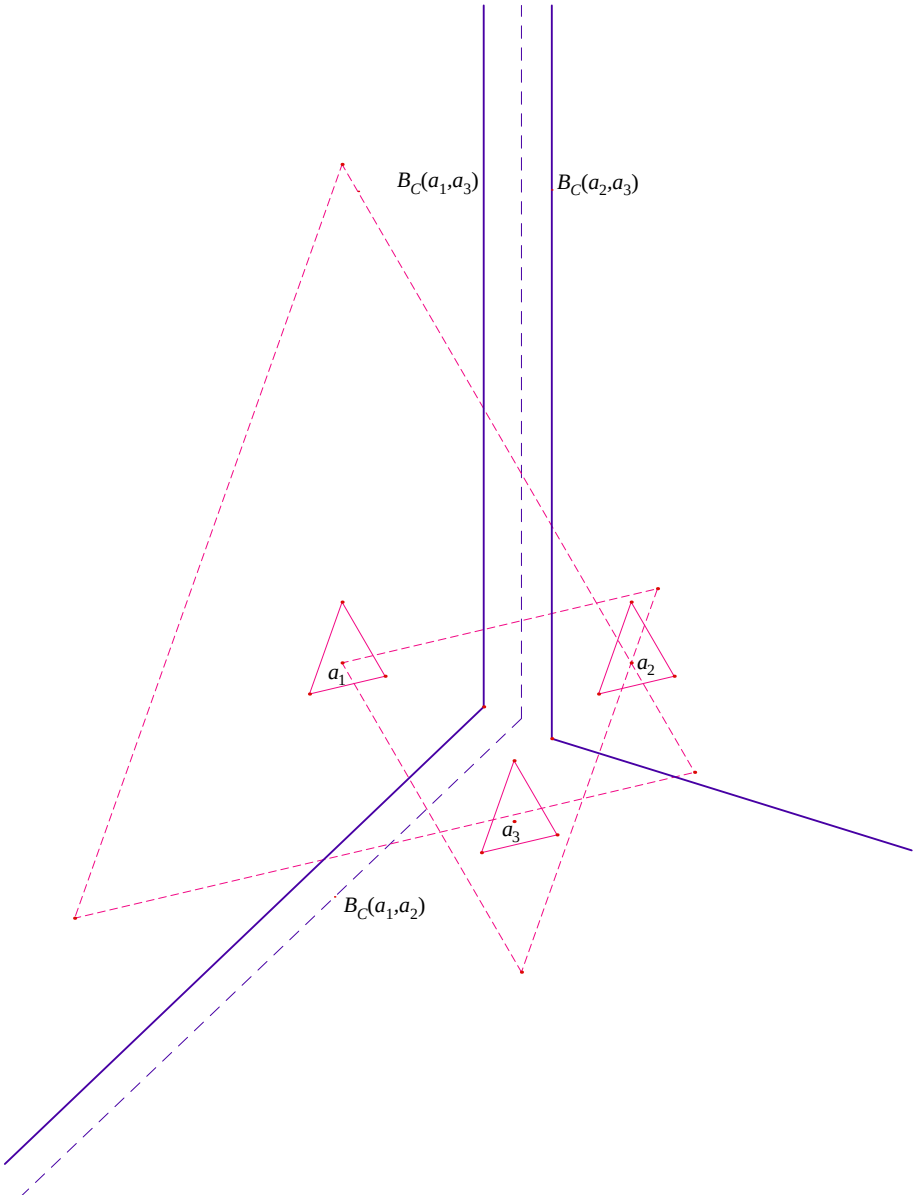

Figure 2.1.5.2: The site a_2 is the nearest neighbour of a_1 with respect to the triangular distance function, but the Voronoi regions of a_1 and a_2 are not adjacent, because a_3 is contained in $F_{12} \cap F_{21}$.

vertex then we have the claim. Otherwise there is a Voronoi vertex v on $B_C^*(a_1, a_j)$ such that q and v lie to the same side of $a_1\, a_j$. The reflected unit circle centered at v passing through a_1 and a_j contains $\overline{a_1\, a_j}$ and $\overline{a_1\, q}$. □

2.1.6 Moving the center of the unit circle

It is interesting to know how the structure of the Voronoi diagram of a set $S = \{a_1, \ldots, a_n\}$ changes, if the center of C is translated to another point in the interior

of C, or equivalently if C is translated by a vector t to C' which still contains the origin O in its interior, see Figure 2.1.6.1.

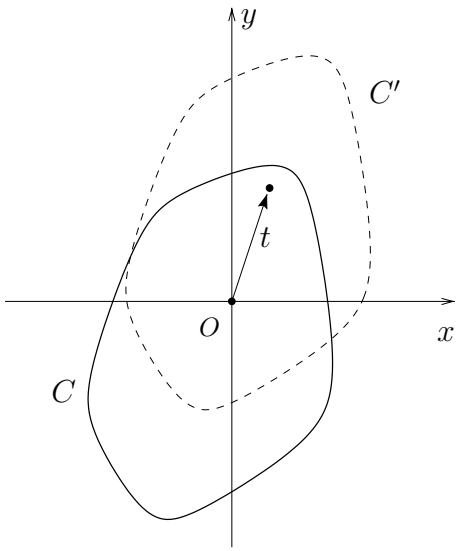

Figure 2.1.6.1: The convex set C and the translated set $C' = C + t$.

For a site $a_k \in S$ we consider the mapping $T_k : \mathbf{R}^2 \to \mathbf{R}^2$ defined by $p \mapsto p + d_C(a_k, p)t$. This is a "scaled translation", point p is translated in the direction of vector t, the Euclidean distance from p to $T_k(p)$ is proportional to the d_C-distance from a_k to p.

Lemma 2.1.6.1 *The mapping T_k is a homeomorphism, and $d_C(a_k, p) = d_{C'}(a_k, T_k(p))$ for all p.*

Proof. It is clear that T_k is a homeomorphism, and a_k is its only fix point.

For an arbitrary point $p \in \mathbf{R}^2$ the distance $d_C(a_k, p)$ equals $\frac{||p-a_k||}{||v-a_k||}$, where v is the foot point of p on ∂C_k, see Figure 2.1.6.2. Let $v' := v + t$ be the corresponding point on the boundary of $C'_k := C_k + t$ and let p' be the intersection of the ray from p in direction t and $\overrightarrow{a_k\, v'}$. The distance $d_{C'}(a_k, p')$ is $\frac{||p'-a_k||}{||v'-a_k||}$. The triangles $\triangle(a_k, v, v')$, $\triangle(a_k, p, p')$ are homothetic because the lines $v\, v'$ and $p\, p'$ are parallel to t, so $d_C(a_k, p) = d_{C'}(a_k, p') = \frac{||p'-p||}{||v'-v||}$, and $p' - p = d_C(a_k, p)t$, therefore $T_k(p) = p'$. □

It turns out that the bisectors of two sites based on C resp. C' are very closely related through this mapping.

Lemma 2.1.6.2 *The mapping T_1 (and also T_2) is homeomorphism from $B_C(a_1, a_2)$ to $B_{C'}(a_1, a_2)$.*

Proof. Let p be an arbitrary point of $B_C(a_1, a_2)$. Due to Lemma 2.1.6.1, $T_1(p) = p + d_C(a_1, p)t = p + d_C(a_2, p)t = T_2(p)$, and $d_{C'}(a_2, T_1(p)) = d_{C'}(a_2, T_2(p)) = d_C(a_2, p) = d_C(a_1, p) = d_{C'}(a_1, T_1(p))$. So $T_1(p)$ is a point in $B_{C'}(a_1, a_2)$. □

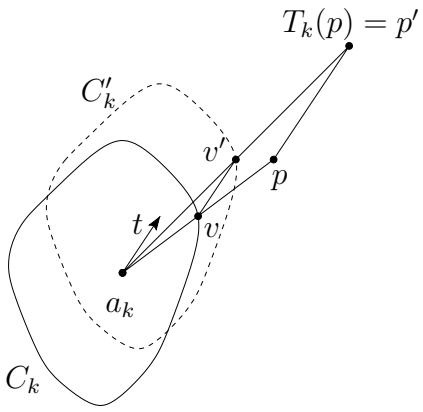

Figure 2.1.6.2: The relation of p and $T_k(p)$.

As a consequence, the structure of a Voronoi diagram based on a convex distance function does not change by moving the center of the convex body: for two sites a_i and a_j the regions $VR_C(a_i, S)$ and $VR_C(a_j, S)$ are adjacent in $V_C(S)$ if and only if $VR_{C'}(a_i, S)$ and $VR_{C'}(a_j, S)$ are adjacent in $V_{C'}(S)$, as is shown in the following theorem.

Theorem 2.1.6.3 *For a unit circle C and a translated circle $C' = C + t$ the two dual graphs $D_C(S)$ and $D_{C'}(S)$ are identical.*

Proof. Let $\overline{a_i\, a_j}$ be an edge in the dual graph $D_C(S)$. There is a point p of the Voronoi diagram $V_C(S)$ such that $p \in \partial\, VR_C(a_i, S) \cap \partial\, VR_C(a_j, S) \subset B^*_C(a_i, a_j)$. Due to Lemma 2.1.6.2, $T_i(p) = p + d_C(a_i, p)t$ is contained in $B^*_{C'}(a_i, a_j)$. We show that $T_i(p)$ is also on the boundaries of $VR_{C'}(a_i, S)$ and $VR_{C'}(a_j, S)$.

Let us consider a site a_k, $k \neq i, j$, and the three points p, $T_i(p)$, and $T_k(p)$. These three points are clearly collinear. Because of $d_C(a_k, p) \geq d_C(a_i, p) = d_C(a_j, p)$, we have

$$T_k(p) - T_i(p) = (d_C(a_k, p) - d_C(a_i, p))t\,,$$

and therefore the three points appear in the order p, $T_i(p)$, $T_k(p)$ on the line. Because of the monotonicity of T_k the inverse image of $T_i(p)$, namely $T_k^{-1}(T_i(p))$, which also lies on this line, appears in front of the other three points.

Now we obtain

$$\begin{aligned} p - T_k^{-1}(T_i(p)) &= p - (T_i(p) - d_{C'}(a_k, T_i(p))t) \\ &= p - (p + d_C(a_i, p)t - d_{C'}(a_k, T_i(p))t) \\ &= (d_{C'}(a_k, T_i(p)) - d_C(a_i, p))t \\ &= (d_{C'}(a_k, T_i(p)) - d_{C'}(a_i, T_i(p)))t\,, \end{aligned}$$

which shows that $d_{C'}(a_k, T_i(p)) \geq d_{C'}(a_i, T_i(p))$. So point $T_i(p)$ can not be contained in $VR_{C'}(a_k, S)$. □

2.2 Polygonal convex distance functions

The class of the polygonal convex distance functions is very important, since any convex set can be approximated with arbitrary ϵ-accuracy by a convex polygon, and each bisector based on a convex polygon has a polygonal shape itself and can be easily constructed, as we will see.

2.2.1 The bisector of two sites

Lemma 2.2.1.1 *If the line segment $\overline{a_1\, a_2}$ is not parallel to an edge of the k-gon C, then the bisector $B_C(a_1, a_2)$ is a polygonal chain completed with two rays at the ends. $B_C(a_1, a_2)$ possesses at most $k-2$ vertices.*

Proof. We assume that the line $a_1\, a_2$ is horizontal. Due to Lemma 2.1.1.1 the bisector $B_C(a_1, a_2)$ is homeomorphic to a line. It can be constructed in the following way. Because $a_1\, a_2$ is not parallel to an edge of C, the upper and lower outer common supporting lines of C_1 and C_2 intersect only vertices, t_{12} resp. t_{21}, and d_{12} resp. d_{21}, see Figure 2.2.1.1.

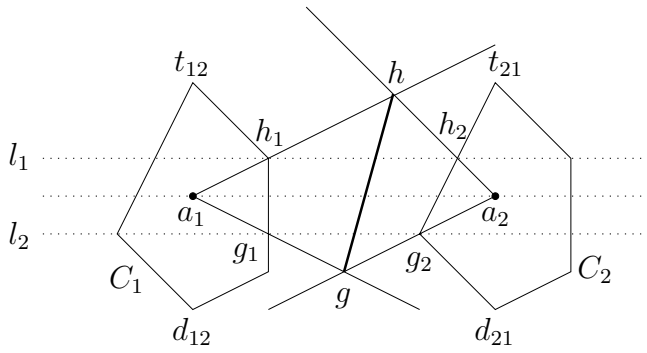

Figure 2.2.1.1: There is no vertex of C_1 and C_2 in the open strip between the lines $h_1\, h_2$ and $g_1\, g_2$.

Let l_i, $i = 1, 2$, be two horizontal lines which pass through at least one vertex of C_1 or C_2 such that in the interior of the strip between the lines l_1 and l_2 there is no other vertex of C_1 or C_2. Let l_1 intersect C_1 and C_2 at $h_1 \in H_{12} + a_1$ and $h_2 \in H_{21} + a_2$. Let l_2 intersect C_1 and C_2 at $g_1 \in H_{12} + a_1$ and $g_2 \in H_{21} + a_2$.

The intersection points h and g of $\overrightarrow{a_1\, h_1}$ and $\overrightarrow{a_2\, h_2}$ resp. $\overrightarrow{a_1\, g_1}$ and $\overrightarrow{a_2\, g_2}$ are in $B_C(a_1, a_2)$. Let u be the intersection point of the lines $h_1\, g_1$ and $h_2\, g_2$, then by Theorem 1.2.1 the points h, g and u are collinear (if $u = \infty$, then the line passing through g and h is parallel to the line $g_1\, h_1$). Let l be an arbitrary horizontal line that lies in the interior between l_1 and l_2, and that intersects $H_{12} + a_1$ and $H_{21} + a_2$ at f_1 resp. f_2. Using again Theorem 1.2.1 for the triangles $\triangle(a_1, h_1, f_1)$ and $\triangle(a_2, h_2, f_2)$, the intersection of $\overrightarrow{a_1\, f_1}$ and $\overrightarrow{a_2\, f_2}$, which is a point in $B_C(a_1, a_2)$, has to lie on the line

segment $\overline{h\,g}$. Therefore the line segment $\overline{h\,g}$ is a part of the bisector $B_C(a_1, a_2)$. We say that $\overline{h\,g}$ is *constructed* by the two edges containing $\overline{g_1\,h_1}$ resp. $\overline{g_2\,h_2}$.

Correspondingly, the bisector $B_C(a_1, a_2)$ has two rays at its ends. If $h_1 = t_{12}$ then one of the ending rays of $B_C(a_1, a_2)$ is parallel to the line passing through a_1 and t_{12}. If $g_1 = d_{12}$ then the other ending ray is parallel to the line passing through a_1 and d_{12}. Hence the bisector is a polygonal chain.

Each vertex of C contributes only one vertex to $B_C(a_1, a_2)$, and each vertex of $B_C(a_1, a_2)$ is constructed by at least one vertex of C. If a horizontal line passes through two vertices of C then the two vertices construct the same vertex of $B_C(a_1, a_2)$. Hence $B_C(a_1, a_2)$ contains at most $k-2$ vertices, since the points t_{12} and d_{12} do not contribute vertices to $B_C(a_1, a_2)$. □

2.2.2 Computing bisectors of two sites

Due to Lemma 2.2.1.1 and Corollary 2.1.1.2, we can compute the bisector of two sites a_1 and a_2 based on a convex polygon C using the plane-sweep technique. We assume that the k vertices of C are stored in cyclic order, the line $a_1\,a_2$ is horizontal, and the site a_1 is left to a_2. In practice, this can be achieved by an appropriate rotation of the coordinate system.

Let U and L be the upper resp. lower horizontal supporting line of C. We sweep a horizontal line SL from U to L, and we stop at every vertex of C.

We start SL at U. If U contains an edge $e = \overline{t_2\,t_1}$ of C then the cone bounded by the rays $\overrightarrow{a_1\,(t_1 + a_1)}$ and $\overrightarrow{a_2\,(t_2 + a_2)}$ is contained in the bisector $B_C(a_1, a_2)$, see Figure 2.2.2.1. In the non-degenerate case the bisector starts with a ray which is parallel to $\overrightarrow{O\,t_1}$ and emanates at the first bisector vertex which will be computed next.

Let u_1 and u_2 always be the actual intersection points of SL with the boundary of C such that $u_1 \in H_{12}$ and $u_2 \in H_{21}$, in the degenerate case we set $u_1 := t_1$ and $u_2 := t_2$. Vertices v_1 and v_2 are always the next clockwise resp. counterclockwise vertices behind u_1 resp. u_2.

The main loop proceeds in the following steps. The sweep-line advances to the closer of v_1 and v_2. The next vertex of the bisector is normally the intersection of the rays $\overrightarrow{a_1\,(u_1 + a_1)}$ and $\overrightarrow{a_2\,(u_2 + a_2)}$. In the special case that $\overrightarrow{a_1\,(u_1 + a_1)}$ and $\overrightarrow{a_2\,(u_2 + a_2)}$ are parallel to $a_1\,a_2$, we first compute the intersection s of the supporting lines of the actual edges of C_1 and C_2. Then the intersection of $a_1\,a_2$ and the line through s and the previous bisector vertex is the new bisector vertex.

We repeat this process until SL reaches the line L and the last piece of $B_C(a_1, a_2)$ is constructed.

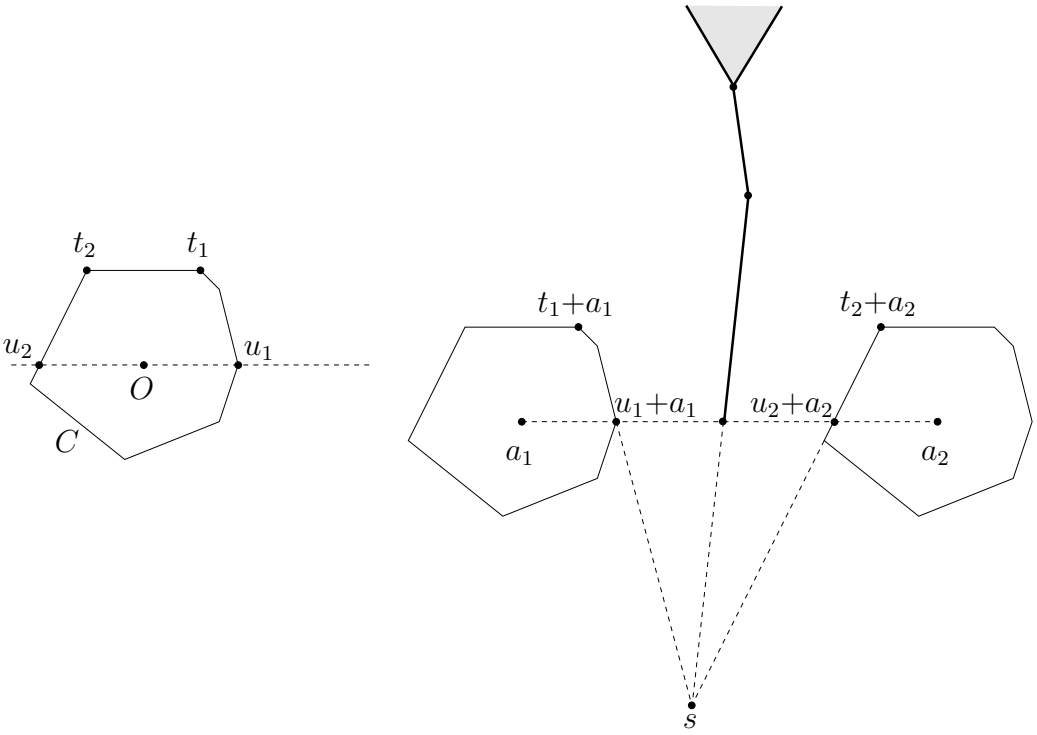

Figure 2.2.2.1: Computing the bisector $B_C(a_1, a_2)$.

Lemma 2.2.2.1 *The bisector of two sites based on a convex k-gon C can be constructed in optimal $O(k)$ time.*

Proof. Each bisector vertex of $B_C(a_1, a_2)$ can be constructed in constant time, so the sweep from U to L runs in $O(k)$ time. This is optimal because each vertex of ∂C contributes a vertex to $B_C(a_1, a_2)$. □

2.2.3 The bisector of three sites

For the sites a_1 and a_2 let $F_{12} \cap F_{21}$, see Definition 2.1.2.11, be bounded by the line segments $\overline{a_1\, u}$, $\overline{a_1\, v}$, $\overline{a_2\, u}$, and $\overline{a_2\, v}$, see Figure 2.2.3.1. So the sets G_{12} and G_{21} are bounded by the rays opposite to $\overrightarrow{a_1\, u}$ and $\overrightarrow{a_1\, v}$, resp. $\overrightarrow{a_2\, u}$ and $\overrightarrow{a_2\, v}$. The unit circle, C, is a convex polygon, so the interiors of $F_{12} \cap F_{21}$ and $G_{12} \cup G_{21}$ are empty iff the line $a_1\, a_2$ is parallel to two line segments of ∂C, and the set $F_{12} \cap F_{21}$ is a triangle iff the $a_1\, a_2$ is parallel to one line segment of ∂C.

For deciding about the existence of $B_C(a_1, a_2, a_3)$ we have Lemma 2.1.2.13 for arbitrary unit circles. Applied to polygonal unit circles we obtain the following, remember that FG_{12} is an abbreviaty for $G_{12} \cup (F_{12} \cap F_{21}) \cup G_{21}$.

Lemma 2.2.3.1 *We consider three sites a_1, a_2, a_3, and their bisector with respect to a convex polygonal unit circle C.*

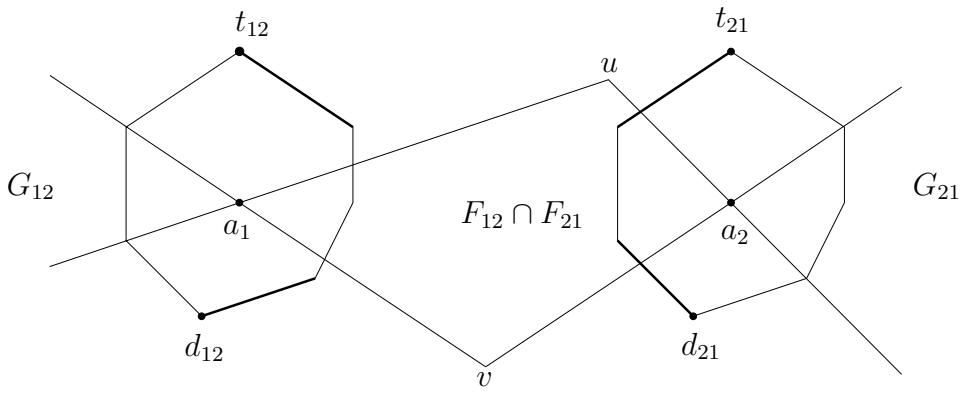

Figure 2.2.3.1: The set $F_{12} \cap F_{21}$ is bounded by the line segments $\overline{a_1\, u}$, $\overline{a_1\, v}$, $\overline{a_2\, u}$, and $\overline{a_2\, v}$.

Case 1. *If a_3 lies in the interior of FG_{12} then $B_C(a_1, a_2, a_3)$ is empty.*

Case 2. *If a_3 lies in the complement of FG_{12} then $B_C(a_1, a_2, a_3)$ consists of exactly one point.*

Case 3. *Otherwise, a_3 lies on the boundary of FG_{12}. If a_1, a_2, a_3 are not collinear then $B_C(a_1, a_2, a_3)$ is a polygonal chain completed with one ray at the end, else $B_C(a_1, a_2, a_3)$ consists of one or two cones.*

Proof. Due to Lemma 2.1.2.13, we only need to prove Case 3. We assume that site a_3 lies on the boundary of FG_{12}.

If a_1, a_2, and a_3 are collinear then the line $a_1\, a_2$ is parallel to one or two line segments of ∂C, therefore the bisectors $B_C(a_1, a_2)$ and $B_C(a_2, a_3)$ contain one or two cones, see Figure 2.1.1.2, and also their intersection consists of one or two cones.

If a_1, a_2, and a_3 are not collinear then the interior of FG_{12} is not empty. Let p be an arbitrary point of $B_C(a_1, a_2)$ whose foot point on ∂C_1 lies on the line segment $e = \overline{d_{12}\, d'}$.

In the case that a_3 lies on the line segment $\overline{a_1\, u}$ as shown in Figure 2.2.3.2, the reflected unit circle passing through a_1 and a_2 centered at p intersects the site a_3, i, e. p is a point of $B_C(a_1, a_2, a_3)$. Thus, $B_C(a_1, a_2, a_3)$ which is the intersection of $B_C(a_1, a_2)$ and $B_C(a_1, a_3)$ is the part of $B_C(a_1, a_2)$ which is contained in the cone of $B_C(a_1, a_3)$. The case $a_3 \in \partial G_{12}$ is similar. □

2.2.4 Computing the bisector of three sites

For an arbitrary convex k-gon C and three sites a_1, a_2, a_3 we can first determine the three sets $F_{12} \cap F_{21}$, G_{12}, and G_{21}, then test the existence of $B_C(a_1, a_2, a_3)$ using Lemma 2.2.3.1. If $B_C(a_1, a_2, a_3)$ exists then we construct the three sets H_{123}, H_{213},

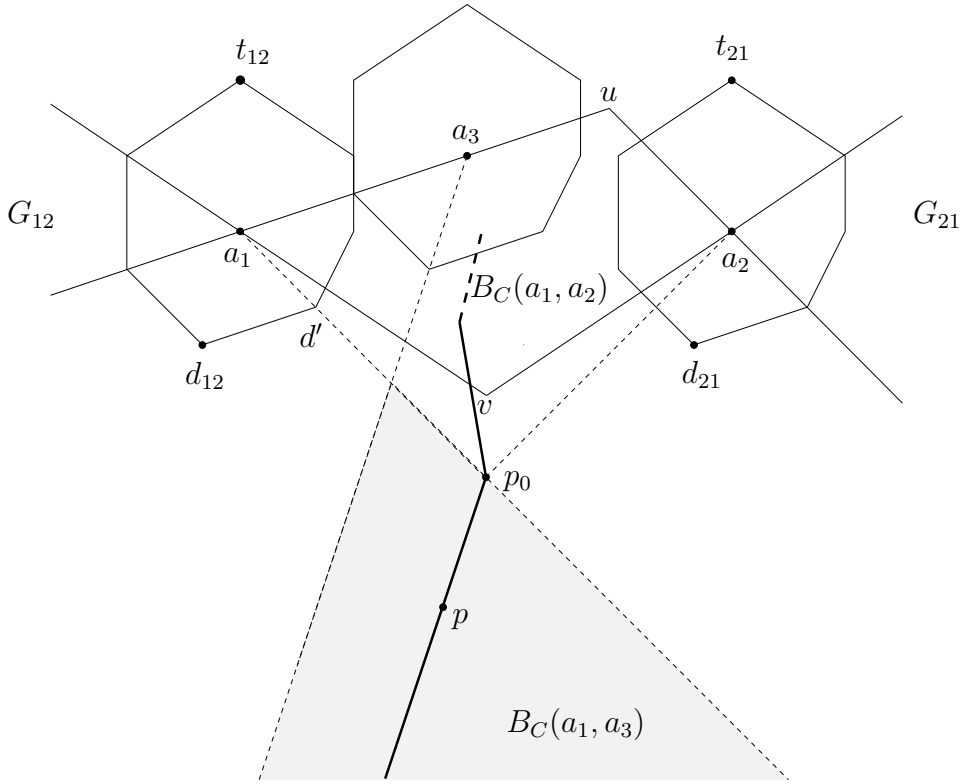

Figure 2.2.3.2: The bisector $B_C(a_1, a_2, a_3)$ is the part of $B_C(a_1, a_2)$ which is contained in the cone of $B_C(a_1, a_3)$.

and H_{312} on ∂C where the vertices of C are stored in an array in cyclical order. All these constructions cost only $O(\log k)$ time because the determination of H_{123} and F_{12} etc. is equivalent to determining the common supporting lines parallel to $a_1\,a_2$, $a_1\,a_3$, and $a_2\,a_3$. This can be achieved by a simple binary search in $O(\log k)$, it is not necessary to use the more general and more complicated technique for common tangents described by Kirkpatrick and Snoeyink [45].

Now we can apply Lemma 2.1.2.8 and obtain the following result.

Lemma 2.2.4.1 *The bisector $B_C(a_1, a_2, a_3)$ based on a convex k-gon C can be computed in $O(\log k + m)$ time, where m is the number of vertices of $B_C(a_1, a_2, a_3)$.*

Proof. The construction of the set FG_{12} costs time $O(\log k)$, as discussed above, or only constant time if the common tangent of C_1 and C_2 are already known. The test of the position of a_3 with respect to FG_{12}, for applying Lemma 2.2.3.1, costs only constant time.

If we have Case 1 of Lemma 2.2.3.1 then $B_C(a_1, a_2, a_3) = \emptyset$.

In Case 2, a_3 lies in the complement of FG_{12}, and we use the search procedure described in the proof of Lemma 2.1.2.8 to construct the point $B_C(a_1, a_2, a_3)$. In the search procedure we choose point a as the middle vertex of H_{213}, find the point

$a' \in H_{123}$, and test whether the point q lies inside or outside the unit circle, see Figure 2.1.2.6.

If we use binary search to find a' and test q then each step can be implemented in $O(\log k)$ time, this means that the bisector point can be found in $O(\log^2 k)$ time. But if we first reduce two of the intervals H_{123}, H_{213} or H_{312} to two single line segments, respectively, in $O(\log k)$ time then we start the search procedure to construct $B_C(a_1, a_2, a_3)$, so $B_C(a_1, a_2, a_3)$ can be found in $O(\log k)$ time. This task for reducing H_{123}, H_{213} or H_{312} was proposed by Kirkpatrick and Snoeyink using a tentative prune-and-search technique, see [44, 46].

In Case 3, if a_1, a_2, and a_3 are collinear then we can construct the one or two cones of $B_C(a_1, a_2, a_3)$ in constant time. In the case that a_3 lies on the boundary of FG_{12}, see Figure 2.2.3.2 we first construct the starting point p_0 of $B_C(a_1, a_2, a_3)$ and then compute the remaining bisector chain in linear time. Due to Lemma 2.2.3.1, the foot point of p_0 on $H_{123} + a_1$ or $H_{312} + a_3$ is a vertex. To find p_0 is equivalent to find the homothetic triangle $\triangle(v_1, v_2, v_3)$ such that v_1 or v_3 is a vertex on ∂C, in particular, the points v_1 and v_3 lie on the same line segment of ∂C. Therefore we start the search procedure at point v_1 or v_3 using binary search to test the position of q defined in the proof of Lemma 2.1.2.8, so p_0 can be found in $O(\log k)$ time. □

2.2.5 The chosen bisector of three sites

As explained in Section 2.1.4, it is useful and common practice to avoid the 2-dimensional bisector parts in the Voronoi diagram, which occur in degenerate cases, by introducing the convention of the chosen bisector. For this purpose we have to adapt the notions for the sets of foot points, too, see Definition 2.1.1.3.

For two sites a_1 and a_2 let H^*_{12} and H^*_{21} be the sets of the foot points of the chosen bisector $B^*_C(a_1, a_2)$ on ∂C_1 resp. ∂C_2, translated back to ∂C. It is clear that H_{12} and H^*_{12} etc. can only differ. Let t^*_{12} denote the upper and d^*_{12} the lower end points of $H^*_{12} + a_1$. In the degenerate case when $a_1\, a_2$ is parallel to an edge of ∂C, if $a_1 \prec a_2$ then the set H^*_{21} is equal to H_{21} but H^*_{12} is H_{12} without the open edge $\overline{(t_{12} - a_1)\,(t^*_{12} - a_1)}$, see Figure 2.2.5.1.

Therefore the sets H^*_{12} and H^*_{21} are always disjoint and partition the boundary of C, even in the degenerate case.

Analogously to Definition 2.1.2.10 for T_{12} and D_{12}, we also define the least steep and the steepest tangents T^*_{12} and D^*_{12} to C_1 at the two boundary points t^*_{12} and d^*_{12} of H^*_{12}, respectively. In particular, T^*_{12} and D^*_{12} are parallel to the two edges of H^*_{12} that are adjacent to t^*_{12} resp. d^*_{12}, see Figure 2.2.5.1. Analogously we have the other two tangents T^*_{21} and D^*_{21} to C_2 at the two boundary points t^*_{21} and d^*_{21} of H^*_{21}, respectively. Also the sets F_{12} and G_{12} etc. need to be adapted to the degenerate

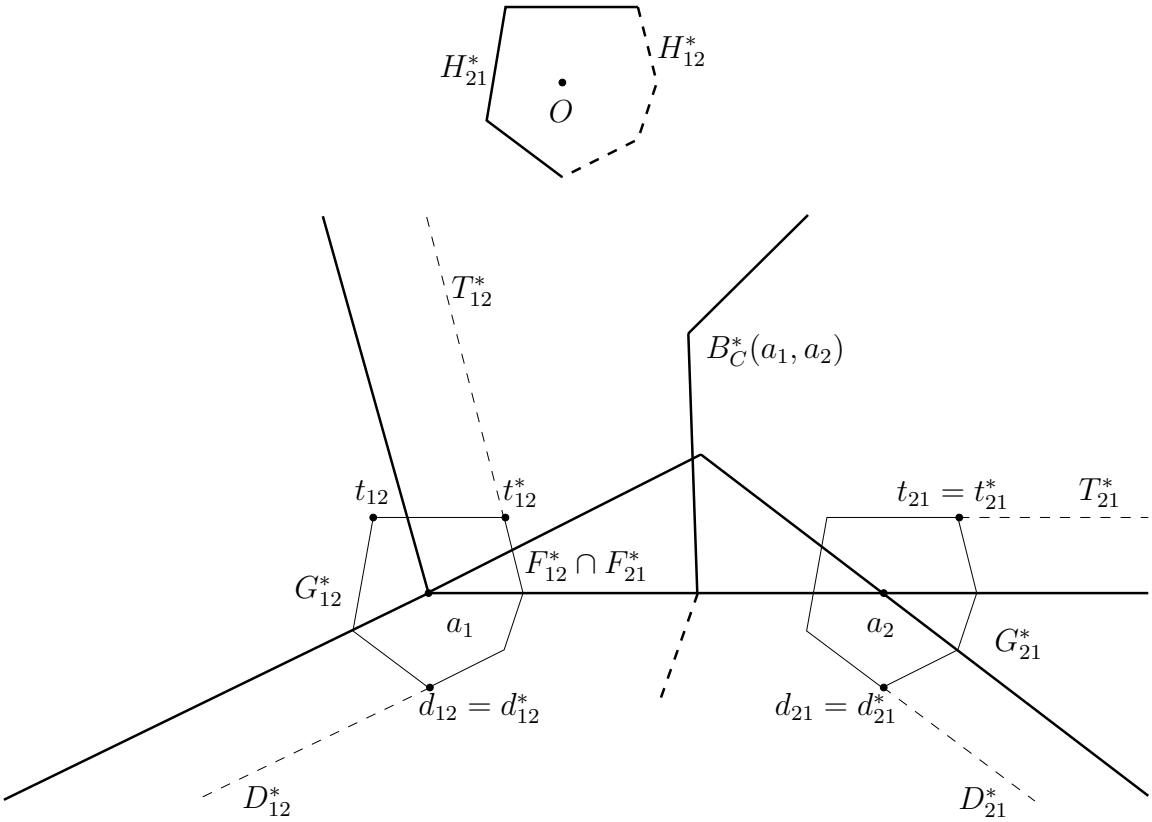

Figure 2.2.5.1: The sets H^*_{21} and H^*_{12} in the degenerate case, $H^*_{12} + a_1$ goes clockwise from t^*_{12} to $d_{12} = d^*_{12}$.

case.

Definition 2.2.5.1 We consider the four cones with apex a_1 defined by the lines through a_1 parallel to T^*_{12} resp. D^*_{12}. Let F^*_{12} denote the cone bounded by the line parallel to D^*_{12} from above and by the line parallel to T^*_{12} from below, and let G^*_{12} be the opposite cone. Analogously we have F^*_{21} and G^*_{21} with apex a_2, see Figure 2.2.5.1.

For $a_1 \prec a_2$, the interiors of F^*_{12} and G^*_{12} are never empty because the two tangents T^*_{12} and D^*_{12} can not be parallel to the line $a_1\, a_2$. The interiors of F^*_{21} and G^*_{21} are empty iff the line $a_1\, a_2$ is parallel to two line segments of ∂C, see Figure 2.2.5.2.

Unfortunately, Lemma 2.1.2.13 does not remain true if we take the chosen bisector instead of the bisector in the special case that a_3 lies on the boundaries of G^*_{12}, G^*_{21}, or $F^*_{12} \cap F^*_{21}$. But we have at least the following results, depending on whether a_3 lies inside or outside or on the boundary of these regions, compare Lemma 2.1.2.12. Let $FG^*_{12} = G^*_{12} \cup (F^*_{12} \cap F^*_{21}) \cup G^*_{21}$.

Lemma 2.2.5.2 *The interior of $F^*_{12} \cap F^*_{21}$ consists of all points that are contained in the interior of each reflected unit circle of C passing through a_1 and a_2. The interior of $G^*_{12} \cup G^*_{21}$ consists of the points that do not lie in any such reflected unit circle.*

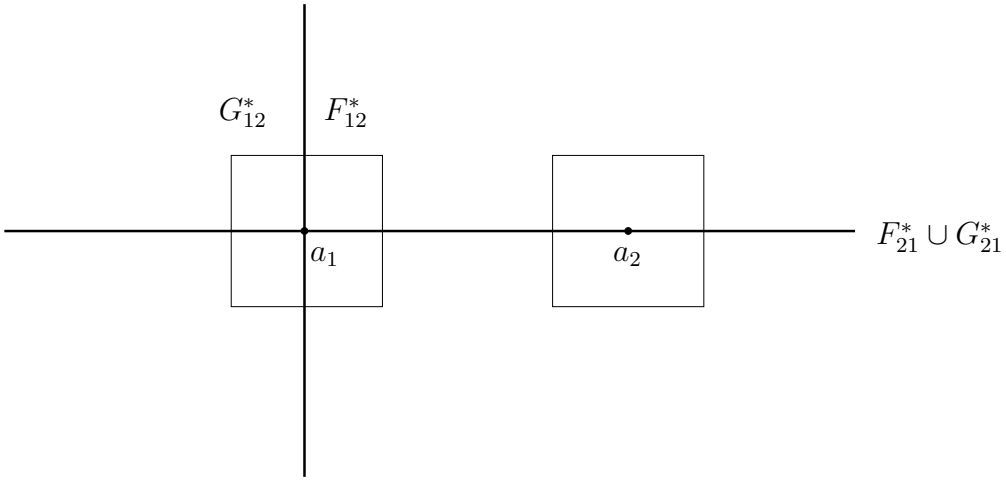

Figure 2.2.5.2: The line $a_1\,a_2$ is parallel to two line segments of ∂C. The sets F_{12}^* and G_{12}^* are two half planes, and F_{21}^* and G_{21}^* together are just the line $a_1\,a_2$.

Proof. Analogously to Lemma 2.1.2.12, in the case that C is a convex polygon each reflected unit circle of C passing through a_1 and a_2 also includes $F_{12}^* \cap F_{21}^*$ in its interior and do not contain any points of $G_{12}^* \cup G_{21}^*$. In particular, if the center points of reflected unit circles lie on the ending rays of $B_C^*(a_1, a_2)$ then such unit circles also contain the boundary of FG_{12}^*.

For the special case that the line $a_1\,a_2$ is parallel to a line segment of ∂C, see Figure 2.2.5.1, the ray from the intersection point of $\overrightarrow{a_1\,t_{12}^*}$ and $\overrightarrow{a_2\,(t_{12}+a_2-a_1)}$ parallel to $\overrightarrow{O\,t_{12}^*}$ is the ending part of $B_C^*(a_1, a_2)$ above $a_1\,a_2$. The site a_1 is always a vertex of each reflected unit circle of C centered at a point of this ray passing through a_1 and a_2. □

As a consequence of Lemma 2.2.5.2 for $a_3 \in FG_{12}^*$ the chosen bisector $B_C^*(a_1, a_2, a_3)$ is empty.

Corollary 2.2.5.3 *If a_3 lies in the interior of FG_{12}^* then the chosen bisector $B_C^*(a_1, a_2, a_3)$ is empty.*

Proof. If a_3 lies in the interior of FG_{12}^* then there is not any reflected unit circle passing through a_1, a_2, and a_3, due to Lemma 2.2.5.2. □

Corollary 2.2.5.4 *Let a_3 be in the interior of the complement of FG_{12}^*. The chosen bisector $B_C^*(a_1, a_2, a_3)$ consists of a single point.*

Proof. Due to Lemma 2.2.5.2, there is at least one reflected unit circle centered at a point of $B_C^*(a_1, a_2)$ that includes the site a_3. Therefore the chosen bisector $B_C^*(a_1, a_2, a_3)$ is not empty. By Lemma 2.1.4.3 and Definition 2.1.4.4 $B_C^*(a_1, a_2, a_3)$ consists of one point. □

The case that a_3 lies on the boundary of FG^*_{12} is the most complicated. Figure 2.2.5.3 shows that $B^*_C(a_1, a_2, a_3)$ may consist of a point or can be empty. We give a criterion for the existence of $B^*_C(a_1, a_2, a_3)$.

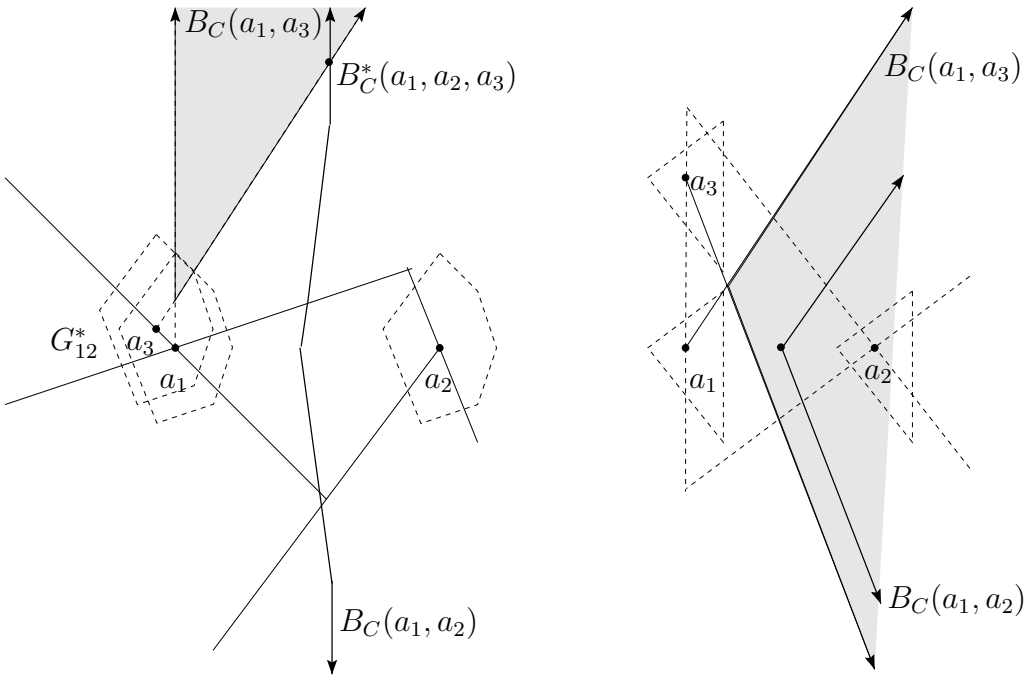

Figure 2.2.5.3: In the picture on the left $B^*_C(a_1, a_2, a_3)$ consists of a point, on the right side $B^*_C(a_1, a_2, a_3) = \emptyset$.

Lemma 2.2.5.5 *Let $a_1 \prec a_2$, and let $F^*_{12} \cap F^*_{21}$ be bounded by the line segments $\overline{a_1\, u}$, $\overline{a_1\, v}$, $\overline{a_2\, u}$, and $\overline{a_2\, v}$, see Figure 2.2.5.4. We consider the special cases concerning the position of a_3.*

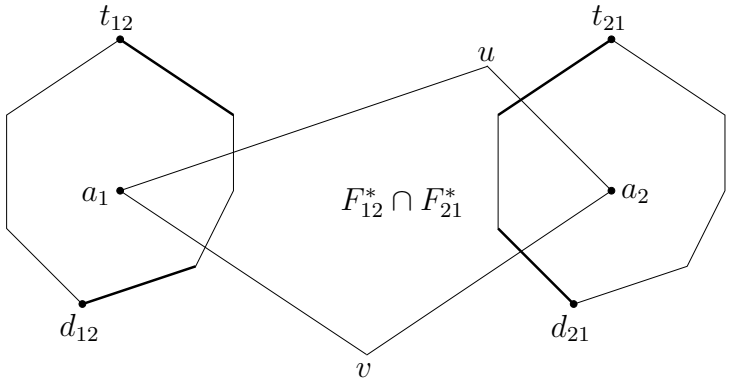

Figure 2.2.5.4: $\overline{a_1\, u}$, $\overline{a_1\, v}$, $\overline{a_2\, u}$, and $\overline{a_2\, v}$ bound the set $F^*_{12} \cap F^*_{21}$.

Case 1. *Site a_3 lies on $\overline{a_1\, u}$ or $\overline{a_1\, v}$.*

If ($a_1 \prec a_3$ and a_1, u, v are not collinear) or ($a_3 \prec a_1$ and $a_3 \in \{u, v\}$) then $B^*_C(a_1, a_2, a_3)$ is a point, otherwise $B^*_C(a_1, a_2, a_3)$ is empty.

Case 2. $a_3 \in \partial G^*_{12}$.

If $(a_3 \prec a_1)$ *or* $(a_1 \prec a_3$ *and* $a_1\,a_2$ *and* $a_1\,a_3$ *are parallel to two adjacent edges of* $\partial C)$ *then* $B^*_C(a_1, a_2, a_3)$ *is a point, otherwise* $B^*_C(a_1, a_2, a_3)$ *is empty.*

Proof. We assume that $a_1\,a_2$ is horizontal.

Let a_3 be on the line segment $\overline{a_1\,u}$. So the bisector $B_C(a_1, a_3)$ contains a two-dimensional cone. If $p \in B^*_C(a_1, a_2, a_3)$ then p must lie on the boundary of the cone of $B_C(a_1, a_3)$. Therefore a_1 or a_3 is a vertex of the reflected unit circle centered at p passing through a_1, a_2, and a_3 depending on whether $a_1 \prec a_3$ or $a_3 \prec a_1$.

Case 1.1. Suppose $a_3 = u$. In this case the lines $a_1\,a_3$ and $a_2\,a_3$ are parallel to two adjacent edges of ∂C. Due to Lemma 2.1.4.3, if $B^*_C(a_1, a_3)$ and $B^*_C(a_2, a_3)$ intersect in a ray if $a_3 \prec a_1$. Therefore $B^*_C(a_1, a_2, a_3)$ is a point if $a_3 \prec a_1$.

Case 1.2. Suppose that a_1, u, and v are collinear, H^*_{12} contains only one edge, see Figure 2.2.5.5. If $a_3 \notin \{u, v\}$ then the sites a_1 and a_3 can not be vertices of any reflected unit circle centered at a point $p \in B^*_C(a_1, a_2)$ through a_1, a_2, a_3. Therefore $B^*_C(a_1, a_2, a_3) = \emptyset$.

In the case $a_3 \in \{u, v\}$ and $a_1 \prec a_3$ the chosen bisector $B^*_C(a_1, a_2, a_3)$ is empty because $B^*_C(a_1, a_2)$ can not intersect the ray from a_1 through the top point t_{12} on ∂C_1.

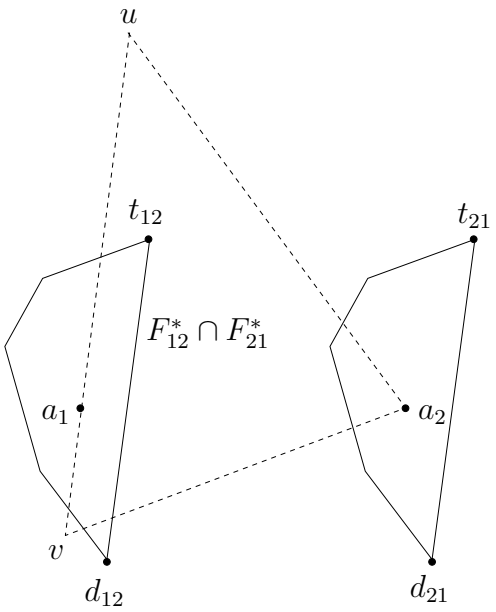

Figure 2.2.5.5: a_1, u, and v are collinear, $H^*_{12} + a_1$ is the open line segment $\overline{t_{12}\,d_{12}}$.

Case 1.3. Suppose that a_1, u, v are not collinear, and a_3 lies on the line segment $\overline{a_1\,u}$. Therefore H^*_{12} contains at least the first and last edges of H^*_{12} parallel to $\overline{a_1\,u}$ resp. $\overline{a_1\,v}$. So the sites a_1, a_2, and a_3 are not collinear. Due to Lemma 2.2.3.1, $B_(a_1, a_2, a_3)$ is a polygonal chain, its starting point is the is in $B^*_C(a_1, a_2, a_3)$ if $a_1 \prec a_3$. If $a_3 \notin \{u, v\}$ and $a_3 \prec a_1$ then the site a_3 can not be a vertex of any reflection centered at a point on $B^*_C(a_1, a_2)$ passing through a_1, a_2, and a_3.

For Case 2 let $a_3 \in \partial G^*_{12}$, and assume that a_3 lies above $a_1\,a_2$. So the line $a_1\,a_3$ is parallel to the first edge of H^*_{21} from above. If $a_1\,a_2$ is parallel to the edge of C adjacent to the edge parallel to $a_1\,a_3$ then due to Lemma 2.1.4.3 $B^*_C(a_1, a_2)$ and $B^*_C(a_1, a_3)$ intersect in a ray if and only if $a_1 \prec a_3$. In this case $B^*_C(a_1, a_2, a_3)$ is their first intersection point. Due to Lemma 2.2.3.1, the starting point of $B_C(a_1, a_2, a_3)$ is in $B^*_C(a_1, a_2, a_3)$ if $a_3 \prec a_1$. □

If a_3 lies on the line segments $\overline{a_2\,u}$, or $\overline{a_2\,v}$, or on ∂G^*_{21} then we can exchange a_1 and a_2 in Lemma 2.2.5.5 to obtain analogous results.

As a consequence of Lemma 2.2.4.1 the chosen bisector $B^*_C(a_1, a_2, a_3)$ can be computed in logarithmic time.

Corollary 2.2.5.6 *For three sites a_1, a_2, and a_3 the chosen bisector $B^*_C(a_1, a_2, a_3)$ based on a convex k-gon can be found in $O(\log k)$ time.*

2.2.6 Computing Voronoi diagrams

The Voronoi diagram based on any convex distance function of a set S containing n sites in the plane is a planar graph with n regions, and each Voronoi vertex has degree ≥ 3, therefore there are $O(n)$ Voronoi vertices by *Euler's formula* [23, Section 7.1]. In the case that the unit circle is a convex polygon consisting of k edges, we count both, Voronoi vertices and other endpoints of line segments in the Voronoi diagram. We have the following result.

Lemma 2.2.6.1 *The Voronoi diagram of a set S containing n sites based on a convex k-gon contains exactly n regions and $\Theta(kn)$ line segments and rays and $\Theta(kn)$ vertices.*

Proof. There are exactly n Voronoi regions by Lemma 2.1.4.7. The bisector of two sites consists of at most $k-2$ vertices by Lemma 2.2.1.1. The upper bound follows because there are only $O(n)$ Voronoi vertices and $O(n)$ Voronoi edges, each Voronoi edge consists of at most $k-2$ line segments and rays. The bound is tight, which can be seen from an example like Figure 2.1.4.1 with collinear (or nearly collinear) sites. □

A couple of different approaches to compute the Voronoi diagram are known from the literature.

A well-known technique to compute the Voronoi diagram of n sites uses the *divide-and-conquer* paradigm. The first divide-and-conquer algorithm for computing the Voronoi diagram based on the Euclidean metric was developed by Shamos and Hoey [76] which was later improved by Lee [61].

The first step of the algorithm is to sort the points lexicographically. Then split the points into a left set L and a right set R, each containing about half of the points. Recursively compute the Voronoi diagrams $V(L)$ and $V(R)$. Finally, merge the two Voronoi diagrams into a single diagram $V(S)$. The merge step can be done in linear time and the entire algorithm takes $O(n \log n)$ time, which is optimal, since finding the closest pair for a set of n points already requires $\Omega(n \log n)$, see [4, 75].

Also for arbitrary convex functions one can also use the divide-and-conquer technique to compute the Voronoi diagram. Lee and Wong [61, 63] give a divide-and-conquer algorithm to compute the Voronoi diagram based on the L_p-metric for $1 \leq p \leq \infty$. Widmayer, Wu, and Wong present also a divide-and-conquer algorithm for computing the Voronoi diagram in a metric where shortest paths are constructed from straight line segments constrained to a fixed set of orientations [80], this is in fact nothing else but a Voronoi diagram for a symmetric, polygonal convex distance function. Chew and Drysdale [17] have found out that the three papers are incomplete. The papers [61, 63] ignore some difficulties that can occur during the construction of the Voronoi diagram. The third paper [80] makes reference to the problems, but gives an incomplete description of how to handle them. Chew and Drysdale give an algorithm to compute the Voronoi diagram based on an arbitrary convex distance function using the divide-and-conquer technique. Their algorithm can overcome the difficulties of the other papers. The step that causes most difficulties is to find the bisector of the sets L and R. Chew and Drysdale have shown that one can find all pieces of the bisector of L and R in linear time using a clockwise-counterclockwise scan procedure. Therefore the Voronoi diagram based on a convex distance function for n sites can be found in $\Theta(n \log n)$ time, assumed that intersection of two bisectors can be found in constant time. Especially, the Voronoi diagram based on a convex polygon with k vertices for n sites can be found in $O(kn \log n)$ time and $O(kn)$ space. But how to deal with the degenerate case is not mentioned in their paper.

A second paradigm for computing the Voronoi diagram is the *sweep-line* technique, see Fortune [31], Dehne and Klein [24], and Klein [50]. In this way the Voronoi diagram of n sites in the plane based on the Euclidean metric can be computed in optimal time $\Theta(n \log n)$, too. The method can be generalized to handle arbitrary convex distance functions. Shute et al. [78] have given an optimal $O(n \log n)$ plane-sweep algorithm to compute a Delaunay triangulation under the L_1 metric or L_∞ metric. Dehne and Klein [24] have presented the first deterministic algorithm for computing the Voronoi diagram of n sites for an arbitrary nice metric in the plane within time $O(n \log n)$.

A third method is to compute a *convex hull* [13] or a *lower envelope* [28] in three dimensions. If n unit circles centered at the n sites expand simultaneously, the places where the so-called wave fronts meet define the Voronoi diagram. If we lift the wave

fronts centered at a site a_i into the third dimension then we have the cone with apex a_i, its equation is $Z = d_C(X, a_i)$ for $X \in \mathbf{R}^2$. The vertical projection of the intersection of two such cones is exactly the bisector of the two sites. The vertical projection of the lower envelope of the n cones is exactly the Voronoi diagram of the n sites. For the special Euclidean case one can also use the algorithm for computing the convex hull in three dimensions: we lift all sites to one paraboloid whose axis of symmetry is the Z-axis, then we compute the convex hull of these points in space. The edges of the lower convex hull, projected back to the XY-plane, are the edges of the Delaunay triangulation from which it is easy to obtain the Voronoi diagram of the sites. The running time is also optimal [4] because there are $O(n \log n)$ time algorithms for computing the three-dimensional convex hull [70].

A fourth method uses the *randomized incremental construction* technique. The Voronoi diagram $V(S)$ of a set S is constructed by inserting the sites one by one, updating the solution after each insertion. The algorithm uses a conflict graph to detect the conflicts between the current site and the regions created previously, see Boissonnat and Yvinec [11]. Because of the simple structure of the Delaunay triangulation in the Euclidean case it is easier to incrementally construct the triangulation using the edge flipping technique of Lawson [55] described in [4] than to directly compute the Voronoi diagram. The Delaunay triangulation of n sites in the plane can be constructed in expected time $O(n \log n)$. The average is taken over the $n!$ different order of inserting the n sites.

A variant of this is an incremental algorithm that works *on-line*, i. e. it constructs the Voronoi diagram $V_C(\{a_1, \ldots, a_i\})$ from $V_C(\{a_1, \ldots, a_{i-1}\}$ without knowing the sites $a_{i+1}, \ldots, a_n$. Boissonnat and Teillaud [8, 9] have first introduced the influence graph, also called Delaunay tree in their papers, to compute on-line the Delaunay triangulation. The influence graph stores the history of the regions created by the algorithm during the incremental construction, and it can be used to detect the conflicts between these regions and the new object. The Voronoi diagram of n sites can be constructed in expected time $O(n \log n)$. The method was later used to solve many other problems.

2.2.7 A simple implementation of an interactive Voronoi applet

For demonstration and experimentation purposes we have developed an interactive program for computing and displaying Voronoi diagrams based on arbitrary convex polygons. The user can define a polygonal convex distance function, as well as insert, delete, and move sites with simple mouse click and drag operations. To make the program excutable on nearly any computer and to make it available through the

World Wide Web the implementation has been carried out in Java.

The resulting applet can be found and tried out on any Java-capable WWW browser at `http://wwwpi6.fernuni-hagen.de/Geometrie-Labor/apps/convex/` in the Internet.

Usage. There are two windows called "Convex Hull" and "Voronoi Diagram". In the first one a set of points and their convex hull, C, are maintained, as well as the so-called center point which is shown in a different color. The second window contains a set of sites and their Voronoi diagram based on the convex distance function d_C. One can add (remove) points by pushing the left (right) mouse button, and drag points around with the left button. The convex hull and the Voronoi diagram are maintained dynamically.

If the display of the circles is turned on then circles centered at every site are shown. Their size can be varied by moving the slider at the top of the window, so one can observe how the circles intersect at the Voronoi edges. One may also verify Theorem 2.1.6.3, i. e. the topological properties of the Voronoi diagram remain the same if the center of the convex polygon in the Convex Hull window is moved within the interior of the convex hull.

The algorithm. The main focus for this program was to get an interactive applet where the user can quickly insert sites and move them around while the Voronoi diagram is displayed dynamically. So we have decided for an incremental algorithm, and we could not use one of the known worst-case optimal algorithms for convex distance functions like the one by Chew and Drysdale [17] to construct the Voronoi diagram, or the other by Drysdale [26] to compute the dual graph which is a generalization of the algorithm of Guibas and Stolfi [35], since the two algorithms use the divide-and-conquer technique.

As already mentioned in the paragraph about randomized incremental construction in Section 2.2.6, it is preferable to compute the dual graph rather than directly the Voronoi diagram, and this remains true for arbitrary convex distance functions. When a new site is inserted, we first have to locate the triangle of the dual graph, our primary structure, that contains the point. For simplicity and practical efficiency we do not even use an influence graph. Already Green and Sibson [33] and Bowyer [12] have observed that such a simple incremental algorithm for computing the Euclidean Voronoi diagram behaves very well in practice, and Devroye et al. [25] have analyzed the reasons for that. For reestablishing the dual graph we use the standard edge flipping technique, adapted to convex distance functions. The Voronoi diagram is directly derived from the dual graph.

Point location. Since we do not want to use an influence graph or any other extra structure specially designed for point location, we do not apply any of the many known results for (dynamic) point location, see e. g. [6, 16, 19, 20, 27, 47]. Instead we only work on the dual graph which exists anyway. The operation we need on this structure is to access a triangle from a neighbouring triangle in constant time, this is supported by any standard data structure to store triangulations. When a new site a_{i+1} is to be inserted, we locate it in the dual graph $D_C(S_i)$ with $S_i = \{a_1, \ldots, a_i\}$ in the following way similar to the methods mentioned in [12, 33].

We start at a certain triangle, choose an arbitrary point inside this triangle, and connect the point to a_{i+1} by a line segment. We walk from neighbor to neighbor across all triangles cut by the line segment, finally we find the triangle T containing a_{i+1}.

Green and Sibson [33] note that one can expect a running time of $O(\sqrt{i})$ for this operation, and Devroye et al. [25] prove an expected time of $O(\sqrt[3]{i})$ for an improved algorithm which first selects $O(\sqrt[3]{i})$ sites at random, then determines the site of them closest to the new point, using an adjacent triangle to this site as the starting triangle for the location procedure as described above. Mücke et al. [67] show that this result can be generalized to three dimensions to obtain an expected query time close to $O(\sqrt[4]{i})$.

This method for point location is very simple to implement and is also very efficient in practice, especially in our interactive program where one site can be dragged around. We proceed as follows. As starting triangle for locating the point a_{i+1} in $D_C(S_i)$ we use the triangle where the point has been located in $D_C(S_i)$ at its previous position. Then the point is only *temporarily inserted*. This means that we compute all necessary information to be able to display the updated structure, but we do not make any changes to the data structure containing $D_C(S_i)$. The advantage of this method, originally described in [38], is that we avoid a costly delete operation, and we can very quickly locate and insert the moving point at different locations because most of the time the moving point is still contained in the same triangle or one of its neighbours, in other words the point location is processed in constant time.

Reestablishing the dual graph. After the point location we insert the new site a_{i+1} into the data structure for the dual graph and create new edges to the three vertices of the containing triangle. Then we use the edge flipping technique to update the data structure until it represents the correct dual graph again. So we must determine all triangles whose *circumcircles* contain the new site. By circumcircle of three sites we mean the reflected unit circle D, passing through the three sites and centered at the chosen bisector of the three sites, which is always a point and can be computed in logarithmic time, see Definition 2.1.5.5 and Section 2.2.4.

As usual, the triangles whose circumcircles include the new site in the interior or

on the boundary are said to be *in conflict* with the new site.

Let us consider the example of a Voronoi diagram based on a triangular unit circle shown in Figure 2.2.7.1. The dashed lines show the Voronoi diagram, and the solid lines indicate the edges of the dual graph, while the unit circles of one particular sits are drawn as dotted lines around each site $a_1, \ldots, a_6$. Site a_7 is to be inserted. It is located in the triangle $T = \triangle(a_3, a_5, a_6)$, so there are edges from a_7 to each of the three sites in the new dual graph. Now the conflicts have to be resolved. Figure 2.2.7.1 also shows that a_7 is contained in the circumcircles (dashed-dotted lines) of $\triangle(a_3, a_4, a_5)$ and $\triangle(a_2, a_3, a_6)$. Therefore, edge $\overline{a_3\, a_6}$ has be changed (flipped) to $\overline{a_7\, a_2}$ and $\overline{a_3\, a_5}$ to $\overline{a_7\, a_4}$. Figure 2.2.7.2 shows the Voronoi diagram and the dual graph after inserting a_7. Observe that the edge $\overline{a_3\, a_4}$ has vanished because site a_7, although not on the convex hull, has an infinite Voronoi region that separates a_3 from a_4.

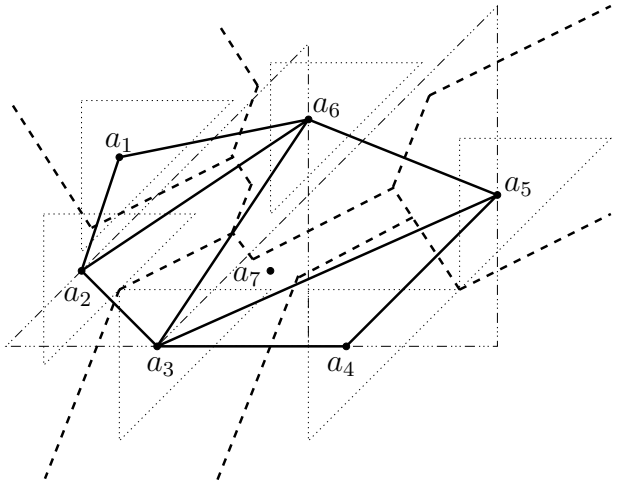

Figure 2.2.7.1: The new site a_7 lies in $\triangle(a_3, a_5, a_6)$, and in the interior of the circumcircles of $\triangle(a_3, a_4, a_5)$ and $\triangle(a_2, a_3, a_6)$.

In the following we give a detailed discussion of all possible cases that can occur when inserting a new site.

We start with the normal case that the new site is contained in the interior of a circumcircle of a triangle. The next lemma shows that the edge flipping as described in the example is correct.

Lemma 2.2.7.1 *Consider a site a_{i+1} that has to be inserted into the dual graph $D_C(\{a_1, \ldots, a_i\})$, and assume that a_{i+1} is contained in in the interior of the circumcircle of $\triangle(a_1, a_2, a_3)$. The edges $\overline{a_{i+1}\, a_j}$ for $j = 1, 2, 3$, are part of the new dual graph $D_C(\{a_1, \ldots, a_i, a_{i+1}\})$. If such a new edge properly[1] intersects one of the edges of $\triangle(a_1, a_2, a_3)$ then this "old" edge is no longer in the new dual graph.*

[1] I. e. the intersection is not only a common endpoint.

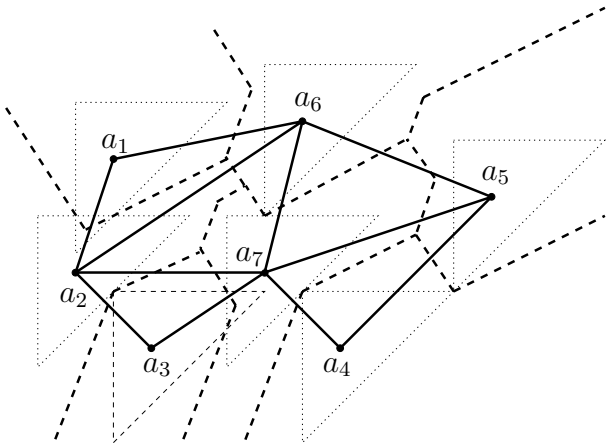

Figure 2.2.7.2: The Voronoi diagram and the dual graph of Figure 2.2.7.1 after inserting a_7.

Proof. Let point $c = B^*_C(a_1, a_2, a_3)$ be the center of the circumcircle of $\triangle(a_1, a_2, a_3)$. We have $d_C(a_{i+1}, c) < d_C(a_1, c)$ because a_{i+1} lies in the interior of this circumcircle. We consider the continuous function f defined by

$$f(p) = d_C(a_{i+1}, p) - d_C(a_1, p), \quad \text{for } p \text{ on the segment } \overline{a_1\, c}.$$

Since $f(c) < 0$ and $f(a_1) = d_C(a_1, a_{i+1}) > 0$, there exists a point q on the line segment $\overline{a_1\, c}$ such that $d_C(a_{i+1}, q) = d_C(a_1, q) < d_C(a_1, c)$, Therefore the intersection of $B_C(a_1, a_{i+1})$ and $\overline{a_1\, c}$ is a connected set, there is a point q_0 on $\overline{a_1\, c}$ such that the chosen bisector $B^*_C(a_{i+1}, a_1)$ intersects the segment $\overline{c\, a_1}$ at q_0. This construction of q guarantees that the reflected unit circle, D, centered at q_0 passing through a_{i+1} and a_1 is enclosed in the circumcircle of $\triangle(a_1, a_2, a_3)$ and contains no sites a_j for $4 \leq j \leq i$ in its interior, only at most one of a_2 and a_3 lies on its boundary. If a_2 and a_3 do not lie on its boundary then the line segment $\overline{a_{i+1}\, a_1}$ is an edge in the new dual graph, due to Lemma 2.1.4.9 (1).

Assume that a_2 lies on its boundary. So a_1 and a_2 lie on the same edge of circumcircle of $\triangle(a_1, a_2, a_3)$ and D, in particular, a_1 (i. e. $a_1 \prec a_2$) is a vertex of the two circles. Therefore the edge $\overline{a_{i+1}\, a_1}$ is in the new dual graph, due to Lemma 2.1.4.9 (2).

Analogously, the edges $\overline{a_{i+1}\, a_2}$ and $\overline{a_{i+1}\, a_3}$ are part of it, too. Because there can not be any properly intersecting edges in the dual graph, the corresponding old edges disappear. □

The next case shows the special treatment which is necessary for edges on the "outside" of the dual graph. For this purpose we say that an edge $\overline{a_1\, a_2}$ is *on the boundary of the dual graph* or a *dual boundary edge*, for short, iff the Voronoi diagram contains an infinite Voronoi edge of $B^*_C(a_1, a_2)$. We use the convention that the infinite part of the Voronoi edge is always to the left of the directed line segment $\overline{a_1\, a_2}$,

sometimes such an edge is on the boundary of the dual graph in both directions.

For a dual boundary edge $\overline{a_1\,a_2}$ we can also define its circumcircle. Let the set $F^*_{12} \cap F^*_{21}$ be bounded by the line segments $\overline{a_1\,u}$, $\overline{a_2\,u}$, $\overline{a_1\,v}$, and $\overline{a_2\,v}$, see Figure 2.2.7.3, where v is to the right of $a_1\,a_2$. The *circumcircle of the dual boundary edge* $\overline{a_1\,a_2}$

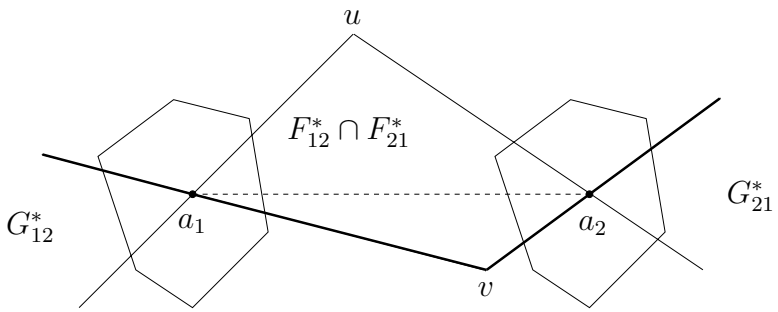

Figure 2.2.7.3: Definition of the circumcircle of the dual boundary edge $\overline{a_1\,a_2}$.

is defined as the region containing u bounded by the two rays $\overrightarrow{v\,a_1}$ and $\overrightarrow{v\,a_2}$. In other words the circumcircle is the limit of the sequence of reflected unit circles centered at $B^*_C(a_1, a_2)$ when the center point tends to infinity. In the Euclidean case the circumcircle of $\overline{a_1\,a_2}$ is the half plane left to $a_1\,a_2$, and $\overline{a_1\,a_2}$ is an edge on the boundary of the Delaunay triangulation of the sites $a_1, \ldots, a_i$ iff $\overline{a_1\,a_2}$ is an edge of their convex hull, i. e. the circumcircle of $\overline{a_1\,a_2}$ does not contain any other site. For convex distance functions we have an analogous result: the circumcircle of a dual boundary edge does not contain any site in its interior. It may however contain other sites on its boundary, see Lemma 2.1.4.9 for the exact conditions.

As observed in Figure 2.2.7.1 and Figure 2.2.7.2, the dual boundary edge $\overline{a_3\,a_4}$ of the dual graph $D_C(\{a_1, \ldots, a_6\})$ is not contained in the new dual graph after inserting site a_7, although it has not been replaced by a crossing edge during an edge flip. We consider such dual boundary edges and give a criterion for deciding their existence in the new dual graph.

The following lemma describes how dual boundary edges are treated if a new site is inserted.

Lemma 2.2.7.2 *Let $\overline{a_1\,a_2}$ be a dual boundary edge of the dual graph $D_C(\{a_1, \ldots, a_i\})$. If the new site a_{i+1} lies in the interior of the circumcircle of $\overline{a_1\,a_2}$ then $\overline{a_{i+1}\,a_1}$ and $\overline{a_{i+1}\,a_2}$ are in the new dual graph $D_C(\{a_1, \ldots, a_i, a_{i+1}\})$. Furthermore the edge $\overline{a_1\,a_2}$ is not in the new dual graph iff a_{i+1} lies in $F^*_{12} \cap F^*_{21}$.*

Proof. There is a sufficiently large reflected unit circle centered somewhere on the end ray of $B^*_C(a_1, a_2)$ passing through a_1 and a_2 that contains a_{i+1} but does not contain any other site in its interior, due to Lemma 2.1.4.9. Analogously to the proof

of Lemma 2.2.7.1, we can show that the edges $\overline{a_{i+1}\,a_1}$ and $\overline{a_{i+1}\,a_2}$ are part of the new dual graph.

If a_{i+1} lies in $F^*_{12} \cap F^*_{21}$ then $\overline{a_1\,a_2}$ is not in the new dual graph, due to Lemma 2.1.2.12 and Lemma 2.1.4.9. Conversely, each reflected unit circle contains a_{i+1}, due to Lemma 2.1.4.9, so a_{i+1} must be in $F^*_{12} \cap F^*_{21}$. □

In Figure 2.2.7.1 we can see that site a_7 lies in the circumcircle of the dual boundary edge, therefore the edge $\overline{a_3\,a_4}$ is not in the new dual graph, due to Lemma 2.2.7.2.

Now let us see how to deal with a new site a_{i+1} that lies on the boundary of a circumcircle. If it is the circumcircle of a triangle $\triangle(a_1, a_2, a_3)$ then we first consider the case that a_{i+1} and the other sites lie on the different edges of the circumcircle. Here, the bisectors $B^*_C(a_{i+1}, a_1)$, $B^*_C(a_{i+1}, a_2)$, and $B^*_C(a_{i+1}, a_3)$ intersect exactly in the center of the circumcircle, so the three edges connecting a_{i+1} and the three vertices of the triangle are in the new dual graph, see Figure 2.2.7.4. If a_{i+1} lies on the same

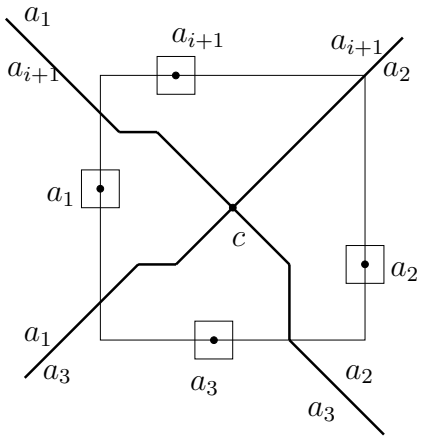

Figure 2.2.7.4: Each of the sites a_{i+1}, a_1, a_2, and a_3 lies on a different edge of the circumcircle of $\triangle(a_1, a_2, a_3)$.

edge of the circumcircle as another site, this also includes the case of a circumcircle of a dual boundary edge, then we have Lemma 2.1.4.9 (2) to decide which edges are in the dual graph.

For example, in Figure 2.2.7.1 site a_7 lies on the boundary of the circumcircle of the triangle $\triangle(a_1, a_2, a_6)$. In particular, a_7 and a_2 lie on the same edge of the circumcircle and $a_2 \prec a_7$, so the edge $\overline{a_7\,a_1}$ is not in the new dual graph, due to Lemma 2.1.4.9 (2).

The last case we have to consider concerns new sites that are not contained in any circumcircle, a phenomenon that does not occur for smooth convex distance functions like the Euclidean one. Even for polygonal distances it can only happen in some cases when the site is outside the convex hull of the other sites. For example, Figure 2.2.7.5

shows the Voronoi diagram after adding site a_8 to the lower right part of the diagram shown in Figure 2.2.7.2. Site a_8 does not lie in any circumcircle of $D_C(\{a_1, \ldots, a_7\})$.

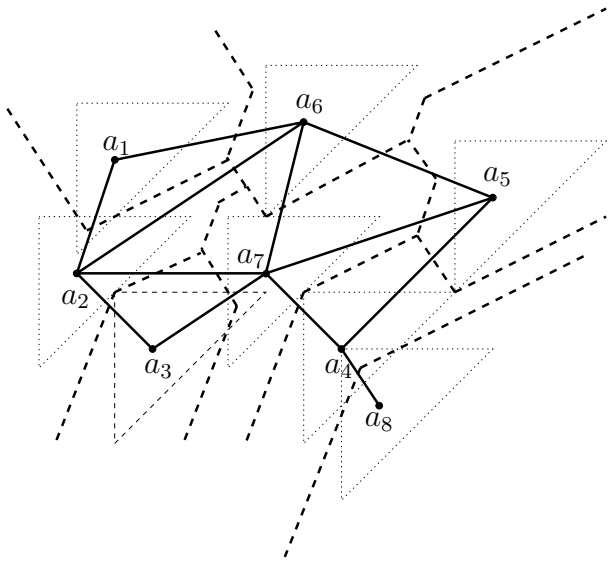

Figure 2.2.7.5: The Voronoi diagram and the dual graph of Figure 2.2.7.2 after inserting a_8. The site a_8 does not lie in any circumcircle of $D_C(\{a_1, \ldots, a_7\})$, the new region of a_8 is only adjacent to the region of a_4.

Lemma 2.2.7.3 *Let a_{i+1} be not in the interior or on the boundary of any circumcircle of $D_C(\{a_1, \ldots, a_i\})$. Then a_{i+1} lies in a unbounded Voronoi region, say $VR_C(a_1, \{a_1, \ldots, a_i\})$. The new dual graph $D_C(\{a_1, \ldots, a_{i+1}\})$ differs from the old one only by the new edge $\overline{a_{i+1}\, a_1}$.*

Proof. First, all edges in the dual graph $D_C(\{a_1, \ldots, a_i\})$ remain in the new dual graph $D_C(\{a_1, \ldots, a_{i+1}\})$, due to Lemma 2.1.4.9.

The new site a_{i+1} lies in a Voronoi region, say $VR_C(a_1, \{a_1, \ldots, a_i\})$. Due to Lemma 2.1.5.6, $VR_C(a_1, \{a_1, \ldots, a_i\})$ is unbounded, and the ray $\overrightarrow{a_1\, a_{i+1}}$ does not intersect a Voronoi edge on the boundary of the Voronoi region of a_1. Otherwise a_{i+1} lies in the circumcircle of a triangle or of a dual boundary edge.

Let $\overline{a_3\, a_1}$ and $\overline{a_1\, a_2}$ be the two consecutive dual boundary edges such that the ray $\overrightarrow{a_1\, a_{i+1}}$ lies in the region bounded by the two rays $\overrightarrow{a_1\, a_2}$ and $\overrightarrow{a_1\, a_3}$, see Figure 2.2.7.6. In particular, the sites a_3 and a_2 can be identical. Because a_{i+1} can not lie in the circumcircles of the dual boundary edges $\overline{a_1\, a_2}$ and $\overline{a_3\, a_1}$, it must lie in the set $G^*_{13} \cap G^*_{12}$. Therefore $\overline{a_{i+1}\, a_2}$ and $\overline{a_{i+1}\, a_3}$ are not in the dual graph $D_C(\{a_1, \ldots, a_{i+1}\})$, due to Lemma 2.2.5.2.

We show that the new dual graph is constructed by adding the dual boundary edge $\overline{a_1\, a_{i+1}}$ into $D_C(\{a_1, \ldots, a_i\})$ using Lemma 2.1.4.9, i. e. the new Voronoi diagram

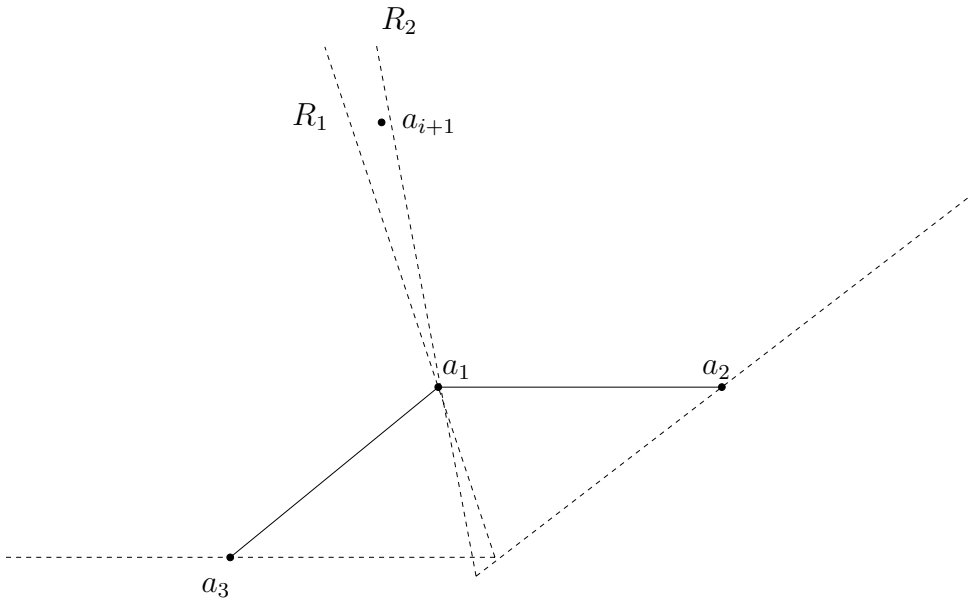

Figure 2.2.7.6: The new site a_{i+1} lies in $G^*_{13} \cap G^*_{12}$ bounded by the rays R_1 and R_2. There is not any sites in the circumcircles of the dual boundary edges $\overline{a_1\, a_2}$ and $\overline{a_3\, a_1}$ drawn by dashed lines.

is constructed by added the whole chosen bisector $B^*_C(a_1, a_{i+1})$ in the Voronoi diagram $V_C(\{a_1, \ldots, a_i\})$.

Because the circumcircle of dual edge $\overline{a_1\, a_2}$ is the limit of the sequence of reflected unit circles centered at $B^*_C(a_1, a_2)$ when the center point tends to infinity, so each reflected unit circle passing through a_1 and a_{i+1} can intersect the circumcircles of the dual boundary edges $\overline{a_1\, a_2}$ and $\overline{a_3\, a_1}$ in two connected components, one of them contains a_1, due to Corollary 2.1.2.2. So such reflected unit circles do not include any other sites in its interior, otherwise these sites also lie in the circumcircles of $\overline{a_1\, a_2}$ or $\overline{a_3\, a_1}$, a contradiction. If there are reflected unit circles that include a site a_j then a_1 and a_j must lie on a line segment of one circumcircle of $\overline{a_1\, a_2}$ or $\overline{a_3\, a_1}$, and we have $a_1 \prec a_j$, otherwise $\overline{a_1\, a_2}$ or $\overline{a_3\, a_1}$ is not a dual edge, a contradiction. Therefore the edge $\overline{a_j\, a_{i+1}}$ is not in the dual graph $D_C(\{a_1, \ldots, a_{i+1}\})$, due to Lemma 2.1.4.9. □

Reestablishing the Voronoi diagram. Once the new dual graph is computed we want to derive the new Voronoi diagram. For each edge of the old dual graph which is not in the new dual graph we remove the corresponding Voronoi edge. For each new edge we construct part of the corresponding bisector. If the centers of the two circumcircles exist, they determine the endpoints of the Voronoi edge, else the edge is infinite at one or the two sides.

Chapter 3

Bisectors and Voronoi diagrams in 3-space

Voronoi diagrams for convex distance functions in 3-dimensional space are interesting and have important applications, but not much is really known about their structure and how to compute them.

Most of the few known results focus on their complexity. Boissonat et al. [7] show an upper bound of $O(n^2)$ for the complexity of a Voronoi diagram of n point sites under L_1 and L_∞, as well as for a tetrahedral distance, and generalizations of this for higher dimensions. Tagansky [79] obtains a more general bound of $O(k^3\alpha(k)n^2 \log n)$ for polyhedral distances with k facets in 3-space. Lê [57] shows that the complexity of Voronoi diagrams under L_p distances is bounded in any dimension, independent of p. Chew et al. [18] prove an upper bound of $O(n^2\alpha(n) \log n)$ for the complexity of a Voronoi diagram of lines under a polyhedral distance.

Even much less is known about the structure of bisectors and Voronoi diagrams. Therefore, this chapter is primarily devoted to this subject. There are some more structural results by Lê. In [58] he proves that for non-smooth distances in 3-space the bisector of three sites may consist of many disconnected pieces, and in [59] he describes an algorithm which is suitable for ellipsoid distances.

One of the reasons for the lack of results on Voronoi diagrams for higher dimensions based on arbitrary convex distance functions is the surprising, really abnormal, structure of the bisectors which behave totally different from what is known for the Euclidean distance.

There is an astonishing result by Shaidenko [73] and by Goodey [32] concerning ellipsoids in any dimension greater or equal to three. Applied to the 3-dimensional case it says that for any convex, non-ellipsoidal body K in $\mathbf{R}^3$ there are two homothetic copies of K such that the intersection of their boundaries is not planar. So we can always find four non-coplanar points in the intersection of their boundaries, and

therefore the bisector of these four sites under distance K contains at least two points.

This means that it is extremely hard, or impossible, to find convex distance functions in 3-space which can guarantee to have only one point in the bisector of four sites in general position. In other words, this phenomenon is not an exception, but the rule: it strikes nearly any convex distance, except for simplex distances and the affine transforms of the Euclidean distance.

In Section 3.1 we present our results for general convex distance functions. We investigate the bisector systems of two, three, and four sites, and show that especially the bisector of four sites can be unexpectedly complicated. Even for strictly convex and smooth distances it may consist of arbitrarily many single points, see Section 3.1.5. Some of the results of Sections 3.1.1 to 3.1.6 have already appeared as journal articles and in conference proceedings, see [39, 40, 51]. This is followed by results on polyhedral distances in Section 3.2, where we give bounds for the complexity of these bisectors in terms of the number of facets of the unit polytope. We also present algorithms to compute the bisectors. Special convex distances, namely the L_p distances are treated in Section 3.3.

3.1 General convex distance functions

In this section we consider bisector systems with respect to a convex distance function d_C in 3-space. The bisectors of two or three sites are defined in exactly the same way as for the two-dimensional setting, see Definitions 2.1.0.1 and 2.1.0.2. Additionally, the bisector, $B_C(a_1, a_2, a_3, a_4)$, of four sites becomes interesting here. It is, of course, defined to be the intersection of $B_C(a_1, a_4)$ and $B_C(a_1, a_2, a_3)$.

The Voronoi diagram in 3-space is defined analogously to Definitions 2.1.4.1, 2.1.4.5, and 2.1.4.6 in Chapter 2, if we apply the three-dimensional lexicographic order.

We will see that the central projection on the unit sphere turns out as a useful means, the behavior of the bisector can be read from the intersection behavior of the so-called silhouttes on the unit sphere.

As was to be expected, in general the bisector of two sites is homeomorphic to a plane, see Section 3.1.1. But in contrast to the Euclidean metric, the bisector of three sites may be disconnected, and each connected component is homeomorphic to a line, see Section 3.1.2. Some basic facts about the bisector of four sites are given in Section 3.1.3, and in Section 3.1.4 we show that two bisectors of three sites, whose intersection is a bisector of four sites, may intersect in permuted order. Moreover, the bisector of four sites can consist of many points. In Section 3.1.5 we construct, for a given number $n \geq 0$, a convex distance function d_C, whose unit sphere C is

smooth, strictly convex, and symmetric about the origin, and four sites p, q, r, s in 3-space such that the bisector $B_C(p,q,r,s)$ consists of *exactly* $2n+1$ *points*. We can show that this is not a mere degeneracy: each of the four sites can be moved independently within a small 3-dimensional neighbourhood, and still the number of points in the bisector is at least $2n+1$. Since each of these points is a vertex in the Voronoi diagram of $\{p,q,r,s\}$ based on C, this result implies that there is no upper bound to the complexity of a Voronoi diagram of four sites based on an arbitrary convex distance function in 3-space.

3.1.1 The bisector of two sites

Let C be a convex body in 3-space. For two sites a_1, a_2 let C_i be the copies of C translated to a_i, $i=1,2$. Let π be an arbitrary plane passing through these two sites. Then the intersection $B_C(a_1,a_2)\cap\pi$ is the two-dimensional bisector of a_1 and a_2 based on the unit ball $C_1\cap\pi$. We call the set of top and bottom points (see Section 2.1.1) of $C_1\cap\pi$, for all such planes π, the *silhouette*.

Definition 3.1.1.1 Let Γ_{ij} be the set of all points on the surface of C that admit a supporting line parallel to $\overline{a_i\,a_j}$. We call Γ_{ij} the *silhouette for direction* $a_i\,a_j$.

In some degenerate cases a bisector can contain 3-dimensional pieces, branchings, or self-intersections. To avoid this, we make the following *assumption on general position*: no line through two sites is parallel to a line segment which is contained in ∂C. This assumption is appropriate because a non-general position does not persist after a small perturbation of the sites.

By the way, one could replace this assumption on general position by the stronger assumption of strict convexity of C, because if there is no line segment in ∂C then there is, of course, no such line segment which is parallel to a direction from site to site.

Under the assumption of general position we obtain a number useful properties.

Lemma 3.1.1.2 *The silhouette* Γ_{12} *for direction* $a_1\,a_2$ *is a simple closed curve.*

Proof. The silhouette is (doubly) connected due to the convexity of C. It is a simple curve due to the assumption. □

By Lemma 3.1.1.2, a silhouette cuts the surface of C into two open "half-spheres" which are homeomorphic to a plane. Let H_{ij} be the relatively open half-sphere of C bounded by the silhouette Γ_{ij} that intersects the ray $\overrightarrow{O\,(a_j-a_i)}$. The two half-spheres H_{ij} and H_{ji} share the same boundary Γ_{ij}, and they represent a disjoint partition of ∂C, i. e., $H_{ij}\,\dot\cup\,\Gamma_{ij}\,\dot\cup\,H_{ji}=\partial C$.

Lemma 3.1.1.3 *The bisector $B_C(a_1, a_2)$ is homeomorphic to a plane.*

Proof. Analogously to the proof of Lemma 2.1.1.1 we can show that the central projection at a_1 is a homeomorphism of $B_C(a_1, a_2)$ onto $H_{12} + a_1$. □

Remark that the assumption on general position is crucial, since the converse of Lemma 3.1.1.3 is also true: in non-general position, i. e., if the line $a_1\,a_2$ is parallel to a line segment of ∂C, the bisector $B(a_1, a_2)$ is definitely not homeomorphic to a plane. As examples one may look at the bisector for a cylindric unit ball, which contains an unbounded 3-dimensional component, or the bisector for a cone, which consists of an infinite triangle glued to a 2-dimensional surface, in such a special position of the two sites.

Corollary 3.1.1.4 *Each ray from a_1 through a point of $H_{12} + a_1$ intersects the bisector $B_C(a_1, a_2)$ exactly once.*

Analogously to the bent strip of Lemma 2.1.1.1 in 2-space the bisector of two sites in 3-space lies in a region bounded by two cones.

Corollary 3.1.1.5 *The bisector $B_C(a_1, a_2)$ lies in the intersection of the cone spanned by a_1 and $\Gamma_{12}+a_1$ containing a_2 and the cone spanned by a_2 and $\Gamma_{21}+a_2$ containing a_1.*

We consider the following interesting relation between three points on the bisector and their foot points on ∂C_i for $i = 1, 2$. Let $\pi(p, q, r)$ denote the plane passing through three non-collinear points p, q, and r.

Lemma 3.1.1.6 *Let p, q, r be three non-collinear points of $B_C(a_1, a_2)$, and let p_i, q_i, r_i be their foot points on ∂C_i for $i = 1, 2$, respectively. The three planes $\pi(p, q, r)$, $\pi(p_1, q_1, r_1)$, and $\pi(p_2, q_2, r_2)$ intersect in a line called the Desargue line of p, q, r, or they are parallel.*

Proof. We apply Theorem 1.2.1 to the triangles $\triangle(a_1, p_1, q_1)$ and $\triangle(a_2, p_2, q_2)$, see Figure 3.1.1.1, the points p, q and the intersection c_1 of $p_1\,q_1$, and $p_2\,q_2$ are collinear or $p\,q$, $p_1\,q_1$ and $p_2\,q_2$ are parallel. Using Theorem 1.2.1 again to the triangles $\triangle(a_1, q_1, r_1)$ and $\triangle(a_2, q_2, r_2)$, resp. $\triangle(a_1, p_1, r_1)$ and $\triangle(a_2, p_2, r_2)$, we obtain that all three points c_1, $c_2 = q_1\,r_1 \cap q_2\,r_2$, and $c_3 = p_1\,r_1 \cap p_2\,r_2$, if they exist, lie on all three planes $\pi(p, q, r)$, $\pi(p_1, q_1, r_1)$, and $\pi(p_2, q_2, r_2)$. So c_1, c_2, and c_3 are collinear and they are on the common intersection of the three planes. The same holds if only two of c_1, c_2, and c_3 exist. In the remaining case the three planes are parallel. □

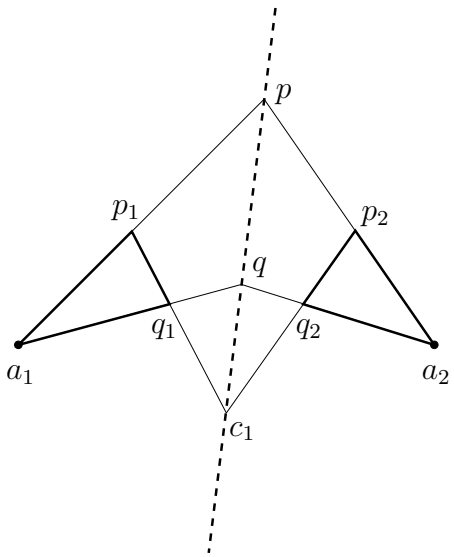

Figure 3.1.1.1: The three points p, q, and c_1 are collinear.

3.1.2 The bisector of three sites

There is a close relationship between the bisector of three sites in 2-space and in 3-space. Let p be a point of $B_C(a_1, a_2, a_3)$ in 3-space, and let v_i be its central projection centered at a_i, for $i = 1, 2, 3$, see Figure 3.1.2.1. The plane π through v_1, v_2, v_3 is parallel to the plane through a_1, a_2, a_3. Let K be the intersection of π and C_1. We choose an interior point w_1 in K, and let $w_i = w_1 - a_1 + a_i$, for $i = 2, 3$. The lines $w_i\, v_i$, $i = 1, 2, 3$, intersect in a common point r that is the bisector of w_1, w_2, w_3 with respect to the unit circle K in the plane π.

Conversely, for each plane π parallel to a_1, a_2, a_3 that intersects C_1 we consider a 2-dimensional bisector problem using $C_1 \cap \pi$ as the unit circle. It is not hard to see that we can construct the corresponding bisector point r on π, if it exists, and obtain the points v_i on $C_i \cap \pi$. From this, we finally get a point $p \in B_C(a_1, a_2, a_3)$ as the intersection of the lines $a_i\, v_i$.

Definition 3.1.2.1 The mapping from $p \in B_C(a_1, a_2, a_3)$ to its foot points (v_1, v_2, v_3) is called the *construction by central projection.*

Lemma 3.1.2.2 *Let a_1, a_2, and a_3 be in general position. The construction by central projection is continuous in both directions.*

Proof. The mapping from $B_C(a_1, a_2, a_3)$ to its foot points is a central projection which is continous by Theorem 1.1.4.

For the other direction it is clear that the mapping is bijective, due to general position. The proof of continuity is analogous to the proof of Lemma 2.1.1.1 for two dimensions. □

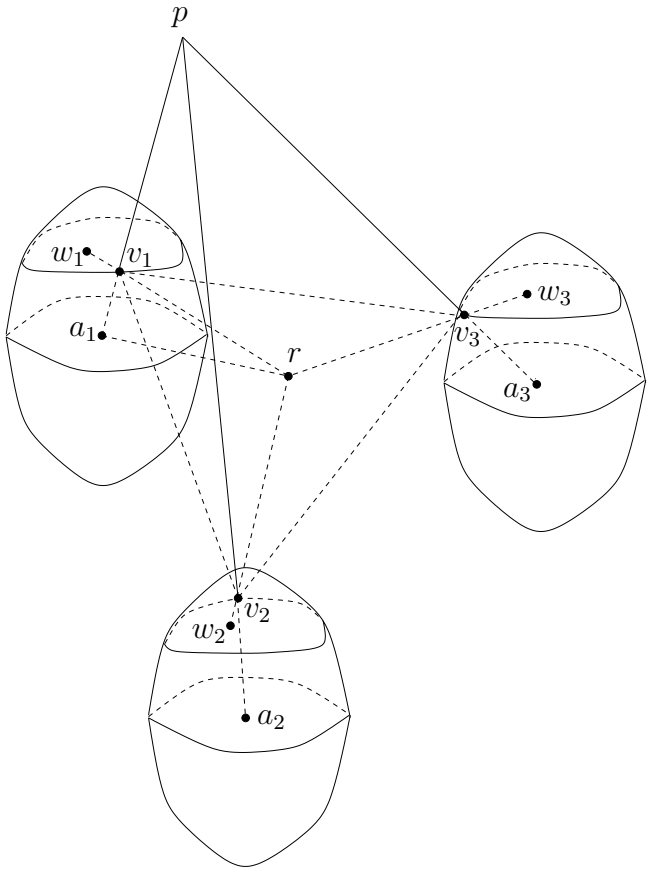

Figure 3.1.2.1: The construction of a bisector point p by central projection shows the close relationship between the 3-bisectors in two and three dimensions.

For the intersection of half-spheres we introduce an abbreviation, let $H_{ijk} = H_{ij} \cap H_{ik}$. This notation is, of course, commutative in the second and third index, i. e. $H_{ijk} = H_{ikj}$.

Now we again assume that a_1, a_2, and a_3 are in general positon as described after Definition 3.1.1.1. Under this assumption each of $B_C(a_1, a_2)$, $B_C(a_1, a_3)$, and $B_C(a_2, a_3)$ is homeomorphic to a plane by Lemma 3.1.1.3. We will investigate the relationships between H_{ijk} and $B_C(a_1, a_2, a_3)$.

Lemma 3.1.2.3 *The intersected half-spheres H_{123}, H_{213}, and H_{312} are disjoint and partition the unit sphere, i. e., for their closures we have $\overline{H_{123}} \cup \overline{H_{213}} \cup \overline{H_{312}} = \partial C$.*

Proof. We have $H_{123} \cap H_{213} = \emptyset$ by definition, due to $H_{12} \cap H_{21} = \emptyset$.

The silhouettes Γ_{12}, Γ_{13}, and Γ_{23} have at least two points in common, namely the points of ∂C touched by the supporting planes parallel to a_1, a_2, a_3 from above and below. At these points, each silhouette separates into two branches. The boundary of H_{123} consists of one branch of Γ_{12} and one branch of Γ_{13}. The "unused" branches

are contained in $\overline{H_{312}}$ and $\overline{H_{213}}$, respectively. Therefore, they must partition the unit sphere. □

In some cases, the intersected half-spheres H_{ijk} can be empty or disonnected. The 3-bisectors copy their behavior, as the next two lemmas show.

Lemma 3.1.2.4 *The bisector $B_C(a_1, a_2, a_3)$ is not empty iff all three intersected half-spheres H_{123}, H_{213}, and H_{312} are not empty.*

Proof. Let p be a point of $B_C(a_1, a_2, a_3)$. Its central projection centered at a_1 lies in $(H_{12} \cap H_{13}) + a_1 = H_{123} + a_1$, compare the proof of Lemma 3.1.1.3. So $H_{123} \neq \emptyset$, and analogously for the other intersected half-spheres.

Conversely, assume that H_{123}, H_{213}, and H_{312} are all not empty. We consider a plane π parallel to a_1, a_2, a_3 which intersects the unit sphere in more than just one point. For brevity, we write $H'_{12} = H_{12} \cap \pi$, etc., for the intersection of the half-spheres with the plane. It is clear that not all three of H'_{123}, H'_{213}, and H'_{312} can be empty, by Lemma 3.1.2.3.

We even show that at most one of them is empty. So assume the contrary, say $H'_{123} = H'_{213} = \emptyset$. Then $H'_{12} \cap H'_{13} = \emptyset$, thus $H'_{12} = H'_{31}$, and analogously $H'_{21} = H'_{32}$. Therefore, $H'_{312} = H'_{31} \cap H'_{32} = H'_{12} \cap H'_{21} = \emptyset$, a contradiction.

Now we consider all possible positions of the plane π. Due to the relative openness of H_{123}, H_{213}, and H_{312} and the fact just proven, there must be a position of π such that all three of H'_{123}, H'_{213}, and H'_{312} are non-empty. More precisely, there must be such a position in any connected component of H_{123}.

For such particular position of π, we consider the 2-dimensional bisector problem using the unit circle $C \cap \pi$. By Corollary 2.1.2.9, there is a bisector point r based on the convex set $C \cap \pi$, and the bisector point $p \in B_C(a_1, a_2, a_3)$ can be derived from this, using the construction by central projection. □

Corollary 3.1.2.5 *The bisector of three collinear sites a_1, a_2, and a_3 is empty.*

Proof. The three silhouettes are identical, therefore one of the three sets H_{123}, H_{213}, and H_{312} must be empty. □

The bisector of three sites can be disconnected and each component is homeomorphic to a line, as already observed in [58]. The reasons for this become clear in the next lemma.

Lemma 3.1.2.6 *The bisector $B_C(a_1, a_2, a_3)$ is connected iff all three intersected half-spheres H_{123}, H_{213}, and H_{312} are connected. The number of connected components of $B_C(a_1, a_2, a_3)$ plus 2 equals the number of connected components of the three sets. Each connected component of $B_C(a_1, a_2, a_3)$ is homeomorphic to a line whose foot set on C_i ends at two points in $(\partial H_{123} \cap \partial H_{213} \cap \partial H_{312}) + a_i$, $i = 1, 2, 3$.*

Proof. Assume that $B_C(a_1, a_2, a_3)$ is not empty and connected. From Lemma 3.1.2.4 we know that the three sets H_{123}, H_{213}, and H_{312} are not empty, and in its proof we have even seen that we can find, using the construction by central projection, the image of a bisector point in each connected component of $H_{123} + a_1$, etc. But the central projection is continuous and therefore maps connected sets to connected sets, so H_{123} etc. must be connected. For an empty $B_C(a_1, a_2, a_3)$, which is connected by definition, one of the three sets must be empty by Lemma 3.1.2.4, and therefore the other two must be connected.

Conversely, if H_{123}, H_{213}, and H_{312} are all connected, then the construction by central projection delivers one bisector point for every plane parallel to a_1, a_2, a_3 that intersects $H_{123} + a_1$, $H_{213} + a_2$, and $H_{312} + a_3$. Since this construction is a continuous mapping of a connected set of planes to the bisector, $B_C(a_1, a_2, a_3)$ must be connected, too. Thereby it is clear that the foot set of a connected component ends at a point at which all three sets meet.

For the number of connected components we consider a moving plane parallel to a_1, a_2, a_3, sweeping the whole unit sphere, and we observe the bisector points constructed by central projection. For the first part of $B_C(a_1, a_2, a_3)$ that is constructed, we "use up" one connected component of each of H_{123}, H_{213}, and H_{312}. Whenever a new piece of $B_C(a_1, a_2, a_3)$ begins, this is caused by a new connected component of one of the three sets, because any connected component of one of them makes a non-empty contribution to the bisector, see the proof of Lemma 3.1.2.4. The connected components are homeomorphic to a line by Lemma 3.1.2.2. □

We give a simple example for constructing a disconnected 3-bisector. Figure 3.1.2.2 shows three sites a_1, a_2, a_3 as well as the intersections of the unit spheres centered at these sites with a plane parallel to a_1, a_2, a_3, at three levels, see Figure 3.1.2.3 for an impression of the unit sphere in 3-space. At all levels, the intersection is a triangle, but the triangle in the middle is rotated against the triangles above and below. Considering the three situations as planar bisector problems, there is a 3-bisector in the upper and lower case, but no 3-bisector point in the middle. This corresponds to the fact that there is an empty set H'_{213} in the middle position, while all three sets exist in the other situations. Therefore, the 3-bisector in 3-space is interrupted, by Lemma 3.1.2.6.

Corollary 3.1.2.7 *If the unit sphere C is smooth then the bisector of three sites consists of only one connected component.*

Proof. As a consequence of smoothness the three sets H_{123}, H_{213}, and H_{312} are connected, and Lemma 3.1.2.6 applies. □

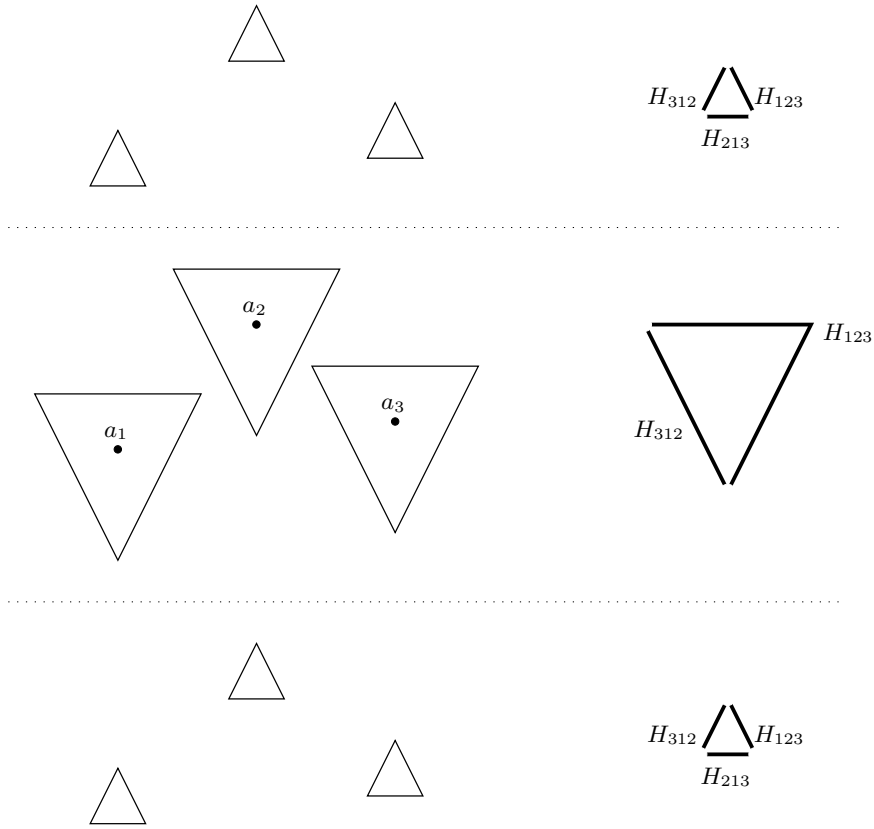

Figure 3.1.2.2: To the left, three planar intersections through three unit spheres as the one shown in Figure 3.1.2.3. To the right, the corresponding sets H_{123}, H_{213}, and H_{312}.

Corollary 3.1.2.5 and Corollary 3.1.2.7 show that the behaviour of the bisector of three sites for smooth distances is quite similar to the Euclidean case: if the three sites are collinear then the bisector is empty and it is homeomorphic to a line otherwise.

3.1.3 The bisector of four sites

Let H_{1234} denote $H_{123} \cap H_{124}$, this notation is commutative in the second, third, and fourth index. We show first that the four sets H_{1234}, H_{2134}, H_{3124} and H_{4123} also separate ∂C into disjoint sets.

Lemma 3.1.3.1 *Let a_1, a_2, a_3, a_4 be in general position. The sets H_{1234}, H_{2134}, H_{3124} and H_{4123} partition the boundary of C into disjoint subsets.*

Proof. Because of the general position the four sets H_{1234}, H_{2134}, H_{3124}, and H_{4123} are disjoint by definition.

Let v be an arbitrary point on ∂C and w. l. o. g. let $v \in H_{123}$ and $v \notin \Gamma_{14}$, so v does not lie on the boundary of H_{1234}. The point v must be contained in $H_{124} \cup H_{412}$, but not in H_{214}, and it is also in $H_{134} \cup H_{413}$, but not in H_{314} by Lemma 3.1.2.3.

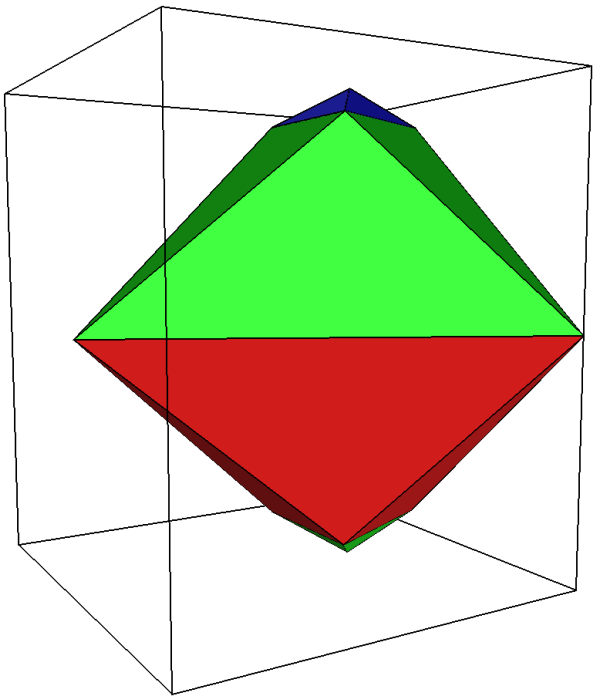

Figure 3.1.2.3: The unit sphere of the example in Figure 3.1.2.2, together with its bounding box.

So if $v \in H_{124}$ then $v \in H_{134}$, i. e. $v \in H_{1234}$, or if $v \in H_{412}$ then $v \in H_{413}$, i. e. $v \in H_{4123}$. □

As a consequence, we have the following result on the bisector of four sites for a simplex distance C, i. e. a polyhedron with only four facets.

Lemma 3.1.3.2 *Let C be a tetrahedron and let a_1, a_2, a_3, a_4 be in general position. The bisector $B_C(a_1, a_2, a_3, a_4)$ is empty or just one point.*

Proof. Let $B_C(a_1, a_2, a_3, a_4) \neq \emptyset$. So each of the four sets H_{1234}, H_{2134}, H_{3124}, and H_{4123} contains exactly one facet of ∂C.

Assume that there are two points p and q in $B_C(a_1, a_2, a_3, a_4)$, and $p \neq q$. Let p_i and q_i be the foot points on ∂C_i, for $i = 1, 2, 3, 4$. So the points $p_1 - a_1$ and $q_1 - a_1$ both lie in the interior of the same facet H_{1234}, and analogously for the other points. the four lines $(p_i - a_i)\,(q_i - a_i)$, $i = 1, 2, 3, 4$, intersect in one point, this means that the four facets of ∂C intersect in a point, this is a contradiction. □

From this follows that the Voronoi diagram based on a tetrahedron (simplex) has a simple structure, similar to the Euclidean one, as already observed by Rote [71].

Corollary 3.1.3.3 *The complexity, i. e. that is the number of vertices, edges, and facets, of the Voronoi diagram of n sites in general position for a tetrahedral unit sphere is in $O(n^2)$.*

Proof. The bisector of two sites contains at most four facets. Upon insertion of a new site no "old" facet is split into several new facets, it can only become smaller. Thus, the Voronoi region of each site has only $O(n)$ facets. □

For general convex distances the existence of the bisector of four sites depends on the existence of a homothety which maps four sites in the surface of a reflected unit ball.

Lemma 3.1.3.4 *The bisector $B_C(a_1, a_2, a_3, a_4)$ of four sites is not empty if and only if there is a tetrahedron T which is homothetic to the tetrahedron $T(a_1, a_2, a_3, a_4)$ and whose four vertices lie in the surface of the reflected unit ball.*

Proof. Let $p \in B_C(a_1, a_2, a_3, a_4)$, so $d_C(a_1, p) = d_C(a_2, p) = d_C(a_3, p) = d_C(a_4, p)$. In other words, the reflected unit sphere centered at p and scaled with factor $d_C(a_1, p)$ passes through the four sites. So we have found a homothetic tetrahedron T such that its four vertices lie on the unit sphere, and vice versa. □

In the Euclidean case, for any four non-coplanar sites there exists exactly one euclidean shpere that passes through the four sites. Therefore there is exactly one bisector point for four non-coplanar sites. But for general distances this is much more complicated.

The result by Shaidenko [73] and by Goodey [32], mentioned at the beginning of the chapter, says that for two convex bodies K_1 and K_2 in $\mathbf{R}^n$, $n \geq 3$, the intersection $\partial K_2' \cap \partial K_1$ is contained in a hyperplane for all translates K_2' of K_2 with $K_2' \neq K_1$ if and only if K_1 and K_2 are homothetic ellipsoids.

Therefore, by Lemma 3.1.3.4, for any non-ellipsoidal body C in $\mathbf{R}^3$ we can find four non-coplanar sites whose bisector contains at least two points. Remark that is not contradiction to Lemma 3.1.3.2, because we do not know if the four sites are in general position.

For the tetrahedron, for example, it is not hard to see that four points which are contained in the intersection of the surfaces of two homothetic tetrahedra are never in in general position, i. e., there are always two of the points whose connecting line is parallel to a facet, see Figure 3.1.3.1.

The interesting question remains for which convex bodies C, except for tetrahedra and ellipsoids, the assertion of Lemma 3.1.3.2 also holds. Our conjecture is that there is no further convex body C with this property. In Section 3.2.5, we will prove this for all polyhedra.

If we additionally assume C to smooth, we can show that the bisector of four sites always exists, except for degenerate cases. This again, as in Corollary 3.1.2.7, shows the similarity to the Euclidean sphere.

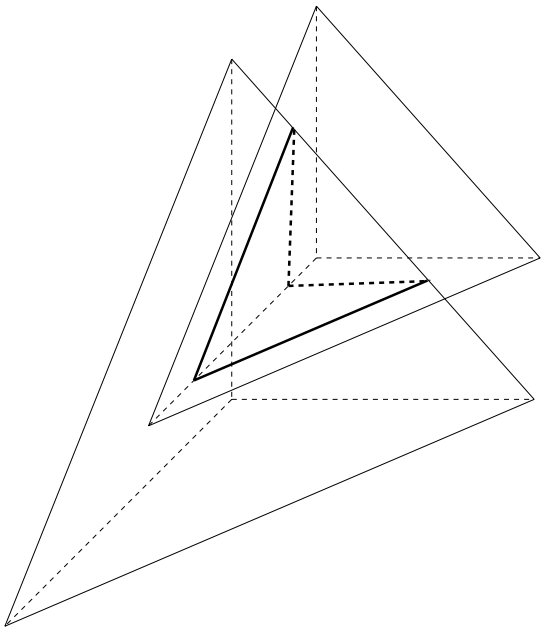

Figure 3.1.3.1: The intersection of the surfaces of two different homothetic tetrahedra is always contained in at most three faces of one of them. So at least two of any four points in this intersection lie on the same facet.

Lemma 3.1.3.5 *Assume a smooth unit sphere C, and let a_1, a_2, a_3, and a_4 be non-coplanar and in general position. Then $B_C(a_1, a_2, a_3, a_4)$ is not empty. After removing a compact subset, $B_C(a_1, a_2, a_3)$ decomposes into components lying on different sides of $B_C(a_1, a_4)$ (in other words, different "ends" of the "line" $B_C(a_1, a_2, a_3)$ lie on different sides of the "plane" $B_C(a_1, a_4)$).*

Proof. The silhouette $\Gamma_{14} + a_1$ cuts ∂C_1 into two half-spheres one is $H_{14} + a_1$ that is intersected by $\overline{a_1\, a_4}$. We know that there is a homeomorphism $F_2 : H_{14} + a_1 \to B_C(a_1, a_4)$.

Let t_1, d_1 be the top and bottom points on ∂C_1 such that the two outer common supporting planes of C_1, C_2, and C_3 intersect C_1 in t_1 resp. d_1.

One of the two points, say t_1, lies in $H_{14} + a_1$, while the other, d_1, lies on the opposite half-sphere, since the four points a_1, a_2, a_3, a_4 are not coplanar. There is a homeomorphism $F_3 : L \to B_C(a_1, a_2, a_3)$, in which L is the foot set of $B_C(a_1, a_2, a_3)$ on ∂C_1 from t_1 to d_1 without the endpoints.

We consider F_2 and F_3 on $(H_{14} + a_1) \cap L$. For all points v in a small environment of t_1, the distance $d(a_1, F_2(v))$ is bounded, whereas $d(a_1, F_3(v))$ tends to infinity, so $\overline{a_1\, F_3(v)} \cap B_C(a_1, a_4) = F_2(v)$. On the other hand, for points v in a small environment of d_1, $\overline{a_1\, F_3(v)} \cap B_C(a_1, a_4) = \emptyset$. This shows that different ends of $B_C(a_1, a_2, a_3)$ lie on different sides of $B_C(a_1, a_4)$ such that they must intersect. □

As a consequence of Lemma 3.1.3.5 the bisector of four sites in general position based on a smooth distance consists of an odd number of connected components.

3.1.4 The intersection of two related bisectors of three sites

The Voronoi region of a site is bounded by pieces of bisectors, and for computing the structure of such a region one must look closely at the intersection of all bisectors related to this site. From the construction by central projection, see Figure 3.1.2.1, the bisector of three sites, which is always one-dimensional, is naturally ordered. One might hope that two such bisectors, which appear in the common boundary of two Voronoi regions, intersect nicely, i. e. the intersections appear in the same order (or reverse) on both bisectors. This will be disproved in the following.

The intersection of two related 3-bisectors, say $B(a_1, a_2, a_3)$ and $B(a_1, a_2, a_4)$, is the 4-bisector $B(a_1, a_2, a_3, a_4)$. We consider a point, p, of the 4-bisector and its central projections, v_i, centered at a_i, for $i = 1, 2, 3, 4$, compare Figure 3.1.2.1. The tetrahedron $T(v_1, v_2, v_3, v_4)$ is homothetic to the tetrahedron $T(a_1, a_2, a_3, a_4)$ and also homothetic to $T(v_1 - a_1, v_2 - a_2, v_3 - a_3, v_4 - a_4)$. In this way, for each point of the 4-bisector we have one tetrahedron homothetic to $T(a_1, a_2, a_3, a_4)$ whose vertices lie on ∂C.

Now we imagine several of such homothetic tetrahedra whose vertices lie on ∂C, and we consider a sweep plane parallel to a_1, a_2, a_3, passing through C. It is also parallel to one of the faces of the tetrahedra. The plane visits these faces in the same, natural order as the corresponding points of the 4-bisector lie on $B(a_1, a_2, a_3)$. This holds because the central projection of the 3-bisector $B(a_1, a_2, a_3)$ on $\partial C + a_1$ is strictly monotonic in the direction orthogonal to the plane through a_1, a_2, a_3.

But this order in which the tetrahedra are visited is not necessarily the same for all four faces. We can indeed construct an example of a 4-bisector containing at least seven points such that the corresponding tetrahedra are visited in totally different order, depending on the face.

To this end, we define seven tetrahedra as shown in the left picture of Figure 3.1.4.1, following an idea of Santos, see [40]. Their coordinates are shown in Table 3.1, remark that all 28 vertices are in convex position.

The four families of parallel faces of the seven tetrahedra are visited in the orders given by the following four rows.

1	2	3	4	5	6	7
5	6	7	4	3	2	1
7	6	5	4	1	2	3
3	2	1	4	7	6	5

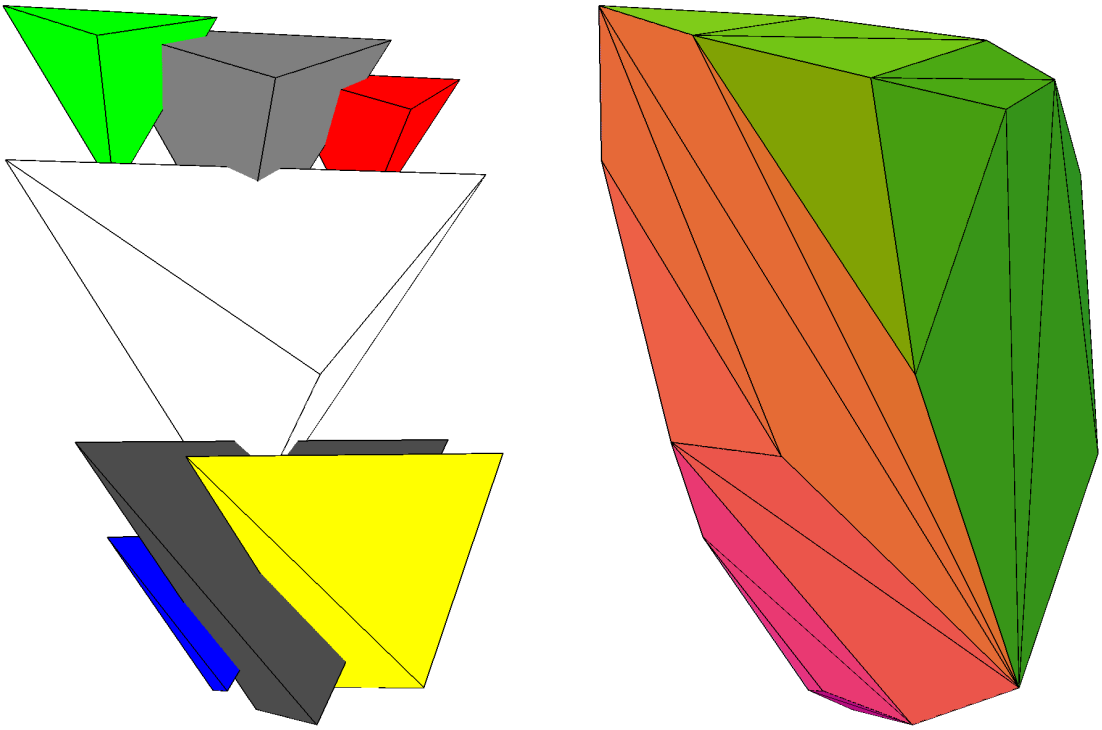

Figure 3.1.4.1: The left picture shows seven homothetic tetrahedra whose parallel faces appear in permuted order. The right picture shows their convex hull, we observe that all vertices of the tetrahedra are in convex position, i. e. they appear as vertices of the convex hull. The convex hulls here and in Figure 3.1.2.3 were computed by Quickhull [5], the pictures were rendered using Geomview [1].

So, if we now choose the convex hull of the seven tetrahedra, see the right picture in Figure 3.1.4.1, or any other convex body C containing the 28 vertices in ∂C as our unit sphere, and if we choose four sites that lie on the vertices of a tetrahedron which is homothetic to the other seven, then the given permutations also apply to the order in which the pieces of the 4-bisector appear on the four 3-bisectors. This strange behavior is illustrated in Figure 2.1.2.2, which schematically shows how the central projections centered at a_1 of three 3-bisectors $B(a_1, a_2, a_3)$, $B(a_1, a_2, a_4)$, and $B(a_1, a_3, a_4)$ and their intersections look like.

The described phenomenon does, of course, not depend on polyhedral shape of the unit sphere. We can easily construct a strictly convex and smooth body whose surface also passes through the 28 vertices of the seven tetrahedra.

T_1:	−14.0	18.0	2.0	T_5:	2.0	−18.0	14.0
	−2.0	18.0	2.0		2.0	−18.0	2.0
	−8.0	10.0	8.0		8.0	−10.0	8.0
	−8.0	10.0	−4.0		−4.0	−10.0	8.0
T_2:	−9.0	19.0	0.0	T_6:	−9.0	−7.0	0.0
	9.0	19.0	0.0		9.0	−7.0	0.0
	0.0	7.0	9.0		0.0	−19.0	9.0
	0.0	7.0	−9.0		0.0	−19.0	−9.0
T_3:	2.0	18.0	−2.0	T_7:	−2.0	−18.0	−2.0
	14.0	18.0	−2.0		−2.0	−18.0	−14.0
	8.0	10.0	4.0		4.0	−10.0	−8.0
	8.0	10.0	−8.0		−8.0	−10.0	−8.0
T_4:	−13.5	9.0	0.0				
	13.5	9.0	0.0				
	0.0	−9.0	13.5				
	0.0	−9.0	−13.5				

Table 3.1: The coordinates of the seven homothetic tetrahedra of Figure 3.1.4.1.

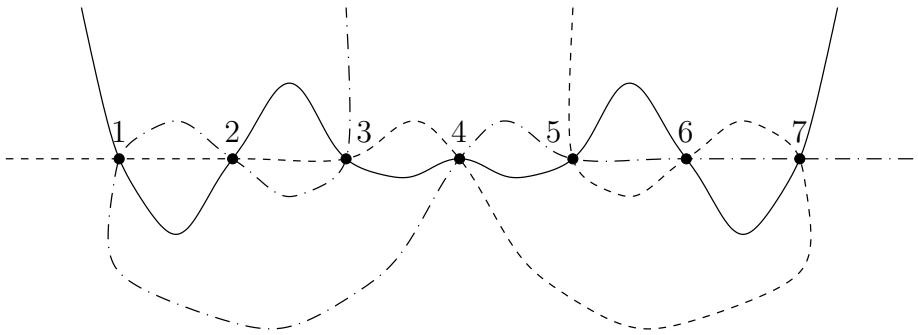

Figure 3.1.4.2: Schematic view on the intersections of the three related 3-bisectors under the polyhedral distance of Figure 3.1.4.1.

3.1.5 The complexity of the bisector of four sites

In this section we show that for general convex distance functions there is *no upper bound* on the complexity of a bisector of four points in space, not even if the unit sphere is strictly convex and smooth.

Theorem 3.1.5.1 *For each integer $n \geq 0$ there exists a smooth, symmetric convex distance function d in 3-space and four sites a_1, a_2, a_3, a_4, such that*

$$|B_C(a_1, a_2, a_3, a_4)| = 2n + 1$$

holds for the cardinality of the d-bisector of the four points.

Due to Lemma 3.1.3.4, we have to construct a smooth convex body C symmetric about the origin, and four points that lie on the surface of exactly $2n+1$ homothetic copies of C. Instead, we prove the following equivalent theorem.

Theorem 3.1.5.2 *For each integer $n \geq 0$ there exist a smooth, symmetric convex body C in 3-space and four points p, q, r, s such that there are exactly $2n+1$ tetrahedra homothetic to the tetrahedron $T(p,q,r,s)$ whose vertices lie on the surface of C.*

The rest of this section is devoted to the proof of Theorem 3.1.5.2, i. e. to the construction of C, and to the proof that even a small perturbation of the four points does not destroy the property that $2n+1$ homothetic tetrahedra lie on the surface of C.

The idea is as follows. Suppose we have two symmetric convex functions, f and g. We place their graphs in the (x,y)-plane and the (z,y)-plane, respectively, such that both graphs pass through the origin and are symmetric with respect to the z-axis; see Figure 3.1.5.1.

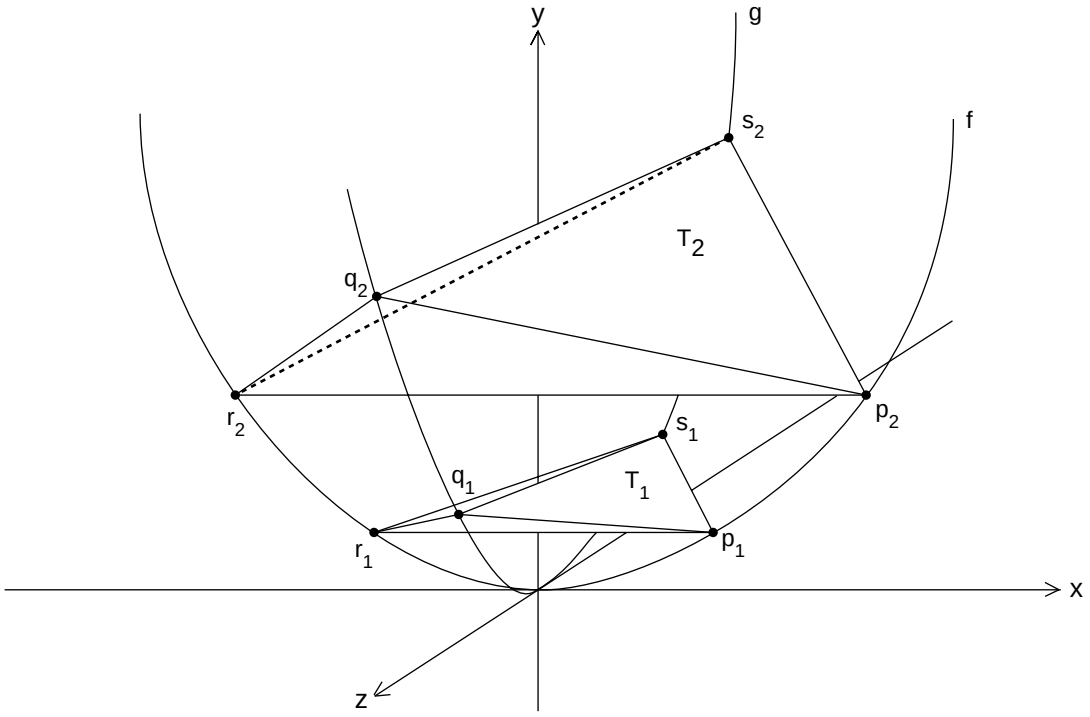

Figure 3.1.5.1: Constructing homothetic tetrahedra.

For $i = 1, 2$ let $x_i \in (0,1)$ be two distinct values and let $p_i = (x_i, f(x_i), 0)$ and $r_i = (-x_i, f(x_i), 0)$, resp. $q_i = (0, g(x_i), x_i)$ and $s_i = (0, g(x_i), -x_i)$ be points on the curves defined by f resp. g in 3-space. Let $T_i = T(p_i, q_i, r_i, s_i)$ be two tetrahedra.

Since all faces of a tetrahedron are triangles, two tetrahedra are homothetic iff all corresponding edges are parallel. Considering T_1 and T_2, by construction we have parallel edges $\overline{p_1\, r_1}$ and $\overline{p_2\, r_2}$ as well as $\overline{q_1\, s_1}$ and $\overline{q_2\, s_2}$.

For the edges $\overline{p_1\,q_1}$ and $\overline{p_2\,q_2}$ we have

$$\begin{aligned} p_1 - q_1 &= (x_1, f(x_1) - g(x_1), -x_1) \\ p_2 - q_2 &= (x_2, f(x_2) - g(x_2), -x_2) \end{aligned}$$

which shows that the edges are parallel if

$$\frac{f(x_2) - g(x_2)}{f(x_1) - g(x_1)} = \frac{x_2}{x_1}$$

This can be achieved if we choose

$$g(x) = f(x) + \varepsilon|x|$$

for some constant $\varepsilon > 0$. With this choice, we also obtain parallelism of the other corresponding edges of T_1 and T_2 by symmetry.

But our given construction is independent of the concrete choice of x_1 and x_2. This shows that each value $x \in (0, 1)$ gives rise to a tetrahedron homothetic to T_1 whose vertices lie on the curves of f, which for example may be a lower half-circle, or g. We may now take the convex hull of the two curves in space as the lower half of a convex body C, the other half can defined by symmetry. Both curves, f and g, lie in the surface of C. We conclude that we have *infinitely many* homothetic tetrahedra whose vertices lie on the surface of this body!

However, after fixing C, this "infinity" property would disappear under the slightest perturbation of the four points. Since we want to give an example that is stable under perturbation, we have to modify the construction. As a consequence, the bisector of four points $B_C(p, q, r, s)$ will no longer be a continuum but will consist of $2n + 1$ discrete points.

In the following, we will refine this idea to a full proof of Theorem 3.1.5.2. For $n = 0$ there is nothing to prove; from now on we assume that $n \geq 1$. There are some technical difficulties.

In Section 3.1.5 we choose $2n + 1$ equidistant points $x_i \in [0, 1]$ and define a convex function F which coincides with f at exactly these points. For smoothness, we construct a function G by patching g with pieces of ellipses. These functions F and G will take over the role of f and g in our idea. The lower half of a convex body C is generated by "wrapping ellipses" around the two curves, the upper half is then obtained by symmetry. In Section 3.1.5 we prove that C is smooth and convex. In Section 3.1.5 we show that there are exactly $2n + 1$ distinct homothetic tetrahedra that have their vertices on the surface of C. In Section 3.1.5 we show that the bisector of two points, $B_C(a_1, a_2)$, and the bisector of three points, $B_C(a_1, a_3, a_4)$, intersect transversally, from which we conclude that a perturbation of the four points is possible. We will see that an *odd* number of homothetic tetrahedra is no coincidence but inevitable if perturbations of the four points are allowed.

Defining a symmetric body C

For $i \in \{0, \ldots, 2n\}$, let $x_i = \frac{i}{2n+1}$ be $2n+1$ equidistant points in $[0,1]$ and let f be the lower half-circle

$$f(x) = 1 - \sqrt{1-x^2}$$

and $g(x) = f(x) + \varepsilon|x|$ as mentioned above. The constant $\varepsilon > 0$ will be determined later. The function $F : [x_1, x_{2n}] \to \mathbf{R}$, with

$$F(x) = f(x) + \varepsilon(-1)^i(x - x_i)(x - x_{i+1}) \quad \text{for} \quad x \in [x_i, x_{i+1}], \quad i = 1, \ldots, 2n-1$$

coincides with f only at the points $x_1, \ldots, x_{2n}$, but otherwise runs alternately below and above f. For the time being, F is only defined in $[x_1, x_{2n}]$.

Lemma 3.1.5.3 *The function F is continuously differentiable in $[x_1, x_{2n}]$, and, if $0 < \varepsilon < 1/2$, strictly increasing and strictly convex.*

Proof. Clearly F is continuous, and for $x \in (x_i, x_{i+1})$ we have

$$F'(x) = f'(x) + \varepsilon(-1)^i(2x - x_i - x_{i+1})$$

Moreover, the left and right derivatives of F at x_i are equal.

$$\lim_{x \nearrow x_i} F'(x) = f'(x_i) + \delta\varepsilon(-1)^{i-1} = f'(x_i) - \delta\varepsilon(-1)^i = \lim_{x \searrow x_i} F'(x)$$

where $\delta = 1/(2n+1)$. Hence, F is continuously differentiable.

For $\varepsilon < f'(x_1)/\delta$, we have $F'(x) > 0$, this shows that F is strictly increasing.

For $x \in (x_i, x_{i+1})$, the second derivative of F is

$$F''(x) = f''(x) + 2\varepsilon(-1)^i$$

which shows that F'' is undefined at all x_i, but elsewhere F'' is strictly positive if $\varepsilon < f''(x_1)/2$.

A function which is smooth in $[x_1, x_{2n}]$ and strictly convex in all subintervals (x_i, x_{i+1}) is also strictly convex in $[x_1, x_{2n}]$. It is easy to show that $\min(f'(x_1)/\delta, f''(x_1)/2) \geq 1/2$ so we may choose any $\varepsilon < 1/2$. □

The following lemma will be applied to F but will also be used to smoothen g.

Lemma 3.1.5.4 *Let $K : [x_1, x_{2n}] \to (0,1)$ be a continuously differentiable, strictly increasing, and strictly convex function that fulfills $K'(x_1) > 2K(x_1)/x_1$.*

The function K can be extended to an interval $[-a_K, a_K]$ with $x_{2n} < a_K$ such that $K(0) = 0$, $K'(0) = 0$, $K(\pm a_K) = 1$, and $K'(\pm a_K) = \pm\infty$ holds, and the extended function K is symmetric, strictly convex, and continuously differentiable in $(-a_K, a_K)$ with infinite limits of the derivative in the endpoints.

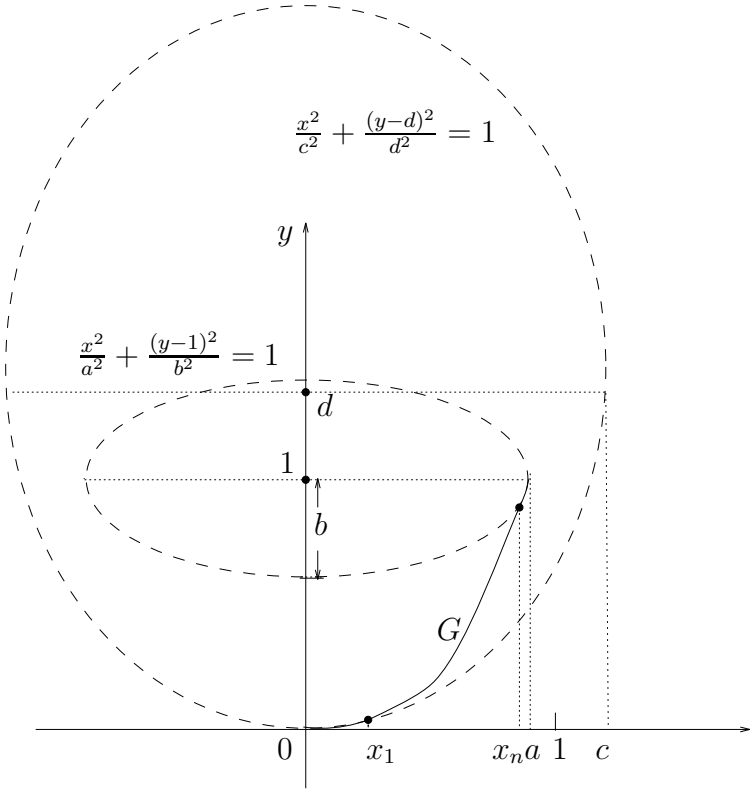

Figure 3.1.5.2: Patching with pieces of ellipses.

Proof. The idea is to patch K with pieces of ellipses in the intervals $[0, x_1]$ and $[x_{2n}, a_K]$, as shown in Figure 3.1.5.2.

We define the following quantities

$$\begin{aligned} a_K &= \sqrt{\frac{x_{2n}(1-K(x_{2n})) + x_{2n}^2 K'(x_{2n})}{K'(x_{2n})}} \\ b_K &= \sqrt{(1-K(x_{2n}))^2 + x_{2n}K'(x_{2n})(1-K(x_{2n}))} \\ c_K^2 &= -\frac{x_1 d_K^2}{K'(x_1)(K(x_1)-d_K)} \\ d_K &= \frac{K(x_1)(K(x_1)-x_1K'(x_1))}{2K(x_1)-x_1K'(x_1)} \end{aligned}$$

and two ellipses as follows.

$$\frac{x^2}{a_K^2} + \frac{(y-1)^2}{b_K^2} = 1 \tag{3.1}$$

$$\frac{x^2}{c_K^2} + \frac{(y-d_K)^2}{d_K^2} = 1 \tag{3.2}$$

The condition $K'(x_1) > 2K(x_1)/x_1$ assures that everything is well defined. Substituting $(x_1, K(x_1))$ for (x, y) in (3.2), and plugging in the expression for c_K and d_K, shows that ellipse (3.2) passes through $(x_1, K(x_1))$. To prove that ellipse (3.2) has

the same tangent as K at this point, we show that

$$\frac{d}{dx}\left(\frac{x^2}{c_K^2}+\frac{(y-d_K)^2}{d_K^2}\right)=0$$

holds for $x = x_1$ and $y = K(x_1)$. This identity can be derived by substituting the expression for c_K.

Analogously, by substituting the expressions for a_K and a_K into (3.1) we can show that ellipse (3.1) passes through $(x_{2n}, K(x_{2n}))$ and has the same tangent as K at that point.

Now K extends as follows.

$$K(x)=\begin{cases} d_K(1-\sqrt{1-x^2/c_K}), & |x|<x_1 \\ K(x), & x_1\le|x|\le x_{2n} \\ 1-b_K\sqrt{1-x^2/a_K^2}, & x_{2n}<|x|\le a_K \end{cases} \tag{3.3}$$

The extended function K is smooth and the other claims are evident, too. □

From now on let F be the extended function defined on an interval $[-a_F, a_F]$ by the technique of Lemma 3.1.5.4, and in the same sense let G be the function defined on $[-a_G, a_G]$ which results from applying Lemma 3.1.5.4 to g restricted to $[x_1, x_{2n}]$. (One can verify that F and g fulfill the conditions of Lemma 3.1.5.4.)

For construction of the body C, function F will be used as the rib in the (x, y)-plane, and G as the rib in the (z, y)-plane.

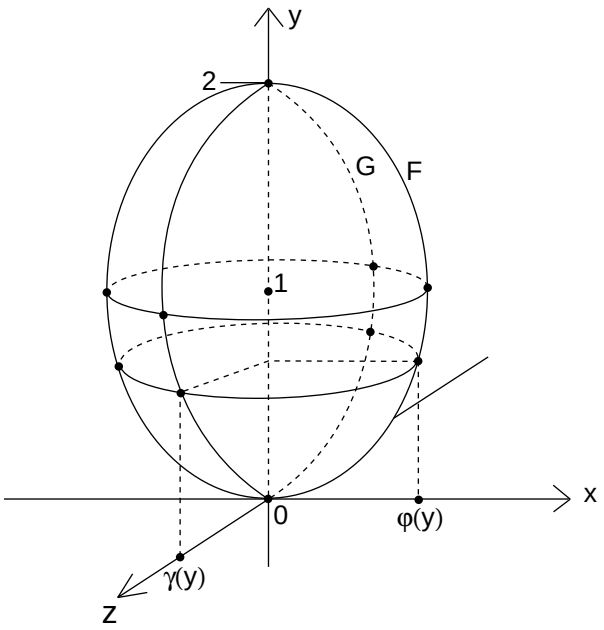

Figure 3.1.5.3: Defining C.

Now, we refer to Figure 3.1.5.3 and reflect F and G at the point $(0, 1, 0)$. For $y \in [0, 2]$ let $\varphi(y)$ and $\gamma(y)$ denote the inverse images of y under F resp. G on the

x-axis resp. on the z-axis. For each $y \in (0,2)$ we wrap around F and G the ellipse parallel to the (x,z)-plane given by

$$\frac{x^2}{\varphi(y)^2} + \frac{z^2}{\gamma(y)^2} = 1.$$

The body C is then defined as the union of all these ellipses and the poles $(0,0,0)$ and $(0,2,0)$. The following fact is obvious.

Lemma 3.1.5.5 *The surface A of C is parametrically described by*

$$A = \{(\varphi(y)\cos v,\ y,\ -\gamma(y)\sin v)\ :\ y \in [0,2],\ v \in [0,2\pi)\}$$

By construction, A is symmetric about the point $(0,1,0)$. In addition, it is also symmetric about the y-axis.

The smoothness and convexity of C

To show that C is convex we use the parametrization of ∂C given in Lemma 3.1.5.5.

Lemma 3.1.5.6 *The surface $A = \partial C$ is smooth.*

Proof. At the origin, the (x,z)-plane is the unique tangent plane of $A = (A_x, A_y, A_z)$. Now let $w = (\varphi(y)\cos v,\ y,\ -\gamma(y)\sin v)$ where $y \in (0,1]$ and $v \in [0,2\pi)$. The direction of the normal vector at w is given by the vector product

$$\begin{aligned}\frac{\partial A}{\partial y} \times \frac{\partial A}{\partial v} &= \left(\frac{\partial A_y}{\partial y}\frac{\partial A_z}{\partial v} - \frac{\partial A_z}{\partial y}\frac{\partial A_y}{\partial v},\ \frac{\partial A_z}{\partial y}\frac{\partial A_x}{\partial v} - \frac{\partial A_x}{\partial y}\frac{\partial A_z}{\partial v},\ \frac{\partial A_x}{\partial y}\frac{\partial A_y}{\partial v} - \frac{\partial A_y}{\partial y}\frac{\partial A_x}{\partial v}\right) \\ &= \Big(-\gamma(y)\cos v,\ \gamma(y)\varphi'(y)\cos^2 v + \gamma'(y)\varphi(y)\sin^2 v,\ \varphi(y)\sin v\Big)\end{aligned}$$

provided the resulting vector is not equal to zero, which is not the case. Since $\varphi : [0,1] \longrightarrow [0,a_F]$ and $\gamma : [0,1] \longrightarrow [0,a_G]$ are the inverse functions of F and G, respectively, their derivatives $\varphi'(y) = (F'(\varphi(y)))^{-1}$ and $\gamma'(y) = (G'(\gamma(y)))^{-1}$ are continuous on $(0,1]$ and we have $\varphi'(1) = 0 = \gamma'(1)$. Thus, if $y = 1$ then w has a normal vector of direction $(-a_G\cos v, 0, a_F\sin v)$. Consequently, the tangent plane of w is parallel to the y-axis. □

It is interesting to observe that a solid like C that is constructed by wrapping ellipses around a skeleton of two closed convex curves is not automatically convex although all its lines of latitude (the ellipses) and of longitude are convex. We will analyze this general problem in Section 3.1.6 and provide a criterion sufficient for convexity that applies to this case. The body C is convex if both functions $\varphi\varphi'$ and $\gamma\gamma'$ are strictly decreasing, see Corollary 3.1.6.7. This condition is ensured by the following lemma.

Lemma 3.1.5.7
For sufficiently small $\varepsilon > 0$, the functions $\varphi\varphi'$ and $\gamma\gamma'$ are strictly decreasing.

Proof. We compute the inverse functions of the first and last piece of F, see Lemma 3.1.5.4, and find that

$$\varphi(y)\varphi'(y) = \begin{cases} \frac{c_F^2}{d_F^2}\sqrt{d_F^2-(y-d_F)^2}\cdot\frac{d_F-y}{\sqrt{d_F^2-(y-d_F)^2}} = \frac{c_F^2}{d_F^2}(d_F-y) & \text{if } y\in[0,F(x_1)] \\ \\ \frac{a_F^2}{b_F^2}\sqrt{b_F^2-(1-y)^2}\cdot\frac{1-y}{\sqrt{b_F^2-(1-y)^2}} = \frac{a_F^2}{b_F^2}(1-y) & \text{if } y\in[F(x_{2n}),1] \end{cases}$$

which shows that $\varphi\varphi'$ is decreasing in these intervals.

Only the middle part, where $y \in (F(x_1), F(x_{2n}))$, needs further attention. For all $1 \le i \le 2n-1$ and for any $y \in (F(x_i), F(x_{i+1}))$, we want to show that

$$\begin{aligned} (\varphi(y)\varphi'(y))' &= \varphi'(y)^2 + \varphi(y)\varphi''(y) \\ &= \frac{1}{F'(\varphi(y))^2} - \varphi(y)\frac{F''(\varphi(y))}{F'(\varphi(y))^3} \\ &= \frac{1}{F'(x)^3}(F'(x) - xF''(x)) \end{aligned}$$

is negative, where $x = \varphi(y) \in (x_i, x_{i+1})$. Let $H(x) = F'(x) - xF''(x)$, then $H'(x) = -xF'''(x) = -xf'''(x) = -3x/(1-x^2)^{5/2} < 0$. The function H is strictly decreasing, so

$$\begin{aligned} H(x) \le H(x_i) &= f'(x_i) - \varepsilon\delta(-1)^i - x_i(f''(x_i) + 2\varepsilon(-1)^i) \\ &= -\frac{x_i^3}{(1-x_i^2)^{3/2}} - \varepsilon(-1)^i(\delta + 2x_i) \end{aligned}$$

is negative if ε is small enough. The function $\varphi\varphi'$ is strictly decreasing in each interval $(F(x_i), F(x_{i+1}))$, thus, as a continuous function, it is strictly decreasing in $[0,1]$.

The proof for $\gamma\gamma'$ is analogous. □

Counting tetrahedra

For $i \in \{1, \ldots, 2n\}$ let T_i be the tetrahedron defined by its vertices $p_i = (x_i, f(x_i), 0)$, $r_i = (-x_i, f(x_i), 0)$, $q_i = (0, g(x_i), x_i)$, and $s_i = (0, g(x_i), -x_i)$ where $x_i = i/(2n+1)$, see Figure 3.1.5.1. Since $f(x_i) = F(x_i)$ holds by construction of F, the vertices of these $2n$ tetrahedra lie on ∂C, the surface of C. All T_i are homothetic, as we have seen at the beginning of this section.

Lemma 3.1.5.8
There are exactly $2n+1$ tetrahedra homothetic to T_1 whose vertices lie on ∂C.

Proof. Let $T = T(p, q, r, s)$ be such a tetrahedron. Since T is homothetic to T_1, the line segment $\overline{r\,p}$ is parallel to the x-axis; see Figure 3.1.5.1. Moreover, p and r have identical y-coordinates, so they lie on the same ellipse. By symmetry, the midpoint of $\overline{r\,p}$ has x-coordinate 0. Similarly, the midpoint of $\overline{q\,s}$ has zero z-coordinate. Since both midpoints differ only in their y-coordinates the vertices of T lie on the curves defined by F and G; that is, $p = (x, F(x), 0)$, $r = (-x, F(x), 0)$, $q = (0, G(z), z)$, and $s = (0, G(z), -z)$.

The tetrahedron T being homothetic to T_1, there must be a constant $c > 0$ such that $p - r = c(p^1 - r^1)$, $q - s = c(q^1 - s^1)$, $q - r = c(q^1 - r^1)$, etc. From the first and the second identity we obtain $x = cx_1 = z$. Now the third equality implies

$$\begin{aligned} G(x) - F(x) &= c(G(x_1) - F(x_1)) \\ &= c\varepsilon x_1 \\ &= \varepsilon x \end{aligned}$$

If $x \in [x_1, x_{2n}]$ then T must be one of the $2n$ tetrahedra $T_1, \ldots, T_{2n}$, by construction. It remains to deal with the pieces of ellipses in the definition of F and G.

If $x \in [0, x_1)$ we consider the function

$$h(x) = G(x) - F(x) - \varepsilon x$$

By definition, $h(0) = 0$ and $h(x_1) = 0$ hold; for the first derivative

$$h'(x) = G'(x) - F'(x) - \varepsilon$$

we have $h'(0) = -\varepsilon < 0$ and $h'(x_1) = -\delta\varepsilon < 0$. Hence, there is a $\xi \in (0, x_1)$ with $h(\xi) = 0$. There is no other zero of h in $(0, x_1)$ and $h'(\xi) \neq 0$, since one can show by simple transformations that the second derivative

$$h''(x) = \frac{c_G d_G}{(c_G^2 - x^2)^{\frac{3}{2}}} - \frac{c_F d_F}{(c_F^2 - x^2)^{\frac{3}{2}}}$$

has only one positive zero. This means that there is one additional tetrahedron homothetic to T_1 with vertices in ∂C.

Finally, we consider the possibility of $x \in (x_{2n}, a_G]$, (because $a_G < 1 < a_F$). Let $H(x) = G(x) - F(x)$. Then

$$\begin{aligned} H'(x) &= \frac{b_G}{a_G}\frac{x}{\sqrt{a_G^2 - x^2}} - \frac{b_F}{a_F}\frac{x}{\sqrt{a_F^2 - x^2}} \\ &= \frac{x(a_G^2 b_F^2 - b_G^2 a_F^2)(x^2 - \frac{a_G^4 b_F^2 - b_G^2 a_F^4}{a_G^2 b_F^2 - b_G^2 a_F^2})}{a_G a_F \sqrt{a_G^2 - x^2}\sqrt{a_F^2 - x^2}(b_G a_F \sqrt{a_F^2 - x^2} + a_G b_F \sqrt{a_G^2 - x^2})} \end{aligned}$$

has only one positive zero χ, with $\chi^2 = \dfrac{a_G^4 b_F^2 - b_G^2 a_F^4}{a_G^2 b_F^2 - b_G^2 a_F^2}$, and

$$\begin{aligned} H''(x) &= \frac{a_G b_G}{(a_G^2 - x^2)^{\frac{3}{2}}} - \frac{a_F b_F}{(a_F^2 - x^2)^{\frac{3}{2}}} \\ &= \left(x^2 - \frac{a_F^{\frac{2}{3}} a_G^{\frac{2}{3}} (a_G^{\frac{4}{3}} b_F^{\frac{2}{3}} - a_F^{\frac{4}{3}} b_G^{\frac{2}{3}})}{(a_F b_F)^{\frac{2}{3}} - (a_G b_G)^{\frac{2}{3}}} \right) \cdot \frac{(a_F b_F)^{\frac{2}{3}} - (a_G b_G)^{\frac{2}{3}}}{(a_G^2 - x^2)^{\frac{3}{2}} (a_F^2 - x^2)^{\frac{3}{2}}} \cdot \\ &\quad \frac{(a_F b_F)^{\frac{2}{3}} (a_G^2 - x^2) + (a_G b_G)^{\frac{2}{3}} (a_F^2 - x^2) + (a_F b_F)^{\frac{1}{3}} (a_G b_G)^{\frac{1}{3}} \sqrt{a_G^2 - x^2} \sqrt{a_F^2 - x^2}}{(a_G b_G)^{\frac{1}{3}} \sqrt{a_F^2 - x^2} + (a_F b_F)^{\frac{1}{3}} \sqrt{a_G^2 - x^2}} \end{aligned}$$

also has only one positive zero ζ, with $\zeta^2 = \dfrac{a_F^{\frac{2}{3}} a_G^{\frac{2}{3}} (a_G^{\frac{4}{3}} b_F^{\frac{2}{3}} - a_F^{\frac{4}{3}} b_G^{\frac{2}{3}})}{(a_F b_F)^{\frac{2}{3}} - (a_G b_G)^{\frac{2}{3}}}$.

With the help of the inequalities $a_G < a_F$ and $b_G < b_F$ one can prove that

$$\zeta < \chi < x_{2n}$$

So $H'(x) > 0$ and $H''(x) > 0$ hold for $x \in [x_{2n}, a_G]$. Therefore, H is convex and strictly increasing in this interval. Due to

$$H(x_{2n}) = \varepsilon x_{2n} \quad \text{and} \quad H'(x_{2n}) = f'(x_{2n}) + \varepsilon - (f'(x_{2n}) - (-1)^{2n}\delta\varepsilon) = \varepsilon(1+\delta) > \varepsilon$$

we have $H(x) > \varepsilon x$ for all $x \in (x_{2n}, a_G]$. Thus, $h(x) = H(x) - \varepsilon x$ is positive in $(x_{2n}, a_G]$. We conclude that h has no zero in that interval. □

This completes the proof of Theorem 3.1.5.2 (and the equivalent Theorem 3.1.5.1).

Stability of the number of spheres passing through four points

Let a_1, a_2, a_3, and a_4 be distinct sites in $\mathbf{R}^3$. For a point p of the bisector $B_C(a_1, a_2, a_3, a_4)$ $= B_C(a_1, a_2, a_3) \cap B_C(a_1, a_4)$ we say that $B_C(a_1, a_2, a_3)$ and $B_C(a_1, a_4)$ intersect *transversally* at p if the tangent plane to $B_C(a_1, a_4)$ and the tangent line to $B_C(a_1, a_2, a_3)$ intersect properly at p.

In this section we want to determine under what conditions the surface $B_C(a_1, a_4)$ and the curve $B_C(a_1, a_2, a_3)$ intersect transversally. In particular, if the number of points in the bisector $B_C(a_1, a_2, a_3, a_4)$ is greater than 1, does this property remain under small perturbations of the four points? To cover more general cases, we allow the convex body C to be not symmetric, although the body defined in Section 3.1.5 is, of course, symmetric. We assume C to be smooth and strictly convex.

Definition 3.1.5.9 Let D denote the reflected unit circle of C about its center. Let p be a point on the bisector, and let p_i denote its foot on ∂C_i, $i = 1, 2$. There exists a homothetic copy of D centered at p passing through a_1 and a_2. Let T_{p_i} and T_{a_i} denote the tangent plane to C_i at p_i and to D at a_i, correspondingly.

Clearly T_{p_i} is parallel to T_{a_i}. We consider the tagent plane to $B_C(a_1, a_2)$ at p, we see the following result.

Lemma 3.1.5.10 *For a point $p \in B_C(a_1, a_2)$ let π denote the tangent plane to $B_C(a_1, a_2)$ at p. If T_{p_1} and T_{p_2} are not parallel then the plane π contains the line $T_{p_1} \cap T_{p_2}$ and also the line $T_{a_1} \cap T_{a_2}$. Otherwise, π is parallel to T_{p_1} and T_{p_2}.*

Proof. Let $q, r \in B_C(a_1, a_2)$ be two points close to p. Let q_i, r_i be their foot points from a_i for $i = 1, 2$. Due to Lemma 3.1.1.6 the three planes $\pi(p, q, r)$, $\pi(p_1, q_1, r_1)$ and $\pi(p_2, q_2, r_2)$ intersect in the Desargue line of p, q, and r.

Now let q and r converge to p, so the plane $\pi(p, q, r)$ converges to the tangent plane π; furthermore the plane $\pi(p_1, q_1, r_1)$ converges to T_{p_1}, and analogously the plane $\pi(p_2, q_2, r_2)$ converges to T_{p_2}. Hence π contains $T_{p_1} \cap T_{p_2}$. If T_{p_1} is parallel to T_{p_2} then π is also parallel to T_{p_1}.

Assume that T_{p_1} and T_{p_2} intersect in a line l_{12}. Since T_{a_1} is parallel to T_{p_1}, and T_{a_2} is parallel to T_{p_2}, clearly T_{a_1} and T_{a_2} also intersect in a line parallel to l_{12}. Let t be an arbitrary point of l_{12}, and let t_i be the intersection of T_{a_i} and the line $p\,t$, for $i = 1, 2$. Then the line passing through p_i and t is parallel to the line passing through a_i and t_i for $i = 1, 2$. From the definition of $p \in B_C(a_1, a_2)$ we obtain

$$\frac{|p - t_1|}{|p - t|} = \frac{|p - a_1|}{|p - p_1|} = \frac{|p - a_2|}{|p - p_2|} = \frac{|p - t_2|}{|p - t|},$$

which shows that the points t_1 and t_2 are identical, so the line $T_{a_1} \cap T_{a_2}$ is also contained in π. □

Lemma 3.1.5.10 shows that the tangent plane to $B_C(a_1, a_2)$ at p is either spanned by $T_{p_1} \cap T_{p_2}$ and p, or $T_{a_1} \cap T_{a_2}$ and p, as well as by $T_{a_1} \cap T_{a_2}$ and $T_{a_1} \cap T_{a_2}$, or is parallel to these planes. This means that we can construct the tangent plane to $B_C(a_1, a_2)$ at p without knowing $B_C(a_1, a_2)$.

Corollary 3.1.5.11 *For a point $p \in B_C(a_1, a_2)$ let C_1 and C_2 be smooth at its foot points. The bisector $B_C(a_1, a_2)$ is also smooth at p.*

Corollary 3.1.5.12 *If there exists a tangent line λ to $B_C(a_1, a_2, a_3)$ at $p \in B_C(a_1, a_2, a_3)$ then λ passes through $T_{a_1} \cap T_{a_2} \cap T_{a_3}$ and $T_{p_1} \cap T_{p_2} \cap T_{p_3}$, or λ is parallel to the intersection line of $T_{a_1} \cap T_{a_2}$ or $T_{a_1} \cap T_{a_3}$.*

Lemma 3.1.5.13 *The curve $B_C(a_1, a_2, a_3)$ and the surface $B_C(a_1, a_4)$ intersect transversally at p if and only if the intersection of the four tangent planes $T_{a_1}, \ldots, T_{a_4}$ to D at $a_1, \ldots, a_4$ is empty and there are three of these planes which intersect in a point.*

Proof. Assume that $B_C(a_1, a_2, a_3)$ is transversal to $B_C(a_1, a_4)$ at p.

Suppose that all intersections of three tangent planes are empty. There are two tangent planes which are parallel, the remaining two are also. By Corollary 3.1.5.12 and Lemma 3.1.5.10 the tangent to $B_C(a_1, a_2, a_3)$ at p lies on the tangent plane to $B_C(a_1, a_4)$, this is a contradiction to the assumption.

Let v be the point $T_{a_1} \cap T_{a_2} \cap T_{a_3}$. Then the tangent to $B_C(a_1, a_2, a_3)$ at p is the line $p\,v$ (Corollary 3.1.5.12). If the plane T_{a_4} contained v, then (from Lemma 3.1.5.10) the tangent plane to $B_C(a_1, a_4)$ would contain the line pv, but this is impossible. So the intersection of the four tangent planes $T_{a_1}, \ldots, T_{a_4}$ must be empty.

Conversely, let $\bigcap_{i=1}^{4} T_{a_i}$ be empty, and let v be the point $T_{a_1} \cap T_{a_2} \cap T_{a_3}$. Assume that the tangent plane π to $B_C(a_1, a_4)$ at p contains tangent line λ to $B_C(a_1, a_2, a_3)$ at p which passes through v. Then, by Lemma 3.1.5.10, λ must intersect $T_{a_1} \bigcap T_{a_4}$ at v, and v is the intersection point of the four tangent planes. □

The following theorem states that a small perturbation of four points does not reduce the size of the bisector of these points.

Theorem 3.1.5.14 *Let $B_C(a_1, a_2, a_3, a_4)$ consist of $n \geq 1$ points. Assume further that $B_C(a_1, a_2, a_3)$ and $B_C(a_1, a_4)$ intersect transversally at each $p \in B_C(a_1, a_2, a_3, a_4)$. Then there are 3-dimensional neighborhoods U_{a_1}, U_{a_2}, U_{a_3}, and U_{a_4} of a_1, a_2, a_3 and a_4, correspondingly, such that for each choice of $a'_1 \in U_{a_1}$, $a'_2 \in U_{a_2}$, $a'_3 \in U_{a_3}$ and $a'_4 \in U_{a_4}$ the set $B_C(a'_1, a'_2, a'_3, a'_4)$ consists of at least n discrete points.*

Proof. Because of strictly convexity and smoothness of C the convex distance function d_C based on C is strictly and smooth. The mapping $f : \mathbf{R}^9 \to \mathbf{R}$ defined by $f(P, Q, X) = d_C(P, X) - d_C(Q, X)$ for $P, Q, X \in \mathbf{R}^3$ is continuously differentiable.

Consider the mapping $H \colon \mathbf{R}^{12} \times \mathbf{R}^3 \to \mathbf{R}^3$ defined by

$$H(P, Q, R, S, X) = \begin{pmatrix} f(P, Q, X) \\ f(P, R, X) \\ f(P, S, X) \end{pmatrix}$$

For the four points a_1, a_2, a_3, a_4 we have $H(a_1, a_2, a_3, a_4, x^{(i)}) = 0$ for $1 \leq i \leq n$, where $x^(i)$ for $1 \leq i \leq n$ are the n points of $B_C(a_1, a_2, a_3, a_4)$. Clearly, H is continuously differentiable with respect to X. Furthermore, $B_C(a_1, a_2, a_3)$ and $B_C(a_1, a_4)$ intersect transversally, this corresponds exactly to the condition that the Jacobian matrix is regular at the intersection points $x^{(i)}$. Hence, the determinant of the Jacobian matrix of H fulfills

$$\det \frac{\partial H}{\partial X}(p, q, r, s, x^{(i)}) \neq 0$$

for $1 \leq i \leq n$.

Now the theorem on implicit functions (cf. [54]) implies that there exist neighborhoods $U^{(i)}$ of (a_1, a_2, a_3, a_4) in $\mathbf{R}^{12}$ and differentiable functions $\varphi^{(i)} : U^{(i)} \to \mathbf{R}^3$ such that for each $i \in \{1, \ldots, n\}$ and for all $(p', q', r', s') \in U^{(i)}$

$$H(p', q', r', s', \varphi^{(i)}(p', q', r', s')) = 0$$

holds. If we choose neighborhoods $U_{a_1}, U_{a_2}, U_{a_3}, U_{a_4}$ of a_1, a_2, a_3 and a_4 small enough so that their Cartesian product is contained in each of the $U^{(i)}$ the assertion follows.

In the remaining part of this section, we want to show that this result is applicable to the special convex distance function described in Section 3.1.5.

Lemma 3.1.5.15 *Let C be the convex body constructed in Section 3.1.5. For each tetrahedron $T_i = T(p_i, q_i, r_i)$ the tangent planes to C at its vertices have empty intersection.*

Proof. We use the notations of Section 3.1.5. Using Lemma 3.1.5.6, we can show that the intersection of the tangent planes to C at p and r is the line l_F, and the intersection of the tangent planes to C at q and s is the line l_G, as given by the following parametrizations.

$$l_F : \begin{cases} X = 0 \\ Y = F(x) - xF'(x) \end{cases} \qquad l_G : \begin{cases} Z = 0 \\ Y = G(x) - xG'(x) \end{cases}$$

If l_F intersects l_G, then we would have

$$G(x) - F(x) - x(G'(x) - F'(x)) = 0 \, .$$

But for the $2n$ tetrahedra T_i with vertices p_i, q_i, r_i, s_i, where $i = 1, \ldots, 2n$, we have

$$G(x_i) - F(x_i) - x_i(G'(x_i) - F'(x_i)) = -\varepsilon\delta(-1)^i x_i \neq 0$$

The last tetrahedron to be considered, according to Lemma 3.1.5.8, has the vertices $p = (\xi, F(\xi), 0)$, $r = (-\xi, F(\xi), 0)$, $q = (0, G(\xi), \xi)$, $s = (0, G(\xi), -\xi)$, where $\xi \in (0, x_1)$, we have

$$h(\xi) = G(\xi) - F(\xi) - \varepsilon\xi = 0 \quad \text{and} \quad h'(\xi) = G'(\xi) - F'(\xi) - \varepsilon \neq 0$$

Therefore,

$$G(\xi) - F(\xi) - \xi(G'(\xi) - F'(\xi)) = \varepsilon\xi - \xi(h'(\xi) + \varepsilon) = -\xi h'(\xi) \neq 0$$

according to Lemma 3.1.5.8. □

Now Lemma 3.1.5.15 and Theorem 3.1.5.1 ensure that all conditions for applying Theorem 3.1.5.14 to the convex body constructed in Section 3.1.5 are fulfilled.

Theorem 3.1.5.16 *For each integer $n \geq 0$ we have constructed a smooth, symmetric convex distance function d in 3-space and four points p, q, r, s, such that the bisector $B_C(p, q, r, s)$ contains exactly $2n + 1$ points. If the four points are disturbed independently in small 3-dimensional neighbourhoods, the bisector of the disturbed points still contains at least $2n + 1$ points.*

According to Lemma 3.1.3.5, for four points $a_1, \ldots, a_4$ in 3-space we know that the two ends of the bisector curve $B_C(a_1, a_2, a_3)$ lie on different sides of the bisector surface $B_C(a_1, a_4)$. As we have seen in this section, all intersections of $B_C(a_1, a_2, a_3)$ and $B_C(a_1, a_4)$ must be transversal to permit perturbations of the four points. As a consequence, the bisector $B_C(a_1, a_2, a_3, a_4)$ has to contain an *odd* number of points if perturbations should be allowed.

3.1.6 Wrapping ellipses around a convex skeleton

In this section, we develop an auxiliary result which is used for the proof of the main result, Theorem 3.1.5.2, of Section 3.1.5. This result has already appeared in [51].

Let F and G denote two closed convex curves in the (X, Z)-plane and in the (Y, Z)-plane, respectively, that cross perpendicularly at two points on the Z-axis, as shown in Figure 3.1.6.1. Let C denote the solid that results from wrapping (X, Y)-parallel ellipses around F and G. Surprisingly, C need not be convex (though all intersections with planes containing the Z-axis are!). We analyze under which condition the solid C is convex, and provide one necessary and one sufficient criterion that are easy to use in practice.

Suppose that F and G are smooth and symmetric about the Z-axis. Furthermore, the description of C should be simple (relatively to the descriptions of F and G), and it should allow for exact computations using methods from computer algebra.

The corresponding 2-dimensional problem can be conveniently solved by computing the ellipse through four given points. Can we solve the 3-dimensional problem in the same way, i. e. by wrapping ellipses around the curves F and G that are parallel to the (X, Y)-plane have their axes parallel to the X -and Y-axis, respectively, and are centered at the Z-axis?

In this section we first show that the resulting body C, besides having convex lines of latitudes, has convex lines of longitude (that is, the intersection of C with *any* plane containing the Z-axis is convex). However, C need not be convex; we present a criterion that is equivalent to the convexity of C. Then we derive two simple criteria for convexity, one necessary and one sufficient, that are easy to apply to concrete situations.

We have shown in Section 3.1.5 that general convex distance functions behave differently because there can by any number n of spheres passing through four points

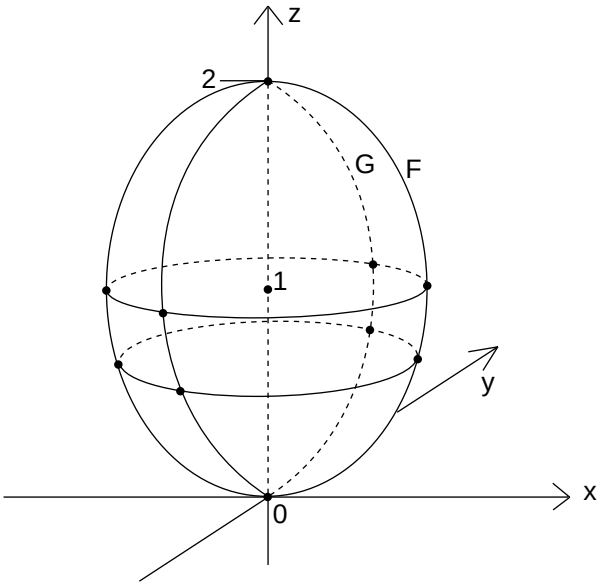

Figure 3.1.6.1: Wrapping ellipses around two convex curves does not always result in a convex solid.

in general position. In order to construct smooth convex example spheres for any given n, we started out with suitable curves F and G and had to flesh them out, we could resort to wrapping ellipses around them.

The lines of longitude

Let $(0,0,0)$ and $(0,0,2)$ be the two "poles" where F and G intersect, as depicted in Figure 3.1.6.1. We restrict ourselves to curves F and G that take on their maximal X-resp. Y-coordinates at $z = 1$. Consequently, we may assume that the lower part of F consists of the concave graph of some function $X = f(Z)$ and its reflection about the Z-axis, where $f(Z)$ is a strictly increasing function in the (Z, X)-plane that is defined for values of Z in $[0, 1]$, has a continuous second derivative on $(0, 1]$, and satisfies $f(0) = 0$. Similarly, let $Y = g(Z)$ be a function in the (Z, Y)-plane with identical properties as f whose graph forms the lower part of G; see Figure 3.1.6.2.

For each $z \in (0, 1]$ let E_z denote the ellipse

$$\frac{X^2}{f(z)^2} + \frac{Y^2}{g(z)^2} = 1 \tag{3.4}$$

that runs through the four points $\big(f(z), 0, z\big)$, $\big(0, g(z), z\big)$, $\big(-f(z), 0, z\big)$, and $\big(0, -g(z), z\big)$ in the plane at height Z parallel to the (X, Y)-plane.

The lower part, V, of the surface of solid C is the union of all ellipses E_z and the origin. By computing normals one can easily show that V is smooth if F and G are.

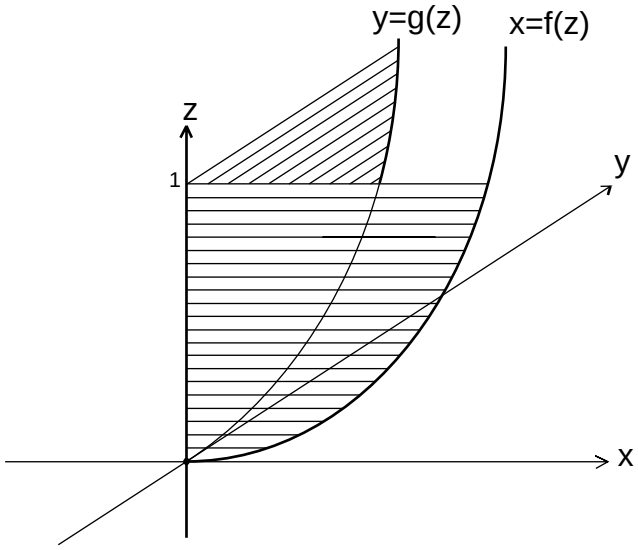

Figure 3.1.6.2: Parametrizing the convex skeleton.

We consider that all lines of longitude on V, defined by

$$F_c = \{(x, y, z); \quad 0 \le z \le 1, \quad (x, y) \in E_z, \quad y = cx\} ,$$

because of symmetry of V we consider only $c \in (0, \infty)$, F_0 and F_∞ are the graphs of f and g, correspondingly.

Lemma 3.1.6.1 *The curves F_c for $c \in (0, \infty)$ are concave.*

Proof. Let $w = (x, y, z)$ be a point on F_c such that $x, y > 0$. From $y = cx$ and from the equation for ellipse E_z we infer

$$x = \frac{f(z)g(z)}{\sqrt{c^2 f(z)^2 + g(z)^2}} , \qquad y = \frac{cf(z)g(z)}{\sqrt{c^2 f(z)^2 + g(z)^2}} .$$

Consequently, a parametrization of the positive part of F_c in the plane $\{Y = cX\}$ is given by

$$\begin{aligned} h_c(z) &= \sqrt{x^2 + y^2} \\ &= \sqrt{1 + c^2} \frac{f(z)g(z)}{\sqrt{c^2 f(z)^2 + g(z)^2}} . \end{aligned}$$

Well, F_c is the graph of h_c in the plane $\{Y = cX\}$.

It is straightforward to verify that

$$\begin{aligned} h_c'(z) &= \sqrt{1 + c^2} \, \frac{c^2 f^3 g' + f' g^3}{(c^2 f^2 + g^2)^{\frac{3}{2}}} \\ h_c''(z) &= \sqrt{1 + c^2} \, \frac{-3c^2 fg(fg' - f'g)^2 + (c^2 f^3 g'' + f'' g^3)(c^2 f^2 + g^2)}{(c^2 f^2 + g^2)^{\frac{5}{2}}} \end{aligned}$$

hold for the derivatives of h_c. With $h_c''(z) \leq 0$ follows that F_c is concave. □

Remark. The assumption for f and g can be slightly weakened. The assertion is true, even if f'' and g'' are discontinuous at finitely many points.

Although both the lines of longitude and the lines of latitude of solid C are convex, the latter by construction, C need not be convex. This will be shown in the subsequent section.

A criterion for convexity

Let $w = (x_0, y_0, z_0)$, where $x_0 > 0$, $y_0 > 0$, be a point of V, and let T denote the tangent plane at w. We have to show that the whole of V lies on one side of T. Let z be a number in $(0, 1]$, we shall compute l, the line of intersection of T with the plane $\{Z = z\}$ and check if ellipse E_z lies on the same side of l. Surface V, and consequently, solid C are convex if and only if this is the case no matter how w and z are chosen.

Lemma 3.1.6.2 *The line l is given by an equation of the form $Y = sX + t$, where*

$$s = -\frac{x_0}{y_0}\frac{g(z_0)^2}{f(z_0)^2}, \qquad t = \left(1 + (z - z_0)\Big(\frac{x_0^2}{f(z_0)^2}\frac{f'(z_0)}{f(z_0)} + \frac{y_0^2}{g(z_0)^2}\frac{g'(z_0)}{g(z_0)}\Big)\right)\frac{g(z_0)^2}{y_0}.$$

Proof. The tangent plane T at w is given by

$$\frac{x_0}{f(z_0)^2}(X - x_0) + \frac{y_0}{g(z_0)^2}(Y - y_0) - \Big(\frac{x_0^2}{f(z_0)^2}\frac{f'(z_0)}{f(z_0)} + \frac{y_0^2}{g(z_0)^2}\frac{g'(z_0)}{g(z_0)}\Big)(Z - z_0) = 0 \quad (3.5)$$

where

$$\left(\frac{x_0}{f(z_0)^2}, \frac{y_0}{g(z_0)^2}, -\Big(\frac{x_0^2}{f(z_0)^2}\frac{f'(z_0)}{f(z_0)} + \frac{y_0^2}{g(z_0)^2}\frac{g'(z_0)}{g(z_0)}\Big)\right)$$

is the normal vector in w.

l is the intersection of T and the plane $\{Z = z\}$, so replaying Z by z in (3.5) gives the equation of l. Solving for Y and applying (3.4) we have the equation in the following form.

$$Y = -\frac{x_0}{y_0}\frac{g(z_0)^2}{f(z_0)^2}X + \left(1 + (z - z_0)\Big(\frac{x_0^2}{f(z_0)^2}\frac{f'(z_0)}{f(z_0)} + \frac{y_0^2}{g(z_0)^2}\frac{g'(z_0)}{g(z_0)}\Big)\right)\frac{g(z_0)^2}{y_0}$$

□

We observe that the ordinate of l must be positive because x_0 and y_0 are positive.

Lemma 3.1.6.3 *E_z lies on the same side of the line l if and only if*

$$\sqrt{s^2 f(z)^2 + g(z)^2} \leq |t| \,.$$

Proof. We determine the two points $v_i = (x_i, y_i), i = 1, 2$, in E_z whose tangents are of slope s, and check if they lie on the same side of line l. The conditions for v_i are

$$\frac{x_i^2}{f(z)^2} + \frac{y_i^2}{g(z)^2} = 1 \,, \qquad -\frac{x_i}{y_i}\frac{g(z)^2}{f(z)^2} = s$$

hence

$$x_i = \pm\frac{sf(z)^2}{\sqrt{s^2 f(z)^2 + g(z)^2}} \,, \qquad y_i = \mp\frac{g(z)^2}{\sqrt{s^2 f(z)^2 + g(z)^2}} \,.$$

Plugging these terms into the equation of l we find that $y_1 - sx_1 - t$ and $y_2 - sx_2 - t$ have the same sign if and only if $\sqrt{s^2 f(z)^2 + g(z)^2} \leq |t|$ holds. □

Now we are ready to prove our main result. Let $T^f_{z_0}(Z) = f(z_0) + f'(z_0)(Z - z_0)$ denote the tangent of $f(Z)$ at z_0 in the (Z, X)-plane. $T^g_{z_0}(Z)$ is defined accordingly.

Theorem 3.1.6.4 *The solid C defined by the functions f and g is convex if and only if for each $z_0, z \in (0, 1]$*

$$|z - z_0| \left| \frac{f'(z_0)}{f(z_0)} - \frac{g'(z_0)}{g(z_0)} \right| \leq \frac{1}{f(z_0)} \sqrt{T^f_{z_0}(z)^2 - f(z)^2} + \frac{1}{g(z_0)} \sqrt{T^g_{z_0}(z)^2 - g(z)^2} \,.$$

Proof. For sake of brevity, let $a(z) = \dfrac{f(z)}{f(z_0)}$ and $b(z) = \dfrac{g(z)}{g(z_0)}$.

Due to Lemma 3.1.6.2 and Lemma 3.1.6.3 the convexity of C is equivalent to

$$\sqrt{\frac{x_0^2}{y_0^2}\frac{g(z_0)^4}{f(z_0)^4} f(z)^2 + g(z)^2} \leq \left(1 + (z - z_0)\Big(\frac{x_0^2}{f(z_0)^2}\frac{f'(z_0)}{f(z_0)} + \frac{y_0^2}{g(z_0)^2}\frac{g'(z_0)}{g(z_0)}\Big)\right)\frac{g(z_0)^2}{y_0}$$

or

$$\sqrt{\frac{x_0^2}{f(z_0)^2} a(z)^2 + \frac{y_0^2}{g(z_0)^2} b(z)^2} \leq 1 + (z - z_0)\Big(\frac{x_0^2}{f(z_0)^2} a'(z_0) + \frac{y_0^2}{g(z_0)^2} b'(z_0)\Big)$$

for each point (x_0, y_0, z_0) in V and each $z \in [0, 1]$. In these expressions, the terms $p = \dfrac{x_0^2}{f(z_0)^2}$ and $q = \dfrac{y_0^2}{g(z_0)^2}$ are two arbitrary nonnegative reals satisfying $p + q = 1$, that is we have

$$\sqrt{pa(z)^2 + qb(z)^2} \leq 1 + (z - z_0)(pa'(z_0) + qb'(z_0))$$

for each z_0, z in $[0, 1]$ and each pair $p, q \geq 0$ such that $p + q = 1$.

We take squares and substitute in the left hand side the expansion

$$a(z) = a(z_0) + a'(z_0)(z - z_0) + a(z) - T^a_{z_0}(z)$$

and the corresponding expansion for $b(z)$. Observing the identities $a(z_0) = 1 = b(z_0)$ and $p - p^2 = pq = q - q^2$ we obtain the condition

$$\begin{aligned}
&(z - z_0)^2 pq(a'(z_0) - b'(z_0))^2 \\
&\leq \; -2p(a(z) - T^a_{z_0}(z))(1 + a'(z_0)(z - z_0) + \frac{1}{2}(a(z) - T^a_{z_0}(z))) \\
&\quad\; -2q(b(z) - T^b_{z_0}(z))(1 + b'(z_0)(z - z_0) + \frac{1}{2}(b(z) - T^b_{z_0}(z))) \\
&\leq \; p(T^a_{z_0}(z)^2 - a(z)^2) + q(T^b_{z_0}(z)^2 - b(z)^2) \; .
\end{aligned}$$

Now the claim follows from the subsequent Lemma 3.1.6.5. □

Lemma 3.1.6.5 *Let $A, B, C \geq 0$. Then the following assertions are equivalent.*

1. *For all $p, q \geq 0$ such that $p + q = 1$ we have $pqC \leq pA + qB$*
2. *$\sqrt{C} \leq \sqrt{A} + \sqrt{B}$*

Proof. Let

$$\mu(p) = pC - \frac{pA}{1 - p} \; .$$

Due to $\lim_{p \to -\infty} \mu(p) = -\infty$ and $\lim_{p \to 1-} \mu(p) = -\infty$ the function μ must take on a local maximum at some value of p less than 1. We have

$$\begin{aligned}
\mu'(p) &= C - \frac{A}{(p-1)^2} \\
\Longrightarrow \qquad \mu'(p) &= 0 \qquad \text{iff} \qquad p = 1 \pm \frac{\sqrt{A}}{\sqrt{C}} \; ,
\end{aligned}$$

so the maximum is taken at $p_0 = 1 - \frac{\sqrt{A}}{\sqrt{C}}$.

If $C < A$ then both (1) and (2) hold; in fact,

$$C < A \leq \frac{A}{1 - p}$$

implies

$$p(C - \frac{A}{1 - p}) < 0 \leq B \; .$$

If $C \geq A$ than $0 \leq p_0 \leq 1$, and by substituting the expression for p_0 into the definition of $\mu(p)$ we obtain the condition

$$p_0 C - \frac{p_0}{1 - p_0} A = (\sqrt{C} - \sqrt{A})^2 \leq B \; .$$

□

Consequences

We start by deriving a simple criterion that is necessary for the convexity of C. It allows to construct simple examples where the solid constructed fails to be convex.

Corollary 3.1.6.6 *For C to be convex it is necessary that the functions f and g satisfy*

$$\left|\frac{f'(z_0)}{f(z_0)} - \frac{g'(z_0)}{g(z_0)}\right| \quad \leq \sqrt{-\frac{f''(z_0)}{f(z_0)}} + \sqrt{-\frac{g''(z_0)}{g(z_0)}}$$

for each z_0 in $[0,1]$.

Proof. By the Taylor formula, see [54], we have for each z in $[0,1]$

$$f(z) = T^f_{z_0}(z) + \frac{1}{2}f''\Big(z_0 + \Theta(z - z_0)\Big)(z - z_0)^2$$

for some $\Theta \in [0,1]$ that depends on z.

Plugging this and the analogous formula for $g(z)$ into the right hand side expression in Theorem 3.1.6.4 yields, after dividing by $|z - z_0|$

$$\begin{aligned}&\left|\frac{f'(z_0)}{f(z_0)} - \frac{g'(z_0)}{g(z_0)}\right| \\ &\quad \leq \frac{1}{f(z_0)}\sqrt{-T^f_{z_0}(z)f''\Big(z_0 + \Theta(z - z_0)\Big) - \frac{1}{4}f''\Big(z_0 + \Theta(z - z_0)\Big)^2(z - z_0)^2} \\ &\quad + \frac{1}{g(z_0)}\sqrt{-T^g_{z_0}(z)g''\Big(z_0 + \rho(z - z_0)\Big) - \frac{1}{4}g''\Big(z_0 + \rho(z - z_0)\Big)^2(z - z_0)^2}\,.\end{aligned}$$

If we let z tend to z_0 then the arguments of f'' and g'' tend to z_0, so the claim follows from the continuity of the second derivatives. □

Example. The functions f and g depicted in Figure 3.1.6.3 generate a smooth body C all of whose lines of latitude and longitude are convex, due to Lemma 3.1.6.1.

But while $f''(\frac{1}{2})$ and $g''(\frac{1}{2})$ are almost zero, the first derivatives differ considerably at $z = \frac{1}{2}$. Therefore, Corollary 3.1.6.6 implies that C is not convex.

Finally, we want to derive a criterion sufficient for the convexity of the solid C.

Corollary 3.1.6.7 *Suppose that both $f(z)f'(z)$ and $g(z)g'(z)$ are decreasing functions. Then the solid C obtained by wrapping ellipses around F and G is convex.*

Proof. Let $z_0 \in (0,1]$ and we consider the function $H(z)$, defined by

$$H(z) = f^2(z) - f^2(z_0) - 2f(z_0)f'(z_0)(z - z_0), \qquad z \in [0,1].$$

$H'(z) = 2f(z)f'(z) - 2f(z_0)f'(z_0)$ is positive for $z \in [0, z_0)$, and $H'(z)$ is negative for $z \in (z_0, 1]$. Since $H(z_0) = 0$, and $H'(z_0) = 0$, we have $H(z) \leq 0$, i. e.

$$f^2(z) \leq f^2(z_0) + 2f(z_0)f'(z_0)(z - z_0)\,.$$

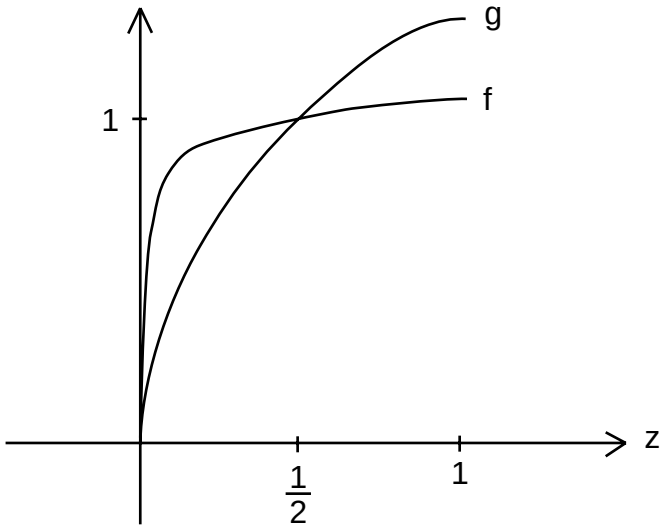

Figure 3.1.6.3: These functions f and g do not generate a convex solid.

After adding $f'(z_0)^2(z-z_0)^2$ on either side we obtain

$$f'(z_0)^2(z-z_0)^2 \leq f(z_0)^2 + 2f(z_0)f'(z_0)(z-z_0) + f'(z_0)^2(z-z_0)^2 - f(z)^2 \ ,$$

hence

$$|z-z_0|\frac{f'(z_0)}{f(z_0)} \leq \frac{1}{f(z_0)}\sqrt{T^f_{z_0}(z)^2 - f(z)^2} \ .$$

An analogous formula holds for $g(z)$. Due to

$$|z-z_0|\left|\frac{f'(z_0)}{f(z_0)} - \frac{g'(z_0)}{g(z_0)}\right| \leq |z-z_0|\left(\frac{f'(z_0)}{f(z_0)} + \frac{g'(z_0)}{g(z_0)}\right) \ ,$$

Theorem 3.1.6.4 applies and yields the convexity of C. □

3.2 Polyhedral convex distance functions

Now we consider the class of polyhedral convex distance funtions in three dimensions. We will see that they have special properties that can be exploited to estimate their complexity and to compute bisectors and diagrams. We also show how to deal with degenerate cases of bisectors.

3.2.1 The bisector of two sites

If the line $a_1\,a_2$ is parallel to a facet f of the polytope C then the intersection of the two convex cones spanned by a_i and $f + a_i$, $i = 1, 2$, is a three-dimensional region of the bisector $B_C(a_1, a_2)$. If $a_1\,a_2$ is not parallel to a facet of C then it is also not parallel to a line segment of ∂C, so the silhouette Γ_{12} is a simple closed curve, due to Lemma 3.1.1.2. By Lemma 3.1.1.3 we have the following result.

Corollary 3.2.1.1 *The bisector $B_C(a_1, a_2)$ is homeomorphic to a plane iff there is no facet of C parallel to the line $a_1\,a_2$.*

We assume for the moment that there is no facet of C parallel to the line $a_1\,a_2$. We want to construct the bisector $B_C(a_1, a_2)$.

Let π be an arbitrary plane perpendicular to $a_1\,a_2$. In a direction parallel to $a_1\,a_2$ we project the facets of H_{12} and H_{21} into the plane π. Let C_{12} resp. C_{21} denote the images of these two sets of facets on π. So C_{12} and C_{21} are two convex subdivisions of the convex set with boundary γ that is the projection of the silhouette Γ_{12}. *A convex subdivision* is a partition of a convex set into a finite number of open convex sets. From two planar convex subdivisions a new convex subdivision can be constructed, namely the set of all intersections of two of their sets. This is called the *overlay of two subdivisions*, see [34]. The overlay of C_{12} and C_{21} can consist of as many as $O(k^2)$ faces, edges, and vertices, where k is the number of facets of C.

Lemma 3.2.1.2 *Let a_1 and a_2 be in general position with respect to the polytope C. The bisector $B_C(a_1, a_2)$ is a polyhedral surface consisting of n facets, n being the number of convex sets of the overlay of the two subdivisions C_{12} and C_{21}.*

Proof. Let s be an arbitrary convex set of the overlay. So there are two facets $s_1 \subset H_{12} + a_1$ on ∂C_1 and $s_2 \subset H_{21} + a_2$ on ∂C_2 such that s is the intersection of the projections of s_1 and s_2. We show that s_1 and s_2 *generate* a facet of $B_C(a_1, a_2)$, this means that there is a facet in $B_C(a_1, a_2)$ whose foot set on C_i is contained in s_i, for $i = 1, 2$.

For a point u_0 in s let $u_1 \in s_1$ and $u_2 \in s_2$ be the two points such that u_0 is the image of u_1 and u_2 of the parallel projection in π. So the line $u_1\,u_2$ is parallel to $a_1\,a_2$. Due to Lemma 3.1.1.3 the intersection of rays $\overrightarrow{a_1\,u_1}$ and $\overrightarrow{a_2\,u_2}$ is a point p in $B_C(a_1, a_2)$. Let T_{u_1} and T_{u_2} be the two supporting planes of s_1 and s_2, und let T_{a_1} resp. T_{a_2} be the two planes translated to a_1 resp. a_2. Due to Lemma 3.1.5.10, the plane passing through $T_{u_1} \cap T_{u_2}$ and $T_{a_1} \cap T_{a_2}$ is the plane tangent to $B_C(a_1, a_2)$ in point p. Therefore all bisector points generated by s_1 and s_2 lie in the plane spanned by $T_{u_1} \cap T_{u_2}$ and $T_{a_1} \cap T_{a_2}$. □

To compute the facet of the bisector corresponding to a facet s of the overlay it is sufficient to perform the construction described above for the vertices of s.

3.2.2 Computing the bisector of two sites

From Lemma 3.2.1.2 we know that the bisector $B_C(a_1, a_2)$ can be computed from the overlay of the two subdivisions of C_{12} and C_{21}. The topological structures of the bisector $B_C(a_1, a_2)$ and the overlay are the same. In particular, each facet touching the boundary of the overlay corresponds to an unbounded facet of the bisector.

It remains to compute the overlay. This can be done by a method of Guibas and Seidel [34]. They describe a topological sweep for constructing the overlay of two subdivisions of size m resp. n in optimal time $O(m+n+L)$. Here L is the size of the output, i. e. the overlay.

Lemma 3.2.2.1 *The bisector $B_C(a_1, a_2)$ of two sites a_1, a_2 in 3-space for a convex polytope C can be computed in optimal time $\Theta(n+k)$, where n is the number of vertices of $B_C(a_1, a_2)$, and k is the number of the facets of C.*

The lemma still holds for degenerate cases where facets of C are parallel to $a_1\,a_2$. We can first compute the bisector for the non-parallel facets as described above and then add the three-dimensional regions which stem from the parallel ones.

3.2.3 The bisector of three sites

Again we concentrate first on general position and explain the degenerate cases afterwards.

The existence and the number of connected components of the bisector of three sites a_1, a_2, and a_3 can be determined using Lemma 3.1.2.4 and Lemma 3.1.2.6.

We also know from Lemma 3.1.2.6 that $B_C(a_1, a_2, a_3)$ consists of a finite number of pieces which are homeomorphic to a line. From the fact that the bisector of two sites is a polyhedral surface by Lemma 3.2.1.2 and $B_C(a_1, a_2, a_3) = B_C(a_1, a_2) \cap B_C(a_1, a_3)$, we can conclude that $B_C(a_1, a_2, a_3)$ must be composed only of line segments and rays.

So we could, in principle, compute $B_C(a_1, a_2, a_3)$ by intersecting two bisectors of two sites, but we will see that there is a more efficient method. We first give some statements about the structure and the complexity.

Lemma 3.2.3.1 *Let p be a vertex in $B_C(a_1, a_2, a_3)$. Then at least one of its foot points on ∂C_1, ∂C_2, and ∂C_3 lies on an edge of that surface. Each connected component of $B_C(a_1, a_2, a_3)$ contains at least one point with a foot point on such an edge.*

Proof. Let p_i be the foot points of p on ∂C_i, $i = 1, 2, 3$. Assume that none of them lies on an edge, see Figure 3.2.3.1. Let T_{p_i} be the tangent plane to C_i at p_i, so T_{p_i} is also the supporting plane of a facet f_i on ∂C_i. Let T_{a_i} be T_{p_i} translated to a_i, $i = 1, 2, 3$. By Corollary 3.1.5.12 the line passing through the intersection points of $\{v\} = \cap_{i=1}^{3} T_{p_i}$ and $\cap_{i=1}^{3} T_{a_i}$ contains p and a line segment of $B_C(a_1, a_2, a_3)$ whose foot set on ∂C_i lies on the facet f_i. But then the point p is an inner point of a line segment of $B_C(a_1, a_2, a_3)$ and not a vertex, see Figure 3.2.3.1.

A connected component of $B_C(a_1, a_2, a_3)$ without any vertex could only be a whole line. Its set of foot points would be a line segment contained in one facet on each of

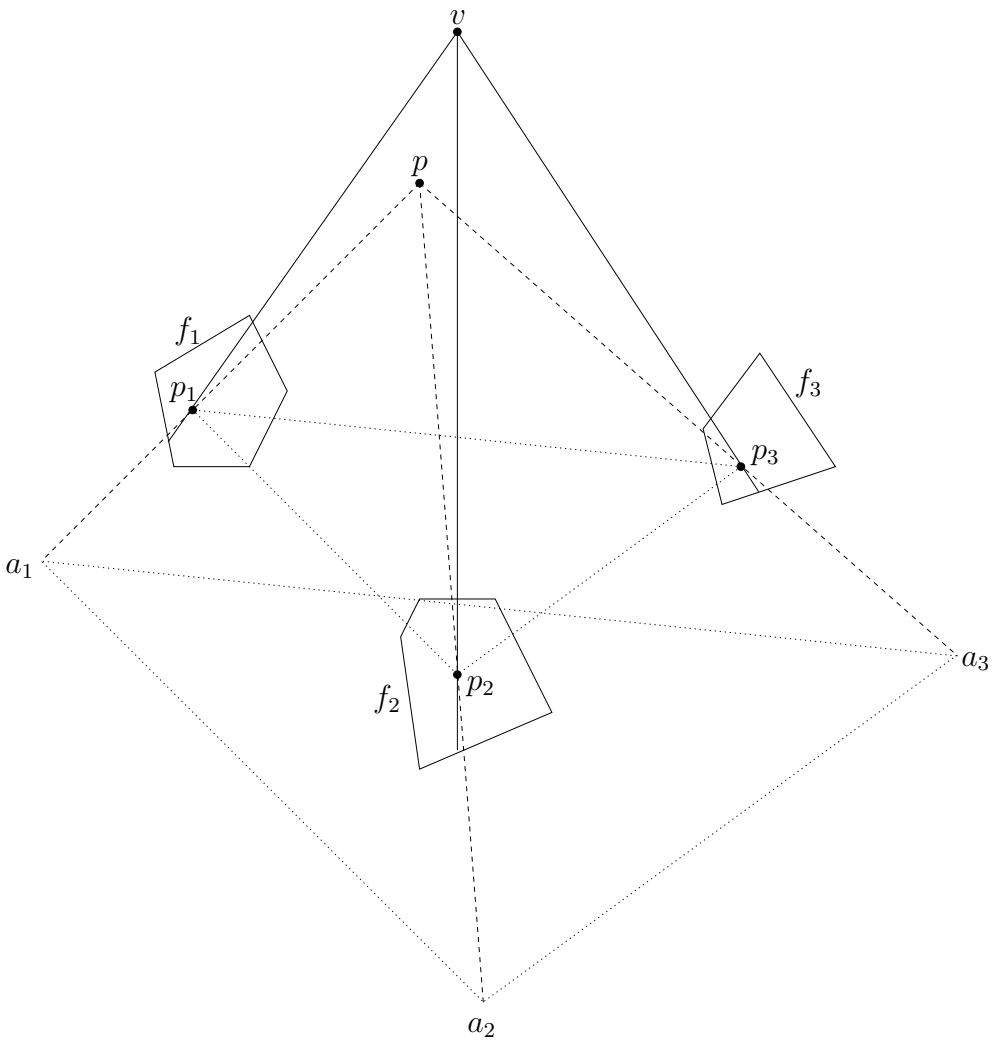

Figure 3.2.3.1: A bisector point $p \in B_C(a_1, a_2, a_3)$ and its foot points p_i which lie on the facets $f_i \subset \partial C_i$, $i = 1, 2, 3$. Point p can only be a vertex of $B_C(a_1, a_2, a_3)$ if at least one of its foot points lies on a edge of a facet.

the three spheres ∂C_1, ∂C_2, and ∂C_3. Translated to C, the end points of these three different line segments would have to coincide, a contradiction. □

By Lemma 3.2.3.1 each change of the directions of line segments of $B_C(a_1, a_2, a_3)$ means that at least one of the three foot sets on C_i changes its facet.

Let k be the number of facets of C, and let n_1 be the number of facets of the set H_{123}, analogously, let n_2 resp. n_3 be the number of facets of H_{213} resp. H_{312}. Due to Lemma 3.1.2.3, we have $k = n_1 + n_2 + n_3$, let $m = n_1 n_2 n_3$.

Lemma 3.2.3.2 *The bisector $B_C(a_1, a_2, a_3)$ contains at most $O(m)$ vertices.*

Proof. Let $\overline{p\,q}$ and $\overline{r\,s}$ be two different edges of $B_C(a_1, a_2, a_3)$ with foot vertices p_i, q_i, r_i, and s_i on ∂C_i. Let p_i, q_i be on the facet f_i, and r_i, s_i on the facet g_i, $i = 1, 2, 3$. Due to Lemma 3.2.3.1, the three lines $p_i\,q_i$, $i = 1, 2, 3$, intersect in a point which is

the intersection of the three corresponding supporting planes f_1, f_2, and f_3. Because of the convexity of the facets f_i and g_i there is at least one i such that f_i and g_i are two different facets. Therefore, two different edges like $\overline{p\,q}$ and $\overline{r\,s}$ in $B_C(a_1, a_2, a_3)$ correspond to two different groups of facets (f_1, f_2, f_3) and (g_1, g_2, g_3). Then by Lemma 3.1.2.3 there are at most m vertices in $B_C(a_1, a_2, a_3)$. □

Clearly, the number m could be in $O(k^3)$ in the worst case if $n_i \in O(k)$. But in this case we have better estimate on the complexity of the bisector $B_C(a_1, a_2, a_3)$.

Lemma 3.2.3.3 *The bisector $B_C(a_1, a_2, a_3)$ contains at most $O(k^2)$ vertices.*

Proof. Let v be a vertex of $B_C(a_1, a_2, a_3)$, so there is an $i \in \{1, 2, 3\}$ such that the projection of v on C_i lies on an edge e of C_i.

For each edge e on $H_{123} + a_1$ we estimate the maximal number of vertices of $B_C(a_1, a_2, a_3)$ whose projections lie on e.

Due to Lemma 3.2.1.2 the part of the bisector $B_C(a_1, a_2)$ whose foot points lie on e is a connected polygonal chain which lies on the cone $\mathcal{K}$ with apex a_1 and passing through e, in particular, each ray from a_1 intersects this chain in a point, and two vertices of the chain correspond to two different edges of ∂C_2. This means that the projections of two vertices on ∂C_2 lie on at least two different edges. Therefore the chain contains at most $O(n_2)$ line segments. Analogously, the part of the bisector $B_C(a_1, a_3)$ is also a connected polygonal chain in the cone $\mathcal{K}$. So the intersection points of these two polygonal chains are exactly the points in $B_C(a_1, a_2, a_3)$ whose number is at most $O(n_2 + n_3)$. Therefore there exist at most $O(n_2 + n_3) \in O(k)$ vertices of $B_C(a_1, a_2, a_3)$ whose projections lie on e. Because the number of edges of H_{123}, H_{213}, and H_{312} is $O(k)$, there are at most $O(k^2)$ vertices in $B_C(a_1, a_2, a_3)$. □

In the degenerate cases the bisector is more complicated. If the plane $\pi(a_1, a_2, a_3)$ through a_1, a_2, and a_3 is parallel to a facet f of C then the intersection of the three convex cones spanned by a_i and $f + a_i$, $i = 1, 2, 3$, is a three-dimensional region of the bisector $B_C(a_1, a_2, a_3)$.

We consider the other degenerate case that the line $a_1\,a_2$ is parallel to a facet f of C and $a_1\,a_3$ is not. Let π be a plane which is parallel to the triangle $\triangle(a_1, a_2, a_3)$ and intersects the facets $f + a_i$, $i = 1, 2$. By Lemma 2.2.3.1 the bisector for the convex set $\pi \cap C_1$ may be a polygonal chain, so the bisector $B_C(a_1, a_2, a_3)$ can contain two-dimensional facets. We can construct such facets in following way. Let e be a line segment of the polygonal chain of the bisector based on $\pi \cap C_i$, and let g_i be the facet of the projection of e on ∂C_i, $i = 1, 2, 3$. So $g_1 = f + a_1$ and $g_2 = f + a_2$, and the line $a_1\,a_2$ is parallel to g_1 and g_2. Let l be the intersection line of the supporting planes of g_i, $i = 1, 2, 3$, let l' be the other intersection line of the supporting planes of g_i translated to a_i, $i = 1, 2, 3$, and let h be the plane passing through l and l'. Then

the intersection of h with the cones spanned by a_1, g_1 resp. a_2, g_2 is a facet in the bisector $B_C(a_1, a_2, a_3)$, due to Corollary 3.1.5.12.

3.2.4 Computing the bisector of three sites

Lemma 3.1.2.6 and its proof have already shown all basic ideas for constructing of three sites. The bisector is naturally ordered, and each of its points can be constructed by central projection from the solution of a two-dimensional bisector problem. Here, in the polyhedral case, the bisector consists only of line segments and rays, so we only need to determine the vertices and the rays' directions, see Lemma 3.2.3.1.

We concentrate on the construction of the foot sets of $B_C(a_1, a_2, a_3)$, since the bisector can easily be derived from the three foot sets (translated to C), which are monotone in diretion perpendicular to $\pi(a_1, a_2, a_3)$, and which are contained in H_{123}, H_{213}, and H_{312}, respectively.

First we construct the silhouettes and the sets H_{123}, H_{213}, and H_{312}. Then we also know the end points of the foot sets of all connected components, they are the points where all three sets meet, see Lemma 3.1.2.6. Here, these end points are vertices of C.

It only remains to simultaneously follow, for each component, its three (translated) foot sets from the common start point down to the common end point through the facets of C. Two cases occur.

Case 1: the actual position is a vertex of C, for at least one of the foot sets. This is the case at the begining for all three, but this can also occur in the middle of a foot set, for one or two, or all three. If the actual position in a foot set is not a vertex then it is clear in which facet the foot set continues. If the actual position in a foot set is a vertex then it continues in one of the adjacent facets below. For a position slightly below the vertex we compute the intersection of a plane parallel to $\pi(a_1, a_2, a_3)$ with the facets which are adjacent to the vertex, and we solve the two-dimensional bisector problem, this determines the facets in which we continue and the directions. The next actual position is the first intersection of one of the foot sets with the boundaries of the facets, by Lemma 3.2.3.1.

Case 2: the actual position is not a vertex of C for all three foot sets. This is only the case if the actual position is at an edge of C for at least one of the foot sets, again by Lemma 3.2.3.1. Then the continuation is clear after a few tests of the facets adjacent to the actual edges. The next actual position is determined as in Case 1.

Lemma 3.2.4.1 *Let C be a polytope consisting of k facets. The bisector $B_C(a_1, a_2, a_3)$ of three sites in general position can be computed in output-sensitive optimal time $O(k + l)$, where l is the number of line segments of $B_C(a_1, a_2, a_3)$.*

Proof. The computation of H_{123}, H_{213}, and H_{312} costs $O(k)$ time.

In Case 1 we only need to compute the intersection of a plane parallel to $\pi(a_1, a_2, a_3)$ with the facets which are adjacent to the actual vertex. Each facet occurs at most once in such a computation because the actual vertex must be its highest point. Thus, all those intersections together require time $O(k)$. The solutions of the two-dimensional bisector problems involve the same facets, so this can also be done in total time $O(k)$, we do not even need to use the binary serch technique from Lemma 2.2.4.1.

For determining the next actual position we simultaneously sweep along the boundaries of the three actual facets until the first intersection of one of the foot sets with a boundary edge is found. Altogether, these steps need time proportional to the number of the vertices of C, which is also $O(k)$.

In Case 2 each step needs only constant time to determine the facets adjacent to the actual boundary edge. □

3.2.5 The bisector of four sites

In Lemma 3.1.3.2 we have seen that the bisector of four sites in general position for a tetrahedron C is at most one point, and we have conjectured that no other convex body, except for the ellipsoids, has the same property. In the following we will show this for all polytopes.

We proceed in two steps and concentrate first on polytopes with exactly five facets. There are two types of polytopes with 5 facets: Type I has 5 vertices and 8 edges, Type II has 6 vertices and 9 edges, see Figure 3.2.5.1. This can easily be shown using Euler's remarkable formula

$$v - e + f = 2$$

for the number v of vertices, e of edges, and f of facets of a polytope, and the relations $v \leq 2(f-2)$, $e \leq 3(f-2)$, see [50, 70].

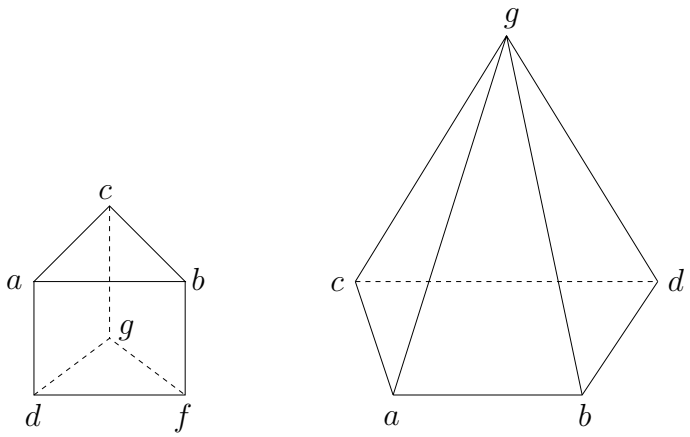

Figure 3.2.5.1: Two different types of polytopes with five facets: to the left, Type I, to the right, Type II.

Lemma 3.2.5.1 *Let C be a polytope with five facets. Then there are four sites in general position such that their bisector based on C consists of at least two points.*

Proof. We choose three facets f_1, f_2, and f_3 of C such that they do not intersect in a vertex of C. For Type I we choose the facets $\triangle(a, b, c)$, $\triangle(d, f, g)$, and $\square(a, b, d, f)$, and for Type II we choose the facets $\triangle(a, b, g)$, $\triangle(c, d, g)$, and $\square(a, b, c, d)$, see Figure 3.2.5.1. Now we assume that the intersection point, u, of the three supporting planes of these facets exists. Point u lies outside C by construction.

For each chosen facet f_i, we consider a line passing through u and intersecting f_i in a line segment l_i of length > 0. The fourth line passes through u and an interior point of C. This line can not intersect any of the chosen facets, so it must intersect the two remaining facets. These two facets are adjacent at edge $\overline{b\,f}$ for Type I and at vertex g for Type II. Therefore the fourth line can be chosen in such way that the length of the line segment, l_4, from the intersection with one facet to the other is arbitrary small.

Now it is easy to choose two points on each of l_1, l_2, and l_3, and a sufficiently short l_4 such that the first points in these three line segments and the start point of l_4 are not coplanar and form a tetrahedron which is homothetic to the tetrahedron formed by the respective second points and the endpoint of l_4, see Figure 3.2.5.2. The center of homothety is u, and it is clear that we have enough freedom to choose the points such that the tetrahedra are in general position.

If the point u does not exist then the construction is quite similar, using parallel lines. □

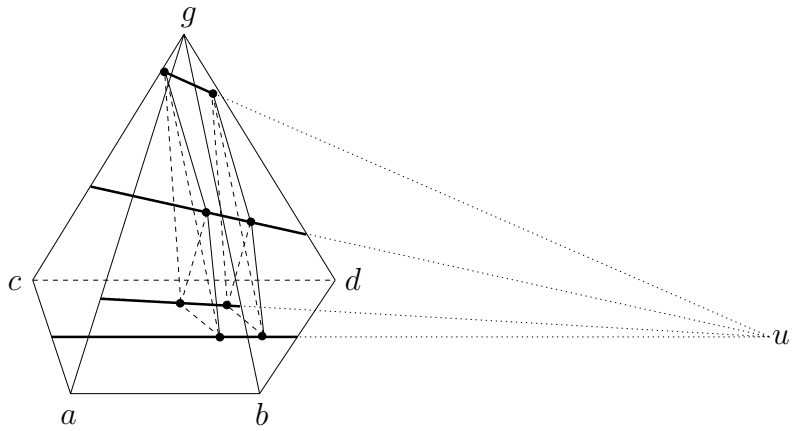

Figure 3.2.5.2: Constructing two homothetic tetraedra in a polytope with five facets.

This result can be generalized to polytopes with more facets, as the next lemma shows.

Lemma 3.2.5.2 *Let C be a polytope with at least six facets. There are four sites in general position such that their bisector based on C consists of at least two points.*

Proof. If each pair of two facets of C is adjacent in at least a vertex then we can proceed similar to Lemma 3.2.5.1 for Type II.

Now we assume that there are two non-adjacent facets f_1 and f_2 of C whose supporting planes intersect in a line l outside of C. The remaining case of only pairs of parallel facets, for example a cube, can be dealt with analogously, see also Section 3.3.2.

Let π be a plane passing through l and an interior point of C, so π does not touch f_1 and f_2. The intersection $\pi \cap C$ is a convex polygon. Let u be the intersection of l and the supporting line of one of this polygon's edges, e. The rest of the construction is similar to the proof of Lemma 3.2.5.1. Point u will be the center of homothety. We have four line segments: l_1 and l_2 are intersections of the facets f_1 resp. f_2 with lines from u through these facets, l_3 is the edge e, and l_4 is a sufficiently short segment on the line from u through one or two other edges of this polygon, see Figure 3.2.5.3. □

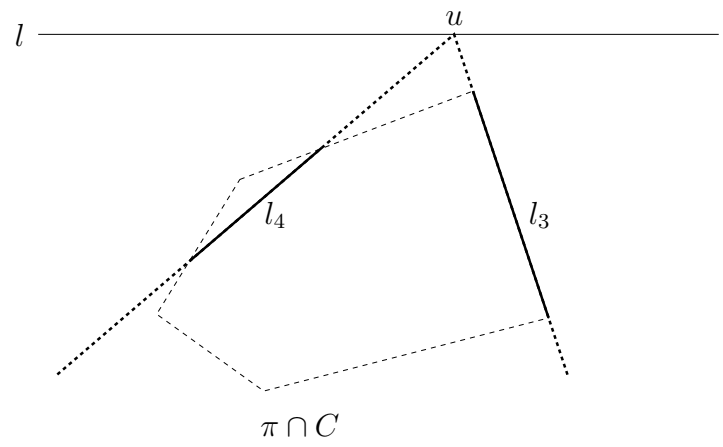

Figure 3.2.5.3: The two rays from u intersect the boundary of the polygon $\pi \cap C$ in a line segment, l_3, and two points, the end points of l_4.

From Theorem 3.1.5.1 and its proof we know that there is no general upper bound for the complexity of a bisector of four sites, even for polytopes. We can, however, bound its complexity in terms of the number of facets of the unit polytope.

Lemma 3.2.5.3 *The bisector $B_C(a_1, a_2, a_3, a_4)$ contains at most $O(k^2)$ connected components for a polytope C containing k facets.*

Proof. $B_C(a_1, a_2, a_3, a_4)$ is a subset of $B_C(a_1, a_2, a_3)$ whose complexity is bounded by $O(k^2)$, see Lemma 3.2.3.3. It is not difficult to see that each line segment of $B_C(a_1, a_2, a_3)$ contains at most two components of $B_C(a_1, a_2, a_3, a_4)$.

Let $\overline{p\,q}$ be a line segment of $B_C(a_1, a_2, a_3)$, and let $\overline{p_i\,q_i}$ be its foot sets on ∂C_i translated to ∂C, $i = 1, 2, 3$. The three lines $p_i\,q_i$, $i = 1, 2, 3$, intersect in a point v which is also the intersection of the three supporting planes of the facets containing

$\overline{p_i\, q_i}$, and v is the center of homothety of the triangles $\triangle(p_1, p_2, p_3)$ and $\triangle(q_1, q_2, q_3)$. Let p_4 be the intersection of the three rays from p_i parallel to $a_i\, a_4$, $i = 1, 2, 3$, and let q_4 be the intersection of the other three rays from q_i parallel to $a_i\, a_4$, $i = 1, 2, 3$. So the tetrahedra $T(p_1, p_2, p_3, r)$, $T(q_1, q_2, q_3, s)$, and $T(a_1, a_2, a_3, a_4)$ are homothetic. The three points p_4, q_4 and v are collinear. Therefore, if there is a bisector point of $B_C(a_1, a_2, a_3, a_4)$ whose foot points lie on $\overline{p_i\, q_i}$, $i = 1, 2, 3$, then the foot point on ∂C_4, translated to ∂C, must be on the line segment $\overline{p_4\, q_4}$.

Because each ray from v can intersect the boundary of ∂C in zero, one, or two points, or a line segment, the intersection $\partial C \cap \overline{p_4\, q_4}$ can consist of at most two points or a line segment in $B_C(a_1, a_2, a_3, a_4)$. By Lemma 3.2.3.3 we have the claim. □

The above proof already contains the main idea of how one can find the bisector of four sites in general position. This is summarized in the following result.

Lemma 3.2.5.4 *The bisector $B_C(a_1, a_2, a_3, a_4)$ can be computed in $O(k^2 + kl)$ time, where l is the number of line segments of $B_C(a_1, a_2, a_3)$.*

Proof. First we compute the four sets H_{1234}, H_{2134}, H_{3124}, and H_{4123} in time $O(k)$. If one of them is empty then $B_C(a_1, a_2, a_3, a_4)$ is also empty.

Otherwise, we compute the bisector $B_C(a_1, a_2, a_3)$ in time $O(k+l)$, as described in Lemma 3.2.4.1, and for each line segment of $B_C(a_1, a_2, a_3)$ we determine which part of it belongs to $B_C(a_1, a_2, a_3, a_4)$, by the method given in the proof of Lemma 3.2.5.3. □

3.3 Special L_p metrics

The L_p metrics are defined by the distance functions

$$\begin{aligned} d_p(q, r) &= (|q_x - r_x|^p + |q_y - r_y|^p + |q_z - r_z|^p)^{1/p}, \quad \text{for } 1 \le p < \infty, \\ d_\infty(q, r) &= \max\{|q_x - r_x|, |q_y - r_y|, |q_z - r_z|\} \end{aligned}$$

for two points $q = (q_x, q_y, q_z)$ and $r = (r_x, r_y, r_z)$, depending on the parameter p.

The bisector of two sites is homeomorphic to a plane by Lemma 3.1.1.3 for all p, for $p \in \{1, \infty\}$ we have to assume general position because here the unit spheres are polyhedra.

Except for $p = 1$ and $p = \infty$, the unit body $U_p := \{q \in \mathbf{R}^3 : d_p(O, q) = 1\}$ is smooth and strictly convex, so the bisector of three sites is homeomorphic to a line, due to Corollary 3.1.2.7. This is also true for $p \in \{1, \infty\}$, as we will show in Lemma 3.3.2.2 and Lemma 3.3.3.2.

Things are much more complicated for the bisector of four sites. For $p = 2$ we have the Euclidean unit sphere, of course, and the bisector of four non-coplanar sites

consists of exactly one point. Unfortunately this property is no longer true for $p \neq 2$, which follows from the results by Shaidenko [73] and by Goodey [32], see Section 3.1.3. If $p \notin \{1, 2, \infty\}$, we even know by Lemma 3.1.3.5 that there is a bisector of four sites which contains at least three points, due to smoothness and strict convexity of U_p.

By Lemma 3.1.3.4 the question about the complexity of the bisector of four sites is equivalent to the question how many unit spheres pass through four given points. For L_p, Bezout's theorem provides an upper bound of $(p-1)^3$, see [37], but this bound can only be achieved if all complex solutions are counted whereas we are only interested in real valued solutions. Surprisingly, there is an upper bound to this number which is independent of p, but depends only on the dimension, as Lê [57] has shown.

The following sections present some results about bisectors for some L_p metrics. For L_4 we show a concrete example that the bisector of four sites can contain three isolated points. For L_∞ and L_1 we refine the results from Section 3.2 and obtain precise assertions about the shape of the bisector and tight bounds for their complexity.

3.3.1 The L_4 metric

We give an example for a bisector of four sites which contains exactly three points. The method for proving this is also interesting in its own right because it uses techniques from computer algebra and is completely independent from the result by Shaidenko and Goodey.

Let $p = (0, 0, 0)$, $q = (1, \frac{1}{2}, -2)$, $r = (-1, -\frac{3}{2}, \frac{1}{3})$, $s = (-3, -4, -\frac{1}{2})$.

Theorem 3.3.1.1

(i) There are exactly three L_4-spheres passing through the four points p, q, r, s.

(ii) There are 3-dimensional neighborhoods U_p, U_q, U_r, U_s for p, q, r, and s, correspondingly, such that for each choice of $p' \in U_p$, $q' \in U_q$, $r' \in U_r$, and $s' \in U_s$ there are at least three L_4-spheres passing through p', q', r', s'.

Proof.

(i) We have to determine the cardinality of the intersection $B(p,q) \cap B(p,r) \cap B(p,s) = B(p,q,r,s)$ which is the set of common zeroes of the three polynomials

$$f(p,q,X), \quad f(p,r,X), \quad f(p,s,X) \tag{3.6}$$

where

$$\begin{aligned} f(p,q,X) &= (X_1 - p_1)^4 + (X_2 - p_2)^4 + (X_3 - p_3)^4 \\ &\quad -(X_1 - q_1)^4 - (X_2 - q_2)^4 - (X_3 - q_3)^4, \end{aligned}$$

and $p_1, p_2, p_3, q_1, \ldots, s_3$ denote the concrete coordinates of the four points p, q, r, s given above (note that these polynomials are of degree 3 since the forth powers cancel out).

Using the MAPLE [15] implementation of Buchberger's algorithm [14] we find that the ideal generated by the polynomials in (3.6) has a Gröbner basis

$$\{\ aX_1 + g_1(X_3),\ bX_2 + g_2(X_3),\ g_3(X_3)\ \} \tag{3.7}$$

where $ab \neq 0$, g_1 and g_2 are polynomials in X_3 of degree 26, and g_3 is a polynomial in X_3 of degree 27. The system (3.7) has the same zeroes (X_1, X_2, X_3) as (3.6) does, but due to the diagonal form of (3.7), it is much easier to determine the zeroes.

An application of Sturm sequences [42], as implemented in MAPLE, yields that g_3 has exactly 3 real roots $x_3^{(1)}, x_3^{(2)}, x_3^{(3)}$ (which lie in the intervals $(-16, -8)$, $(-8, -4)$, $(-4, 0)$). For each of the three values of x_3 one can, from system (3.7), uniquely determine the values of x_2 and of x_1. Let $x^{(i)}$ be $(x_1^{(i)}, x_2^{(i)}, x_3^{(i)})$ for $i = 1, 2, 3$. Consequently, $B(p, q, r, s)$ is of cardinality 3.

(ii) The claim directly follows from Theorem 3.1.5.14. □

3.3.2 The L_∞ metric

Let U_∞ be the unit sphere of the L_∞ metric, U_∞ is an axis-parallel cube with eight vertices $u_1, \ldots, u_8$, twelve edges and six facets, see Figure 3.3.2.1, where

$$\begin{array}{llll} u_1 = (1,1,1), & u_2 = (1,1,-1), & u_3 = (1,-1,-1), & u_4 = (1,-1,1), \\ u_5 = (-1,-1,1), & u_6 = (-1,-1,-1), & u_7 = (-1,1,-1), & u_8 = (-1,1,1). \end{array}$$

With the help of our results from Section 3.1 and Section 3.2 it is not difficult to derive properties of the bisectors of two, three, or four sites in general position. As usual, let $C_i = U_\infty + a_i$.

Lemma 3.3.2.1 *The bisector $B_\infty(a_1, a_2)$ based on the L_∞ metric consists of at most seven facets, each of which is parallel to one of the following nine planes,*

$$\begin{array}{lllll} X = 1, & Y = 1, & Z = 1, & X - Y = 0, & X + Y = 0, \\ Y - Z = 0, & Y + Z = 0, & X - Z = 0, & X + Z = 0. & \end{array}$$

Proof. Because of general position and symmetry of $C = U_\infty$ each of H_{12} and H_{21} consists of exactly three facets which are adjacent to a common vertex, while their boundary, the silhouette Γ_{12}, is always a polygonal chain with six vertices.

Let $f \in H_{12}$ and $g \in H_{21}$, and let h be a facet in $B_\infty(a_1, a_2)$ whose foot sets on ∂C_1 resp. ∂C_2 are contained in $f + a_1$ resp. $g + a_2$. Either f and g are parallel and then h is also parallel to them, or f and g are adjacent to a common edge e on Γ_{12}, then the facet h is parallel the plane spanned by O and e, by Lemma 3.1.5.10.

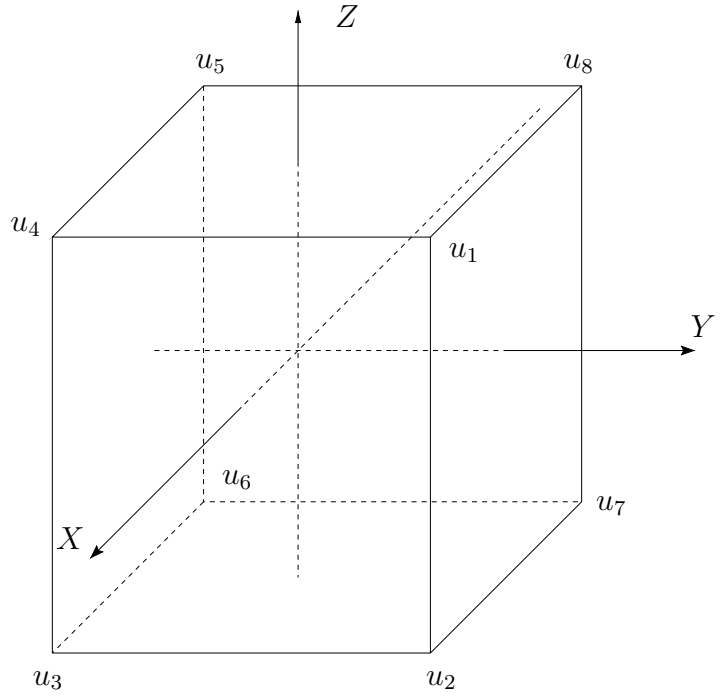

Figure 3.3.2.1: The unit sphere U_∞ of the L_∞ metric.

As for the number of facets of $B_\infty(a_1, a_2)$, we have an upper bound of $3^2 = 9$ by Lemma 3.2.1.2, but at most seven of these seven combinations can really occur, because there are only three different directions for all edges. □

In Section 3.2.3 we have seen that the bisector of three sites based on a convex polytope is not necessarily a connected polygonal chain, but for the L_∞ metric we have the following result.

Lemma 3.3.2.2 *The bisector $B_\infty(a_1, a_2, a_3)$ is empty or a connected polygonal chain completed by two rays.*

Proof. Suppose that $B_\infty(a_1, a_2, a_3)$ is not empty. Then each of H_{123}, H_{213}, and H_{312} is not empty, due to Lemma 3.1.2.4. As mentioned in the previous proof, each of H_{12} and H_{21} consists of exactly three facets of ∂C where every two of the three are adjacent. The set H_{123} consists of a subset of the facets of H_{12}, therefore it is connected. Then by Lemma 3.1.2.6, $B_\infty(a_1, a_2, a_3)$ is a connected polygonal chain completed by two rays. □

This result was also obtained by Le [60], but his proof is very complicated, and the techniques can not easily be generalized to other polytopes.

Lemma 3.3.2.3 *The bisector $B_\infty(a_1, a_2, a_3)$ consists of at most four edges each of which is is parallel to one of the following seven directions,*

$$(1,1,1), \quad (-1,1,1), \quad (1,-1,1), \quad (1,1,-1), \quad (0,0,1), \quad (1,0,0), \quad (0,1,0).$$

Proof. Let s be an edge of the bisector with foot sets are contained in $f_1 + a_1$, $f_2 + a_2$, and $f_3 + a_3$ on ∂C_1, ∂C_2, and ∂C_3, respectively. Therefore $f_1 \subset H_{123}, f_2 \subset H_{213}, f_3 \in\subset H_{312}$.

If two of f_1, f_2, and f_3 are parallel, due to Corollary 3.1.5.12, then the intersections of these two planes with the third plane are parallel to an edge of C that can have one of the directions $(0,0,1)$, $(1,0,0)$, and $(0,1,0)$. Otherwise the facets f_1, f_2, and f_3 intersect in a point v that is a vertex of ∂C and lies on the boundaries of H_{123}, H_{213}, and H_{312}, so the edge h is a ray parallel to the line through O and v that has one of the directions $(1,1,1)$, $(-1,1,1)$, and $(1,-1,1)$.

There are only two possible distinct partitions of the six facets of the unit cube into the three sets H_{123}, H_{213}, and H_{312}. Either each of sets consists of two facets, or one set has three facets, and the others have two resp. one. Then by Lemma 3.2.3.2 we have an immediate upper bound of eight for the number of vertices of $B_\infty(a_1, a_2, a_3)$, but this bound is not tight here. By using Desargue's Theorem 1.2.1 it is not hard to see that the foot sets of the bisector can cross each edge of H_{123} etc. at most once, and only three such edges can be crossed, altogether. □

Now let us turn to the bisector of four sites. We are interested in the number of points the bisector of four sites consists of. From Lemma 3.2.5.2 we know that there are four sites in general position whose bisector contains at least two points. As an example, we give two homothetic tetrahedra whose vertices lie on the facets of U_∞. It is not difficult to check that the following two tetrahedra T_1 and T_2 with vertices p_i, q_i, r_i, s_i, for $i = 1, 2$, are homothetic, see Figure 3.3.2.2, where

$$\begin{array}{llll} p_1 = (1, -\frac{1}{2}, \frac{1}{2}), & q_1 = (-1, -\frac{1}{2}, \frac{1}{2}), & r_1 = (a, \frac{5}{6}, 1), & s_1 = (b, -1, -\frac{5}{6}) \\ p_2 = (1, -\frac{1}{3}, \frac{1}{3}), & q_2 = (-1, -\frac{1}{3}, \frac{1}{3}), & r_2 = (a, 1, \frac{5}{6}), & s_2 = (b, -\frac{5}{6}, -1), \end{array}$$

for $a, b \in (0, 1)$. We see that the points p_1 and p_2 lie in the same facet with $X = 1$, the points q_1 and q_2 lie in the facet with $X = -1$. The two facets with r_1 and s_2 are parallel, as well as the facets with r_2 and s_1. The four lines $p_1\,p_2$, $q_1\,q_2$, $r_1\,r_2$, and $s_1\,s_2$ are parallel, the two tetrahedra T_1 and T_2 have the same size. This is not a coincidence, as the next lemma shows.

Lemma 3.3.2.4 *There are no two homothetic tetrahedra of different size whose vertices are contained in the surface of the unit cube.*

Proof. Assume the contrary with $T(a'_1, \ldots, a'_4)$ and $T(a''_1, \ldots, a''_4)$. Then the two tetrahedra have a common center of their homothety, namely the common intersection p of the lines $a'_i\,a''_i$, $i = 1, \ldots, 4$.

The surface of the unit cube is partitioned into four parts, $H_{1234}, \ldots, H_{4123}$.

For each i we have that a'_i and a''_i are contained in the same part, and a'_i is contained in a different part from a'_j for $i \neq j$, but not on the boundary of a part.

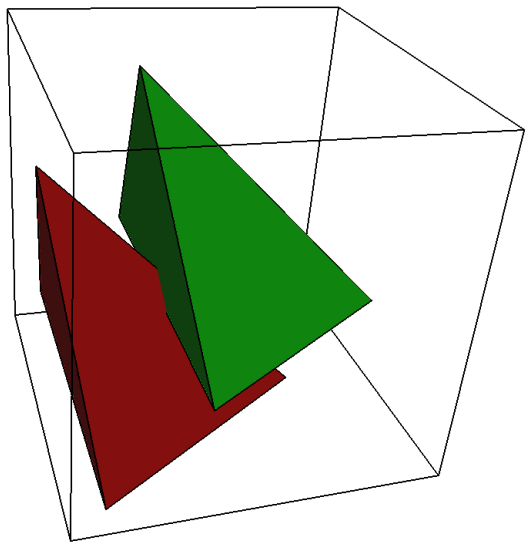

Figure 3.3.2.2: Two homothetic tetrahedra in the unit cube.

Thus each of the four rays from p through a'_i must hit a different face of the unit cube, this is impossible. □

In other words, if the L_∞-bisector of four sites in general position contains two points, then the two cubes centered at the two points which pass through the four sites have the same size. This strongly restricts the possible shapes of the bisector, as we will see now.

Lemma 3.3.2.5 *The bisector of four sites in general position based on the L_∞ metric consists of at most two points or one line segment.*

Proof. Assume that three different homothetic tetrahedra $T(a'_1, \ldots, a'_4)$, $T(a''_1, \ldots, a''_4)$, and $T(a'''_1, \ldots, a'''_4)$ are contained in the surface of the unit cube. Then by Lemma 3.3.2.4 they have the same size.

Assume that a'_1, a''_1, and a'''_1 are not collinear, then a'_i, a''_i, and a'''_i, $i = 2, \ldots, 4$, are also non-collinear. From Desargue's theorem follows that the four planes $\pi(a'_i, a''_i, a'''_i)$ for $i = 1, \ldots, 4$ are parallel. Two of the planes must pass through two parallel facets of the unit cube because at least two of the four sets $H_{1234}, \ldots, H_{4123}$ contain only one facet. The two remaining planes, say $\pi(a'_2, a''_2, a'''_2)$ and $\pi(a'_3, a''_3, a'''_3)$ must be situated between these first two and must contain the triangles $\triangle(a'_2, a''_2, a'''_2)$ and $\triangle(a'_3, a''_3, a'''_3)$. The three points a'_2, a''_2, and a'''_2 lie two different facets, and the three points a'_3, a''_3, and a'''_3 lie the two remaining facets, see Figure 3.3.2.3. But then it is impossible that $\triangle(a'_2, a''_2, a'''_2)$ and $\triangle(a'_3, a''_3, a'''_3)$ are homothetic.

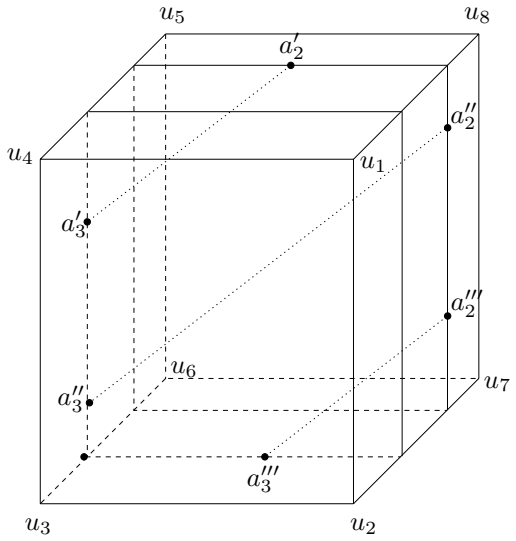

Figure 3.3.2.3: The two triangles $\triangle(a'_2, a''_2, a'''_2)$ and $\triangle(a'_3, a''_3, a'''_3)$ can not be homothetic.

The only remaining possibility is that all four triplets (a'_i, a''_i, a'''_i) for $i = 1, \ldots, 4$ are collinear on parallel lines, and each such triplet must be contained in a single facet of the unit cube. Then we have a situation as shown in Figure 3.3.2.4.

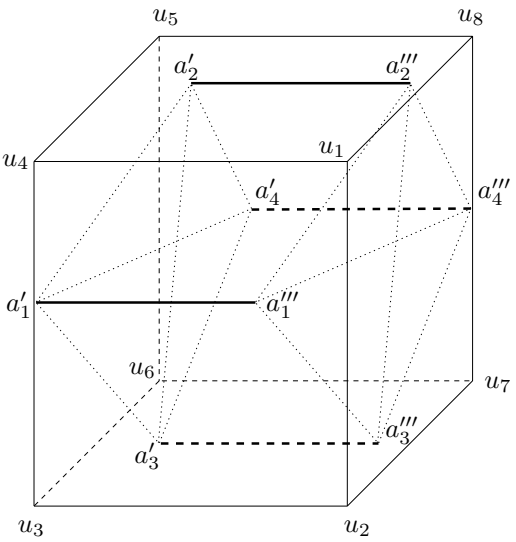

Figure 3.3.2.4: A tetrahedron is contained in the unit cube and can be translated without losing contact to the four facets.

A tetrahedron contained in the unit cube can be translated along a line without losing contact to the four facets. This corresponds to the fact that the bisector of the four sites is a line segment. □

3.3.3 The L_1 metric

Let U be the unit sphere of the L_1 metric in 3-space. U is the regular octahedron with six vertices $u_1 = (1,0,0)$, $\overline{u_1} = (-1,0,0)$, $u_2 = (0,1,0)$, $\overline{u_2} = (0,-1,0)$, $u_3 = (0,0,1)$, and $\overline{u_3} = (0,0,-1)$, see Figure 3.3.3.1.

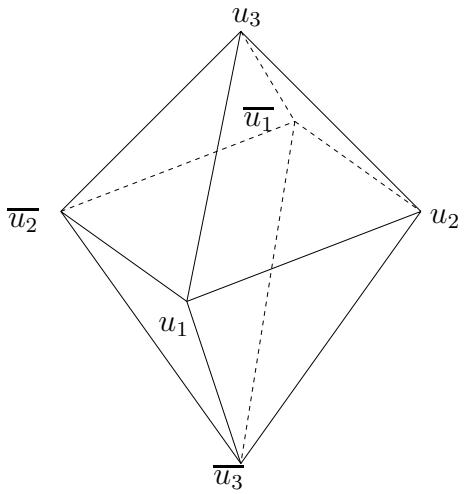

Figure 3.3.3.1: The regular octahedron.

We assume general position for the sites $a_1, \ldots, a_4$.

Lemma 3.3.3.1 *The bisector $B_1(a_1, a_2)$ based on the L_1 metric consists of at most nine facets, each of which is parallel to one of the following planes,*

$$\begin{array}{lll} X+Y+Z=1, & -X+Y+Z=1, & -X-Y+Z=1, \quad X-Y+Z=1, \\ X=0, & Y=0, & Z=0, \\ X=\pm Y, & X=\pm Z, & Y=\pm Z. \end{array}$$

Proof. Because of the symmetry of U the set H_{12} contains exactly four incident triangles, and each triangle contains an edge that lies in the sihouette Γ_{12}.

Let h be a facet in $B_1(a_1, a_2)$ whose foot sets on ∂C_1 resp. ∂C_2 are contained in two triangles $f + a_1$ resp. $g + a_2$. If f and g are parallel then the facet h is also parallel to them and thereby parallel to one of the first four given planes. If f and g contain a common line segment on Γ_{12} then h is unbounded and it is parallel to the plane passing through O and this line segment, this plane has one of the equations $X = 0$, $Y = 0$, or $Z = 0$. If f and g contain a common vertex v on Γ_{12} then the facet h is unbounded and it is parallel to two lines: one is the intersection of the supporting planes of f and g, the other is the line passing through O and v. Such planes have the equations $X = \pm Y$, $X = \pm Z$, or $Y = \pm Z$.

As for the number of facets of $B_1(a_1, a_2)$ we have an upper bound of $4^2 = 16$ by Lemma 3.2.1.2, but it is not hard to see that at most nine of these combinations can occur. □

Lemma 3.3.3.2 *The bisector $B_1(a_1, a_2, a_3)$ is empty or a connected polygonal chain. It contains at most six edges.*

Proof. Suppose that $B_1(a_1, a_2, a_3)$ is not empty. Then, due to Lemma 3.1.2.4, all three sets H_{123}, H_{213}, and H_{312} are not empty. Because each of H_{12} and H_{21} contains exactly four incident triangles of ∂U, so the set H_{123} contains two or four triangles, and each two of them are adjacent by a line segment. Therefore H_{123} is alway simply connected. Due to Lemma 3.1.2.6, the bisector $B_1(a_1, a_2, a_3)$ is a connected polygonal chain.

We assume that H_{123} consists of four triangles of ∂U which are adjacent to a vertex, and each of H_{213} and H_{312} consist of two triangles adjacent to an edge. The three boundaries of H_{123}, H_{213}, and H_{312} must intersect in two vertices t and d of ∂U. The three foot sets of the bisector translated to ∂U must connected t and d.

Assume that there are two vertices p and q of $B_1(a_1, a_2, a_3)$ such that their foot points on ∂C_i lie on an edge $e + a_i$ for an i. Let p_i and q_i be the two foot points of p resp. q translated to ∂U, $i = 1, 2, 3$. The three lines $p_i\, q_i$, $i = 1, 2, 3$, intersect in a point u, or they are parallel. To this is equivalent that there are three rays that intersect only H_{123}, H_{213}, and H_{312}, respectively, and one of them passes through the edge e. But this is only possible if e is an edge of H_{123}, and e is adjecent to t or d. The points p_i and q_i for $i = 2, 3$ must lie in two different triangles of H_{213} resp. H_{312}, otherwise the three lines $p_i\, q_i$, $i = 1, 2, 3$, intersect in t or d, or they are parallel, this means that p or q is not a vertex, a contradiction.

Assume that e is adjacent to t, and p_1 is closer to t than q_1. Because the line segments $\overline{p_i\, t} + a_i$, $i = 1, 2, 3$, lie in the foot sets of the bisector, the point p_2 or p_3 lies on the edge of H_{213} resp. H_{312}. Therefore the point p_2 and q_2 or p_3 and q_3 lie in the same triangle, a contradiction.

Thus $B_1(a_1, a_2, a_3)$ contains at most six edges. □

The bisector of four sites for the L_1 metric is slightly more complicated than that for the L_∞ metric.

By Lemma 3.2.5.2 we know that there are four sites a_1, a_2, a_3, and a_4 in general position such that $B_1(a_1, a_2, a_3, a_4)$ consists of at least two points. We consider some example configurations. The following two tetrahedra $T_1 = T(p_1, p_3, p_5, p_7)$ and $T_2 = T(p_2, p_4, p_6, p_8)$ are homothetic, see Figure 3.3.3.2, where

$$p_1 = (-\tfrac{3}{20}, -\tfrac{3}{4}, \tfrac{1}{10}), \qquad p_3 = (\tfrac{1}{8}, -\tfrac{3}{4}, \tfrac{1}{8}), \qquad p_5 = (-\tfrac{1}{4}, \tfrac{1}{4}, \tfrac{1}{2}), \qquad p_7 = (\tfrac{1}{8}, \tfrac{1}{4}, \tfrac{5}{8}),$$

$$p_2 = (-\tfrac{5}{36}, -\tfrac{7}{18}, -\tfrac{17}{36}), \quad p_4 = (\tfrac{1}{6}, -\tfrac{7}{18}, -\tfrac{4}{9}), \quad p_6 = (-\tfrac{1}{4}, \tfrac{13}{18}, -\tfrac{1}{36}), \quad p_8 = (\tfrac{1}{6}, \tfrac{13}{18}, \tfrac{1}{9}).$$

We see that the points p_7 and p_8 lie on the same triangle $\triangle(u_1, u_2, u_3)$, the other six points lie on six different triangles of U. This corresponds to a bisector $B_1(a_1, a_2, a_3, a_4)$ of four sites in general position. The bisector point which corresponds

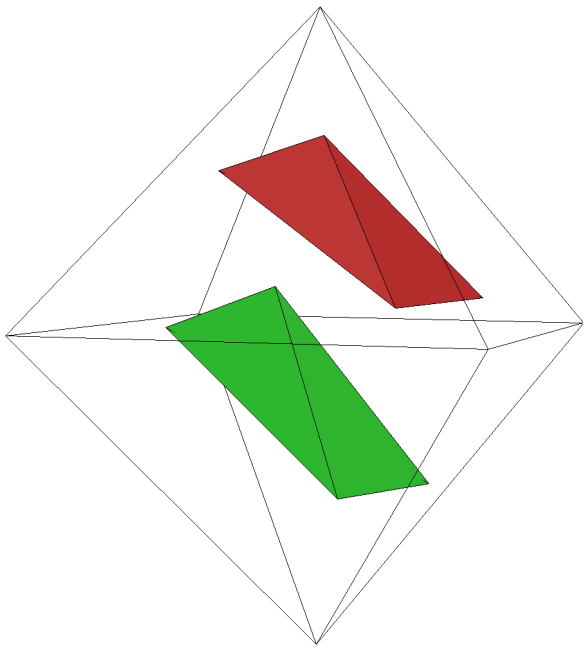

Figure 3.3.3.2: Two homothetic tetrahedra whose vertices lie on the surface of the regular octahedron. The lower tetrahedron corresponds to an isolated bisector point. The upper tetrahedron belongs to a set of tetrahedra whose vertices lie on the same facets and whose common center of homothety is the top vertex, this corresponds to a line segment of the bisector.

to the lower tetrahedron is the result of a transversal intersection of $B_1(a_1, a_2, a_3)$ and $B_1(a_1, a_4)$, by Lemma 3.1.5.13, thus it is an isolated point of $B_1(a_1, a_2, a_3, a_4)$. The upper tetrahedron, however, does not correspond to a transversal intersection, by Lemma 3.1.5.13. It is in fact part of a line segment in $B_1(a_1, a_2, a_3, a_4)$, because the tetrahedron is homothetic to infinitely many tetrahedra with vertices on the same facets of the octahedron, the center of this homothety is the top vertex of U.

The next example corresponds to a bisector of four sites which consists of exactly two points, see Figure 3.3.3.3. It shows two homothetic tetrahedra $T_1 = T(p_1, p_3, p_5, p_7)$ and $T_2 = T(p_2, p_4, p_6, p_8)$, where

$$p_1 = (\tfrac{1}{8}, -\tfrac{1}{4}, \tfrac{5}{8}), \quad p_3 = (-\tfrac{1}{6}, \tfrac{3}{4}, -\tfrac{1}{12}), \quad p_5 = (\tfrac{1}{8}, \tfrac{3}{4}, \tfrac{1}{8}), \quad p_7 = (-\tfrac{3}{4}, -\tfrac{1}{8}, \tfrac{1}{8}),$$

$$p_2 = (\tfrac{1}{4}, -\tfrac{3}{8}, \tfrac{3}{8}), \quad p_4 = (-\tfrac{1}{24}, \tfrac{5}{8}, -\tfrac{1}{3}), \quad p_6 = (\tfrac{1}{4}, \tfrac{5}{8}, -\tfrac{1}{8}), \quad p_8 = (-\tfrac{5}{8}, -\tfrac{1}{4}, -\tfrac{1}{8}).$$

The two tetrahedra are of the same size which is required for a bisector of this kind. In the proof of Lemma 3.3.3.4 we will get an idea of the reason for that.

The bisector of four sites in general position may also consist of two line segments, it is easy to construct such an example in which one tetrahedron touches the four upper facets, and the other tetrahedron touches the four lower facets of the octahedron. In the following we will see that these three configurations we have seen with

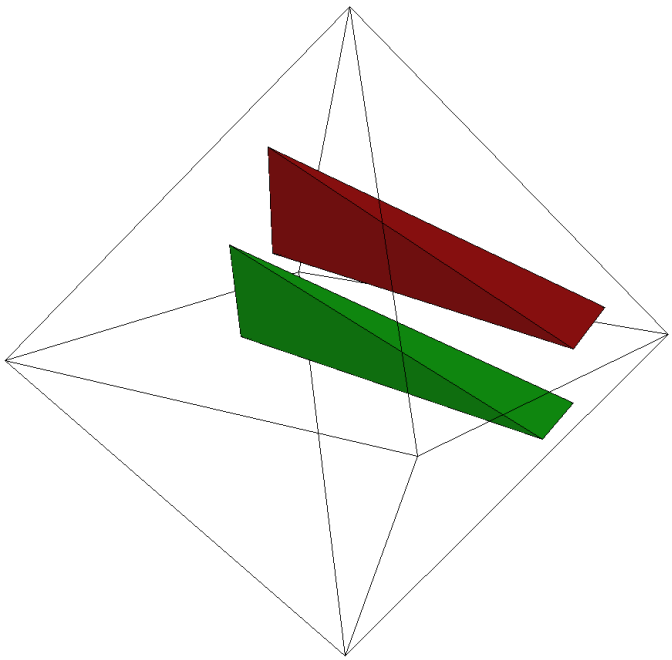

Figure 3.3.3.3: Two homothetic tetrahedra whose vertices lie on the surface of the regular octahedron. Both tetrahedra correspond to isolated bisector points.

two components plus the "normal" ones where the bisector has only one component represent all possibilities.

Lemma 3.3.3.3 *If $B_1(a_1, a_2, a_3, a_4)$ contains at least two connected components then each of H_{1234}, H_{2134}, H_{3124}, and H_{4123} consists of two triangles adjacent by a line segment.*

Proof. Similar to what we have remarked at the beginning of the proof of Lemma 3.3.3.2, each of H_{1234}, H_{2134}, H_{3124}, and H_{4123} can consist of one, two, or four of the eight triangular facets of the unit sphere U.

So assume that we have two of these sets, say H_{1234} and H_{2134}, which contains only one triangle. Then one of the two remaining parts, say H_{3124}, has two triangles adjacent by a line segment, and H_{4123} contains four triangles that are adjacent in a vertex of ∂U. Therefore H_{1234} and H_{2134} must also be adjacent by a line segment.

Now let $T(a_1', a_2', a_3', a_4')$ and $T(a_1'', a_2'', a_3'', a_4'')$ be two homothetic tetrahedra which correspond to two points of the two connected components of $B_1(a_1, a_2, a_3, a_4)$. The points a_1' and a_1'' are both contained in H_{1234}, etc. for other points.

The four lines $a_i' a_i''$, $i = 1, 2, 3, 4$, intersect in the center of the homothy, u, or they are parallel. If u exists then it must lie on the supporting planes of H_{1234} and H_{2134}, otherwise the four lines are parallel to the edge which is adjacent to H_{1234} and H_{2134}.

In any case it is not possible that the line $a'_3\,a''_3$ intersects H_{3124} twice, and that $a'_4\,a''_4$ intersects H_{4123} twice, a contradiction.

Thus each of H_{1234}, H_{2134}, H_{3124}, and H_{4123} contains two triangles of ∂U which are adjacent by a line segment, and all four sets must be adjacent to two antipodal vertices of ∂U. □

Lemma 3.3.3.4 *The bisector $B_1(a_1, a_2, a_3, a_4)$ consists of at most two connected components.*

Proof. Assume that the bisector $B_1(a_1, a_2, a_3, a_4)$ contains three connected components. From each connected component we choose one point, they correspond to three homothetic tetrahedra $T' = T(a'_1, a'_2, a'_3, a'_4)$, $T'' = T(a''_1, a''_2, a''_3, a''_4)$, and $T''' = T(a'''_1, a'''_2, a'''_3, a'''_4)$ that are contained in U with a'_i, a''_i, and a'''_i on ∂U. In particular, the points a'_1, a''_1, and a'''_1, are contained in H_{1234}, and analogously for the other triplets.

It is easy to see that no triplet (a'_i, a''_i, a'''_i) is collinear, because if one triplet was collinear, then the others would be collinear as well, and their bisector components were connected. It is also clear that no triplet (a'_i, a''_i, a'''_i) is contained in the same facet of the octahedron, because otherwise by Lemma 3.1.1.6 the four planes $\pi_1 := \pi(a'_1, a''_1, a'''_1)$, $\pi_2 := \pi(a'_2, a''_2, a'''_2)$, $\pi_3 := \pi(a'_3, a''_3, a'''_3)$, and $\pi_4 := \pi(a'_4, a''_4, a'''_4)$ intersect in a line which lies on the supporting plane of this triplet (a'_i, a''_i, a'''_i), but this is impossible. Therefore plane π_1 intersects H_{1234} in two connected line segments which contain the points a'_1, a''_1, and a'''_1, and analogously for the other triplets. Furthermore, the triplets appear always in the same order, say a'_i, a''_i, and a'''_i.

We consider the possible distribution of the twelve vertices on the eight facets of U. There are no two of the three tetrahedra with the same four facets attached to their vertices, because the tetrahedra represent disconnected components of the bisector. And there are even no two of the three tetrahedra which three facets, for the same reason. Essentially only one possibility remains, due to the fact that the triplets appear the same order. The first tetrahedron, T', touches the four upper facets of U, T'' touches two adjacent upper facets and the two opposite (lower) facets, and T''' touches the four lower facets.

T' represents a line segment of the bisector, by homothety centered at the top vertex of U. But then T' can be scaled such that at least one of its vertices, say a'_1, touches an edge of the lower facets, and then a'_1, a''_1, and a'''_1 are collinear, a contradiction. □

Remark that a bisector of four sites may consist of two rays and a connecting line segment, in the special case that was mentioned in the above proof. One tetrahedron touches the four upper facets of U, the second one touches two upper and two lower

facets, and the last one touches the four lower facets. The rays of the bisector stem from the homothety of the first tetrahedron centered at the top vertex of U and the homothety of the last tetrahedron centered at the botton vertex. The connectivity is realized by parallel translation of the maximally scaled upper tetrahedron to the corresponding position of the lower tetrahedron.

Bibliography

[1] N. Amenta, S. Levy, T. Munzner, and M. Philips. Geomview: A system for geometric visualization. In *Proc. 11th Annu. ACM Sympos. Comput. Geom.*, pages C12–C13, 1995.

[2] F. Aurenhammer. Voronoi diagrams: A survey of a fundamental geometric data structure. *ACM Comput. Surv.*, 23(3):345–405, Sept. 1991.

[3] F. Aurenhammer and H. Edelsbrunner. An optimal algorithm for constructing the weighted Voronoi diagram in the plane. *Pattern Recogn.*, 17:251–257, 1984.

[4] F. Aurenhammer and R. Klein. Voronoi diagrams. In J.-R. Sack and J. Urrutia, editors, *Handbook of Computational Geometry*. Elsevier Science Publishers B.V. North-Holland, Amsterdam, 1999.

[5] C. B. Barber, D. P. Dobkin, and H. Huhdanpaa. The quickhull algorithm for convex hulls. *ACM Trans. Math. Softw.*, 22(4):469–483, Dec. 1996.

[6] H. Baumgarten, H. Jung, and K. Mehlhorn. Dynamic point location in general subdivisions. *J. Algorithms*, 17:342–380, 1994.

[7] J.-D. Boissonnat, M. Sharir, B. Tagansky, and M. Yvinec. Voronoi diagrams in higher dimensions under certain polyhedral distance functions. *Discrete Comput. Geom.*, 19(4):473–484, 1998.

[8] J.-D. Boissonnat and M. Teillaud. A hierarchical representation of objects: The Delaunay tree. In *Proc. 2nd Annu. ACM Sympos. Comput. Geom.*, pages 260–268, 1986.

[9] J.-D. Boissonnat and M. Teillaud. On the randomized construction of the Delaunay tree. *Theoret. Comput. Sci.*, 112:339–354, 1993.

[10] J.-D. Boissonnat and M. Yvinec. *Géométrie Algorithmique*. Ediscience international, Paris, 1995.

[11] J.-D. Boissonnat and M. Yvinec. *Algorithmic Geometry*. Cambridge University Press, UK, 1998. Translated by Hervé Brönnimann.

[12] A. Bowyer. Computing Dirichlet tesselations. *Comput. J.*, 24:162–166, 1981.

[13] K. Q. Brown. Voronoi diagrams from convex hulls. *Inform. Process. Lett.*, 9(5):223–228, 1979.

[14] B. Buchberger. Ein algorithmisches Kriterium für die Lösbarkeit eines algebraischen Gleichungssystems. *Aequationes Mathematicae*, 4(3):374–383, 1970.

[15] B. W. Char, K. O. Geddes, G. H. Gonnet, B. L. Leong, M. B. Monagan, and S. M. Watt. *Maple V Language Reference Manual*. Springer-Verlag, New York, 1991.

[16] S. W. Cheng and R. Janardan. New results on dynamic point location. In *Proc. 31st Annu. IEEE Sympos. Found. Comput. Sci.*, pages 96–105, 1990.

[17] L. P. Chew and R. L. Drysdale, III. Voronoi diagrams based on convex distance functions. In *Proc. 1st Annu. ACM Sympos. Comput. Geom.*, pages 235–244, 1985.

[18] L. P. Chew, K. Kedem, M. Sharir, B. Tagansky, and E. Welzl. Voronoi diagrams of lines in 3-space under polyhedral convex distance functions. In *Proc. 6th ACM-SIAM Sympos. Discrete Algorithms*, pages 197–204, 1995.

[19] Y.-J. Chiang, F. P. Preparata, and R. Tamassia. A unified approach to dynamic point location, ray shooting, and shortest paths in planar maps. *SIAM J. Comput.*, 25:207–233, 1996.

[20] Y.-J. Chiang and R. Tamassia. Dynamization of the trapezoid method for planar point location. In *Proc. 7th Annu. ACM Sympos. Comput. Geom.*, pages 61–70, 1991.

[21] A. G. Corbalan, M. Mazon, and T. Recio. About Voronoi diagrams for strictly convex distances. In *Abstracts 9th European Workshop Comput. Geom.*, pages 17–22, 1993.

[22] A. G. Corbalan, M. Mazon, and T. Recio. Geometry of bisectors for strictly convex distances. *Internat. J. Comput. Geom. Appl.*, 6:45–58, 1996.

[23] M. de Berg, M. van Kreveld, M. Overmars, and O. Schwarzkopf. *Computational Geometry: Algorithms and Applications*. Springer-Verlag, Berlin, 1997.

[24] F. Dehne and R. Klein. "The Big Sweep": On the power of the wavefront approach to Voronoi diagrams. *Algorithmica*, 17(1):19–32, 1997.

[25] L. Devroye, E. P. Mücke, and B. Zhu. A note on point location in Delaunay triangulations of random points. *Algorithmica*, 22:477–482, 1998.

[26] R. L. Drysdale, III. A practical algorithm for computing the Delaunay triangulation for convex distance functions. In *Proc. 1st ACM-SIAM Sympos. Discrete Algorithms*, pages 159–168, 1990.

[27] H. Edelsbrunner, L. J. Guibas, and J. Stolfi. Optimal point location in a monotone subdivision. *SIAM J. Comput.*, 15(2):317–340, 1986.

[28] H. Edelsbrunner and R. Seidel. Voronoi diagrams and arrangements. *Discrete Comput. Geom.*, 1:25–44, 1986.

[29] S. Fortune. Voronoi diagrams and Delaunay triangulations. In D.-Z. Du and F. K. Hwang, editors, *Computing in Euclidean Geometry*, volume 1 of *Lecture Notes Series on Computing*, pages 193–233. World Scientific, Singapore, 1st edition, 1992.

[30] S. Fortune. Voronoi diagrams and Delaunay triangulations. In J. E. Goodman and J. O'Rourke, editors, *Handbook of Discrete and Computational Geometry*, chapter 20, pages 377–388. CRC Press LLC, Boca Raton, FL, 1997.

[31] S. J. Fortune. A sweepline algorithm for Voronoi diagrams. *Algorithmica*, 2:153–174, 1987.

[32] P. R. Goodey. Homothetic ellipsoids. *Math. Proc. Camb. Phil. Soc.*, 93:25–34, 1983.

[33] P. J. Green and R. R. Sibson. Computing Dirichlet tessellations in the plane. *Comput. J.*, 21:168–173, 1978.

[34] L. J. Guibas and R. Seidel. Computing convolutions by reciprocal search. *Discrete Comput. Geom.*, 2:175–193, 1987.

[35] L. J. Guibas and J. Stolfi. Primitives for the manipulation of general subdivisions and the computation of Voronoi diagrams. *ACM Trans. Graph.*, 4(2):74–123, Apr. 1985.

[36] H. W. Hamacher. *Mathematische Lösungsverfahren für planare Standortprobleme*. Verlag Vieweg, Wiesbaden, 1995.

[37] R. Hartshorne. *Algebraic Geometry*, volume 52 of *Graduate texts in Mathematics*. Springer-Verlag, New York, 1977.

[38] C. Icking, R. Klein, P. Köllner, and L. Ma. A Java applet for the dynamic visualization of Voronoi diagrams. In *Abstracts 13th European Workshop Comput. Geom.*, pages 46–47, 1997.

[39] C. Icking, R. Klein, N.-M. Lê, and L. Ma. Convex distance functions in 3-space are different. *Fundam. Inform.*, 22:331–352, 1995.

[40] C. Icking, R. Klein, N.-M. Lê, L. Ma, and F. Santos. On bisectors for convex distance functions in 3-space. In *Proc. 11th Canad. Conf. Comput. Geom.*, 1999.

[41] C. Icking, R. Klein, L. Ma, S. Nickel, and A. Weißler. On bisectors for different distance functions. In *Proc. 15th Annu. ACM Sympos. Comput. Geom.*, pages 291–299, 1999.

[42] N. Jacobson. *Basic Algebra I.* W. H. Freeman, San Francisco, CA, 1974.

[43] P. Kelly and M. Weiss. *Geometry and Convexity: A Study in Mathematical Methods.* John Wiley & Sons, New York, NY, 1979.

[44] D. Kirkpatrick and J. Snoeyink. Tentative prune-and-search for computing Voronoi vertices. In *Proc. 9th Annu. ACM Sympos. Comput. Geom.*, pages 133–142, 1993.

[45] D. Kirkpatrick and J. Snoeyink. Computing common tangents without a separating line. In *Proc. 4th Workshop Algorithms Data Struct.*, volume 955 of *Lecture Notes Comput. Sci.*, pages 183–193. Springer-Verlag, 1995.

[46] D. Kirkpatrick and J. Snoeyink. Tentative prune-and-search for computing fixed-points with applications to geometric computation. *Fundam. Inform.*, 22:353–370, 1995.

[47] D. G. Kirkpatrick. Optimal search in planar subdivisions. *SIAM J. Comput.*, 12(1):28–35, 1983.

[48] R. Klein. Combinatorial properties of abstract Voronoi diagrams. In M. Nagl, editor, *Proc. Internat. Workshop Graph-Theoret. Concepts Comput. Sci.*, volume 411 of *Lecture Notes Comput. Sci.*, pages 356–369. Springer-Verlag, 1989.

[49] R. Klein. *Concrete and Abstract Voronoi Diagrams*, volume 400 of *Lecture Notes Comput. Sci.* Springer-Verlag, 1989.

[50] R. Klein. *Algorithmische Geometrie.* Addison-Wesley, Bonn, 1997.

[51] R. Klein and L. Ma. Wrapping ellipses around a convex skeleton. *Internat. J. Comput. Math.*, 55:173–181, 1995.

[52] R. Klein, K. Mehlhorn, and S. Meiser. Randomized incremental construction of abstract Voronoi diagrams. Technical Report MPI-I-93-105, Max-Planck-Institut Inform., Saarbrücken, Germany, 1993.

[53] R. Klein and D. Wood. Voronoi diagrams based on general metrics in the plane. In R. Cori and M. Wirsing, editors, *Proc. 5th Sympos. Theoret. Aspects Comput. Sci.*, volume 294 of *Lecture Notes Comput. Sci.*, pages 281–291. Springer-Verlag, 1988.

[54] S. Lang. *Analysis I.* Addison-Wesley, New York, NY, 1969.

[55] C. L. Lawson. Software for C^1 surface interpolation. In J. R. Rice, editor, *Math. Software III*, pages 161–194. Academic Press, New York, NY, 1977.

[56] N.-M. Lê. On general properties of strictly convex smooth distance functions in R^d. In *Proc. 5th Canad. Conf. Comput. Geom.*, pages 375–380, 1993.

[57] N.-M. Lê. On Voronoi diagrams in the L_p-metric in R^D. *Discrete Comput. Geom.*, 16:177–196, 1996.

[58] N.-M. Lê. On non-smooth convex distance functions. *Inform. Process. Lett.*, 63(6):323–329, 1997.

[59] N.-M. Lê. Randomized incremental construction of simple abstract Voronoi diagrams in 3-space. *Comput. Geom. Theory Appl.*, 8:279–298, 1997.

[60] N.-M. Lê. Abstract Voronoi diagrams in 3-space. Technical Report HKUST-TCSC-99-11, Hong Kong University of Science and Technology, Theoretical Computer Science Center, 1999.

[61] D. T. Lee. Two-dimensional Voronoi diagrams in the L_p-metric. *J. ACM*, 27(4):604–618, 1980.

[62] D. T. Lee and R. L. Drysdale, III. Generalization of Voronoi diagrams in the plane. *SIAM J. Comput.*, 10:73–87, 1981.

[63] D. T. Lee and C. K. Wong. Voronoi diagrams in L_1 (L_∞) metrics with 2-dimensional storage applications. *SIAM J. Comput.*, 9(1):200–211, 1980.

[64] D. Leven and M. Sharir. Planning a purely translational motion for a convex object in two-dimensional space using generalized Voronoi diagrams. *Discrete Comput. Geom.*, 2:9–31, 1987.

[65] K. Mehlhorn, S. Meiser, and C. Ó'Dúnlaing. On the construction of abstract Voronoi diagrams. *Discrete Comput. Geom.*, 6:211–224, 1991.

[66] H. Meschkowski. *Grundlagen der Euklidischen Geometrie.* BI-Wissenschaftsverlag, Mannheim, 1974.

[67] E. P. Mücke, I. Saias, and B. Zhu. Fast randomized point location without preprocessing in two- and three-dimensional Delaunay triangulations. In *Proc. 12th Annu. ACM Sympos. Comput. Geom.*, pages 274–283, 1996.

[68] C. Ó'Dúnlaing and C. K. Yap. A "retraction" method for planning the motion of a disk. *J. Algorithms*, 6:104–111, 1985.

[69] A. Okabe, B. Boots, and K. Sugihara. *Spatial Tessellations: Concepts and Applications of Voronoi Diagrams.* John Wiley & Sons, Chichester, UK, 1992.

[70] F. P. Preparata and M. I. Shamos. *Computational Geometry: An Introduction.* Springer-Verlag, New York, NY, 1985.

[71] G. Rote. Personal communication, 1999.

[72] J. T. Schwartz and M. Sharir. Algorithmic motion planning in robotics. In J. van Leeuwen, editor, *Algorithms and Complexity*, volume A of *Handbook of Theoretical Computer Science*, pages 391–430. Elsevier, Amsterdam, 1990.

[73] A. V. Shaidenko. Some characteristic properties of the ellipsoid. *Sibirsk Mat. Z.*, 21:232–234, 240, 1980. In Russian.

[74] M. I. Shamos. Geometric complexity. In *Proc. 7th Annu. ACM Sympos. Theory Comput.*, pages 224–233, 1975.

[75] M. I. Shamos. *Computational Geometry.* Ph.D. thesis, Dept. Comput. Sci., Yale Univ., New Haven, CT, 1978.

[76] M. I. Shamos and D. Hoey. Closest-point problems. In *Proc. 16th Annu. IEEE Sympos. Found. Comput. Sci.*, pages 151–162, 1975.

[77] M. I. Shamos and D. Hoey. Geometric intersection problems. In *Proc. 17th Annu. IEEE Sympos. Found. Comput. Sci.*, pages 208–215, 1976.

[78] G. M. Shute, L. L. Deneen, and C. D. Thomborson. An $O(n \log n)$ plane-sweep algorithm for L_1 and L_∞ Delaunay triangulations. *Algorithmica*, 6:207–221, 1991.

[79] B. Tagansky. *The Complexity of Substructures in Arrangements of Surfaces.* Ph.D. thesis, Tel Aviv University, Tel Aviv, 1996.

[80] P. Widmayer, Y. F. Wu, and C. K. Wong. Distance problems in computational geometry with fixed orientations. In *Proc. 1st Annu. ACM Sympos. Comput. Geom.*, pages 186–195, 1985.

Index